DISSERTATION

RELIABILITY-BASED LIFETIME PERFORMANCE ANALYSIS OF LONG-SPAN BRIDGES

Submitted by

Jun Wu

Department of Civil and Environmental Engineering

In partial fulfillment of the requirements

For the Degree of Doctor of Philosophy

Colorado State University

Fort Collins, Colorado

Fall 2010

Doctoral Committee:

Department Head: Luis Garcia

Advisor: Suren Chen

John W. van de Lindt
Paul R. Heyliger
Hiroshi Sakurai

ABSTRACT

RELIABILITY-BASED LIFETIME PERFORMANCE ANALYSIS OF LONG-SPAN BRIDGES

Long-span bridges generally serve as the significant hub in the transportation system for normal transportation and critical evacuation paths when any disaster happens. Thus, the safety and serviceability of long-span bridges are related to huge economic cost and safety of thousands of lives. The objective of this research is to establish a general framework to evaluate the lifetime performance of long-span bridges through taking account of more realistic load situations, such as traffic flow and wind environment. After some background information is introduced in Chapter 1, Chapter 2 covers the modeling of stochastic traffic flow for the bridge infrastructure system in a more realistic way by using the Cellular Automaton model. Based on the detailed information of individual vehicles of the stochastic traffic flow, the general framework to study Bridge/Traffic/Wind dynamic performance is developed in Chapter 3. Chapter 3 and Chapter 4 also report the results of the bridge's serviceability under normal and extreme loads events, respectively. In Chapter 5, the scenario-based fatigue model is further developed based on the dynamic framework developed in Chapter 3. Finally, the reliability-based analysis is conducted in Chapter 6 to study the fatigue damage caused by the coupling effects among bridge, traffic flow and wind throughout the bridge's service life.

DEDICATION

To those I love

ACKNOWLEDGEMENT

I gratefully acknowledge my advisor Dr. Suren Chen, for sharing valuable knowledge, research experience, guidance, encouragement and support through the almost four years of my study at Colorado State University. His mentorship was paramount in providing a well rounded experience consistent with my long-term career goals. My appreciation is beyond words.

I am very pleased to have Dr. John W. van de Lindt, Dr. Paul Heyliger and Dr. Hiroshi Sakurai on my dissertation committee. I enjoyed learning a variety of topics from the courses I took from them in the past years. I would like to thank them for their guidance on my dissertation research. My appreciation also goes to all the teachers of the classes I have taken in Colorado State University, which helped me gain a good amount of useful knowledge. I would also like to thank my fellow graduate students at Colorado State University for their support, encouragement and friendship during my studies. Gratitude is also extended to Professor Xuhong Zhou and Professor Jin Di at Chang'an University for their encouragement and support. The financial support I received from the CSU startup fund and NSF research grant, which has made my dissertation study possible, is also very appreciated.

Last but not the least, the constant support from my parents is highly appreciated. It was from them that I gained so much motivation and ability to face the challenges. The dissertation could not have been completed without their encouragement, love and devotion.

TABLE OF CONTENTS

LIST OF FIGURES

LIST OF TABLES

CHAPTER 1: INTRODUCTION

1.1 Background

In the United States, over 800 long-span bridges are categorized as fracture-critical (Pines and Aktan 2002). Although the amount of long-span bridges is relatively small compared with the short and medium bridges, the importance of the continued integrity in both normal and extreme conditions for these critical infrastructures are easily justified by the critical role in the national and regional transportation network. Generally, long-span bridges accommodate a large volume of traffic and its functionality is critical to local economy during normal service conditions. During some natural disasters like hurricane, flood and earthquake, these long-span bridges may often serve as important evacuation routes. However, according to the special report by the sub-committee on the performance of bridges of ASCE (ASCE 2003), "… most of these [long-span] bridges were not designed and constructed with in-depth evaluations of the performance under combination loadings, under fatigue and dynamic loadings and for the prediction of their response in extreme events such as wind and ice storms, floods, accidental collision or blasts and earthquakes". Therefore, a reasonable lifetime performance prediction of slender long-span bridges under complex service loads becomes crucial.

1.2 Literature Review and Scope of the Dissertation

1.2.1 Service loads of long-span bridge

Long-span bridges (e.g. span length > 152.4m or 500 ft) usually accommodate a number of vehicles simultaneously and are subjected to strong bridge/vehicle dynamic interactions. In addition to traffic loads, slender long-span bridges (e.g. cable-stayed and suspension bridges) are

also susceptible to wind excitations as compared to conventional long-span bridges (e.g. arch or truss bridges). A slender long-span bridge usually experiences complicated dynamic loads from the bridge, stochastic traffic and wind (Guo and Xu 2001; Chen and Cai 2007). The stochastic nature of wind and traffic, as well as the dynamic interactions, makes a realistic estimation of fatigue damage of the bridge over time very challenging (Chen and Cai 2007). The research on bridge dynamics interacted with traffic and wind has experienced three stages: (1) bridge/vehicle interaction; (2) bridge/wind interaction and vehicle/wind interaction; (3) bridge/wind/vehicle interaction. Those three phases of the research will be introduced briefly in the following.

1.2.1.1 Traffic load on bridge

Daily traffic is the main live load which has significant impact on the strength and serviceability of bridges. Bridge/vehicle interactions have been studied since the middle of 20th century (Blejwas et al.1979; Olsson 1985). The impact of a vehicle on a bridge was initially assumed to be a moving load without considering the inertia effect. Later, a vehicle was simplified as a moving mass which can consider the inertia effect on bridges (Sadiku and Leipholz 1987). In recent years, the commonly-used analytical model for vehicle is a dynamic system consisting of mass, spring and damping parts, which have significant effects on dynamic analysis of vehicles and interactions with other systems. Thus, the interaction analysis of bridge and vehicles is to investigate the coupling nature of multiple dynamic systems. By numerically solving the coupled equations in the time domain, the dynamic response (displacement, acceleration and stress) of the bridge and vehicles can be obtained, respectively (Guo and Xu 2001; Kim et al. 2005; Chen and Cai 2006).

The evolution of traffic flow is complicated in terms of vehicle number, vehicle type combination and drivers' behavior such as lane-changing, acceleration or deceleration. AASHTO code (2007) specifies the design truck or tandem to investigate the bridge's strength and fatigue capacity

regarding short and medium bridges. Nevertheless, the current code does not provide the specifications on vehicular load regarding long-span bridges whose main span is more than 152.4m (500 feet). Most existing research did not adopt an appropriate model for traffic flow which is close to the realistic situation on bridge. Only the simplified models of traffic flow were used, such as a uniform fleet or statistical distributions with assumed patterns. Some researchers use WIM (Weigh-In-Motion) data to define the traffic load, but they cannot provide the useful and detailed information like the instantaneous speed and location at each time step. Such simplifications may be applicable for short and medium span bridges as fewer vehicles running on them at a time. But it is hard to apply on long-span bridges as well because long-span bridges accommodate large volume of traffic which is substantially more complex as compared to short and medium ones.

Although oversimplified by structural engineers, the traffic flow models have been studied extensively in the field of transportation engineering and can be categorized into three scales: macroscopic, mesoscopic and microscopic. The former two scales are based on continuous time and space, which are suitable for traffic studies typically focusing on physical characteristics of the whole traffic flow in a large scale (Nagel et al. 1998, Barlovic et al. 1998, Cheybani et al. 2000). The microscopic traffic simulation is based on discrete time and space which can capture the detailed time-variant information of individual vehicles. Cellular Automaton (CA) model proposed in 1992 by Nagel and Schreckenberg belongs to microscopic traffic flow model. The advantage of CA model is to reproduce the basic features of traffic flow through defining the basic data: vehicle density, speed limit, number of lanes and acceleration rate. This time-discrete and space-discrete traffic model can be integrated into the time-history analysis of bridge very well as it can offer the detailed information of individual vehicles.

Despite being a relatively new technology, CA simulation technique has shown its promising future through applications in the actual transportation management. For example, TRANSIMS, a commercial software developed by Las Alamos National Laboratory, is based on the concept of CA model (TRANSIMS Travelogue 1996). In Germany, CA model is used for online traffic simulation in North Rhein Westphalia (http://www.autobahn.nrw.de./) (Schadschneider 2006). The CA model has strong capability of replicating major traffic phenomena on highways including both normal and incident (partial lanes are blocked due to natural disaster, construction, maintenance and accidents) situations with different level of services, i.e. free traffic or busy traffic. Thus it becomes an ideal technology to be integrated into the advanced bridge dynamic analysis considering live load in a more accurate manner.

1.2.1.2 Wind load on bridge and vehicle

Slender long-span bridges are such a type of structure being sensitive to wind which has been proved by several noteworthy collapse accidents due to bridge/wind interaction. The bridge/wind dynamic interaction can be traced back to the failure of Tacoma Bridge in 1940. That striking accident aroused the serious concerns of engineers to study bridge aerodynamics. Generally, the wind-induced force on bridge can be classified into two types: one is the aerodynamic instability problem including the phenomena of flutter and galloping. The occurrence of flutter and galloping solely appear when some conditions are met. Another one is the wind-induced vibration problems including buffeting and vortex shedding. The primary wind-induced phenomena for long-span bridges are flutter and buffeting. When the critical wind speed is achieved, the vibration of bridge becomes self-feeding and divergent which is called flutter. Currently, most slender long-span bridges have been carefully designed to avoid flutter occurrence. Buffeting is the turbulence-induced vibration on bridges and theoretically exists whenever wind turbulence exists. Hence, buffeting can happen over a large range of wind speed (from low to high wind

speeds), and potentially cause serviceability and fatigue problem (Xu et al. 2009; Virlogeux 1992; Gu et al. 1999).

Inspired by the overturned vehicles and other accidents caused by high speed wind, the vehicle/wind interaction analysis started in the 1980s through wind tunnel test and numerical computation (Baker 1986, 1991a, 1991b; Hucho 1987; Cooper 1981; Coleman and Baker 1990; Chen and Cai 2004; Guo and Xu 2006). Wind effect on vehicles is composed of two parts: static wind force and quasi-static turbulent wind force (Baker 1986). Baker developed the basic functions in terms of the aerodynamic coefficient, vehicle speed and wind direction to quantify the wind force on running vehicle (Baker 1986).

1.2.1.3 Bridge/Traffic/Wind dynamic interaction

The comprehensive consideration of coupling effects among bridge, wind and vehicle started around 2003 by using the time-history analysis of the coupled finite element model (Xu and Guo 2003; Cai and Chen 2004; Chen and Cai 2006; Chen et al. 2007). In those studies, both the bridge and vehicle are taken as a completed dynamic system composed of mass, spring and damping matrix. The force exerted by wind on a bridge and vehicles as well as the interaction between the bridge and the vehicles considering the roughness of the pavement were included in those analytical models.

As the preliminary study on Bridge/Traffic/Wind interaction, those models successfully investigated the mechanism of dynamic interactions and identified the most significant parameters influencing the dynamic performance of bridges and can expose the effect of the main factors such as the wind speed, vehicle speed, vehicle type and road roughness. However, there are two major problems remaining in those early studies. Firstly, as the first step to study the complicated Bridge/Traffic/Wind interaction, those studies have considered only one or several

vehicles distributed in an assumed (usually uniform) pattern on a bridge. As stated in the previous section, the movement of traffic flow is necessary to taken into account of for accurate estimation of long span bridges' performance. Secondly, the fully-coupled Bridge/Traffic/Wind analysis considering the realistic traffic flow leads to matrices of mass, stiffness, damping and force vectors with extremely large sizes. The computation cost will be considerably high, if not practically acceptable at all.

1.2.2 Fatigue of bridge

Fatigue damage is one of the most common damage types for current bridges (Li and Chan 2006). The bridge members fail with the development of cracks under repeated range of stress. Traffic loads and wind force are inherently repeated loads and occur throughout the whole life of bridges. Both wind and traffic can be regarded as the main factors causing fatigue problem of long span bridges. In addition to the serviceability issue and damage to some local members, the fatigue problem can also cause the collapse of a whole bridge in some situation. For example, the Point Pleasant Bridge in West Virginia failed in 1967 without warning is an example of fatigue damage. The collapse is caused by the facture at the pinhole of an eye-bar of the bridge (White et al. 1992).

At present, the research on fatigue damage is generally classified into two categories. One is the theoretical research on the mechanism of fatigue damage based on crack growth concepts, the continuous damage mechanics models, the energy-based theories and etc. This branch of research is on small scale and focus mostly on lab work about engineering materials. Another branch is the research on fatigue analysis for large-scale engineering structures such as bridges. Systematic study on fatigue analysis of bridges has been implemented by National Cooperative Highway Research Program like Schilling et al. (1978); Fisher et al. (1980, 1983) and Moses et at. (1986). Among those proposed fatigue models, Miner's rule is still the most popular approach especially for large civil structures. Miner's rule is to use S-N curve (S: stress range, N: number of cycles to

failure) to form a linear damage rule which simplifies the prediction of fatigue life by the assumption of linear accumulation of fatigue damage over time (Rao and Talukdar 2003). As the S-N curve is based on the assumption that the loading is constant while the realistic load is random in nature, the Rainflow Counting Method should be applied to calculate the equivalent stress range and cycles before the application of Miner's rule. In addition to Miner's rule, there are numerical methods which assume the complicated nonlinear damage propagation process, but the steady improvements of the accuracy of those methods over Miner's Rule, a simple linear damage rule, was not observed (Laman 1995).

In most current specifications, a typical fatigue design procedure includes two steps: (1) calculating the stress variation under fatigue design loads; and (2) comparing the calculated stress amplitude and frequencies with the designed one to check if the design is safe. In the first step, the fatigue design load is defined as one design truck per bridge with 15% dynamic allowance in the AASHTO LRFD (AASHTO 2007) for short and medium span bridges yet not applicable for long-span bridges. Existing studies on the fatigue performance of long-span bridges were limited to those only considering wind loads but not traffic loads at the same time (Pourzeynali and Datta 2005; Gu et al. 1999). All these underscore the significance and need for the study in this dissertation.

1.2.3 Application of reliability theory on long-span bridges

Most existing long-span bridges were designed based on deterministic methods (Catbas et al. 2008). However, the loadings (traffic flow, wind, earthquake, wave and etc.) are innately random and the capacity of bridge (mechanical property, material corrosion, structural deformation) is also time-dependent (Torres and Ruiz 2007). Accordingly, it is necessary to use the reliability method to quantify the performance of bridges to consider those uncertainties.

During the last thirty years, there has been numerous reliability research concerning structures. For bridges, a large amount of research effort on reliability-based analyses has been put forth on short and medium bridges (Caprani and O'Brien 2006; Akgul and Frangopol 2004; Akgul and Frangopol 2005a; Akgul and Frangopol 2005b; Czarnecki and Nowak 2008). For the reliability-based analysis of long-span bridges, there were some studies on aerodynamic performance such as flutter instability (Cheng et al. 2005; Pourzeynali and Datta 2002; Ge et al. 2000; Jakobsen and Tanaka 2003) and some studies using the field-monitored stress data to analyze the performance of existing bridges (Frangopol and Imai 2004; Frangopol et al. 2008; Catbas et al. 2008; Imai and Frangopol 2002). However, the study on reliability-based prediction of the performance of long-span bridges considering Bridge/Traffic/Wind interaction has rarely been conducted.

The general reliability analysis include three steps: (1) Defining the limit state function about the concerning capacity of bridges; (2) Determining the basic random variables which are the main parameters on the limit state function such as the mechanical properties of material and the load factor; (3) Computing the reliability index through the reliability method. For the third step, there are several reliability methods (FORM, SORM, RSM, Monte Carlo and etc) to choose from. FORM and SORM are the two basic reliability methods which use first-order and second-order approximation at the minimum distance point to the limit state curve, respectively. Compared to FORM, SORM is usually more accurate for a better approximation of the reliability index, while at the same time with more computational cost. For the large-scale structures such as bridges, FORM has been found to be commonly applied. The Monte Carlo Simulation (MCS) method is a traditional approach which can generate accurate results, but it can be extremely time-consuming (Frangopol 1999). The response surface method (RSM) is a useful and efficient technique to solve the problem of the implicit limit state equation (Frangopol 1999; Bucher and Bourgund 1990). To compute the reliability analysis in an efficient way, the hybrid method which is the combination of the available methods which can take advantage of each method's advantages is

applied to complicated problems on bridge such as bridge/wind interaction (Cheng et al 2005). Based on investigating the existing reliability-based methods, a hybrid method involving the Response Surface Method (RSM) and First Order Reliability Method (FORM) will be applied to study the reliability index of life-time fatigue damage of long-span bridges in my research.

1.3 Summary of Dissertation

This dissertation aims to propose a reasonable reliability-based framework to evaluate lifetime serviceability performance of long-span bridges. More specifically, the objectives of this dissertation include:

(1) Developing a general semi-deterministic Bridge/Traffic/Wind dynamic interaction analysis methodology which can be used by any medium- and long-span bridges with stochastic traffic along with various wind conditions;

(2) Based on the Bridge/Traffic/Wind interaction model, extensive numerical analyses will be conducted to evaluate the safety performance of bridge under normal and extreme conditions;

(3) With the established interaction model, the scenario-based fatigue analytical framework is developed to investigate the fatigue damage of bridge under normal and extreme conditions;

(4) Based on the fatigue model considering coupling effects among bridge, traffic and wind, the reliability-based fatigue assessment model of long-span bridges is proposed to investigate the reliability index of bridge during its service life.

The contents of this dissertation are based on the relevant papers which have already been published, accepted, under review or are to be submitted to referred journals. The dissertation is divided into seven chapters. Chapter 1 herein is to describe the current problem in the related field and introduce the objective and scope of this study.

Chapter 2 explains the application of Cellular Automaton (CA) traffic model on the study of traffic loads on the bridge. Taking a typical long-span cable-stayed bridge as an example, several parameters such as the length of the approaching way, the speed limit, the level of service (free traffic or busy traffic) and the road conditions (normal road condition or incident condition such as the blockage of the partial road) will be taken account of and their influence on the variation of traffic flow like static traffic loads on bridge and average movement speed will be investigated.

Based on the traffic flow model introduced in Chapter 2 and the equivalent dynamic wheel load (EDWL) approach proposed by Chen and Cai (2007), Chapter 3 is to develop the scenario-based Bridge/Traffic/Wind interaction framework under normal road condition. Three typical vehicle types (car, light truck and heavy truck) are studied firstly with different driving speed under breeze and moderate wind speed to quantify the dynamic impact of single vehicle on the bridge. Then, the EDWL approach is performed to compute the collective impacts of traffic flow on bridge. Representative scenarios of different level of road service (free, moderate and busy traffic flow) have been researched to gain more realistic understanding of the structural performance under probabilistic traffic and dynamic interactions.

Chapter 4 is to study the probabilistic dynamic behavior of long-span bridges under extreme events with the help of the analytical framework established in Chapter 3. The extreme events include the partial-block road conditions, the extreme high wind speed and the bumper-to-bumper case (the bridge is fully occupied by vehicles with the maximum capacity) due to evacuation. The baseline model is defined as the normal road condition under breeze. Through comparison of extreme cases with the baseline model, the better understanding of extreme events of long-span bridges from the perspectives of strength and serviceability design is achieved, which may contribute to future design specification about long-span bridges.

Chapter 5 is to develop the scenario-based fatigue analytical framework of bridges considering Bridge/Traffic/Wind interaction. The proposed approach starts with identifying the site-specific wind and traffic conditions for the bridge, including local traffic volume, vehicle combinations, as well as variations in a typical day and a typical week. The cumulative dynamic stress levels and cycles under each representative combination of loadings are calculated and accordingly the fatigue damage is obtained through the input of the stress history to the fatigue analytical model. The parametric study of a typical long-span cable-stayed bridge will give some insights of the fatigue mechanism.

Chapter 6 is about the reliability-based fatigue life analysis of long-span bridges. The limit state function is set as the difference between the accumulated fatigue damage factor of the studied member of bridge and unit according to Miner's rule. By considering uncertainties associated with the basic data of the traffic flow, wind and structural properties of a typical bridge, the reliability analysis can integrate the common scenarios of bridge and considering each scenario's occurrence chance during the bridge's life, which can render a more realistic estimation on the reliability index of fatigue.

Finally, Chapter 7 concludes the whole dissertation and some discussions about future studies will also be reported.

1.4 References

AASHTO (2007). LRFD Bridge Design Specification, 4th ed., Washington, D.C.

Akgul, F., Frangopol, D. M. (2004). "Lifetime performance analysis of existing steel girder bridge superstructures." Journal of Structural Engineering, 12, 1875-1888.

Akgul, F., Frangopol, D. M. (2005a). "Lifetime performance analysis of existing reinforced concrete bridges. I: theory." Journal of Infrastructure Systems, 6, 122-128.

Akgul, F., Frangopol, D. M. (2005b). “Lifetime performance analysis of existing reinforced concrete bridges. II: Application.” Journal of Infrastructure Systems, 6, 129-141.

ASCE (2003). Assessment of performance of vital long-span bridges in the United States, ASCE Sub-committee on performance of Bridges, edited by Richard J. Kratky.

Baker, C. J. (1986). “Simplified analysis of various types of wind-induced road vehicle accidents.” Journal of Wind Engineering and Industrial Aerodynamics, 22(1), 69-85.

Baker, C. J. (1991a). “Ground vehicles in high cross winds Part I: steady aerodynamic forces.” Journal of Fluids and Structures, 5, 69-90.

Baker, C. J. (1991b). “Ground vehicles in high cross winds Part II: unsteady aerodynamic forces.” Journal of Fluids and Structures, 5, 91-111.

Barlovic, R., Santen, L., Schadschneider,A. and Schreckenberg, M. (1998). “Metastable states in cellular automata for traffic flow.” Eur. Phys. J. B, 5, 793-800.

Blejwas, T. E., Feng, C. C., Ayre, R. S. (1979). “Dynamic interaction of moving vehicles and structures.” Journal of Sound and Vibration 67, 513-521.

Bucher, C. G., Bourgund, U. (1990). “A fast and efficient response surface approach for reliability analysis.” Structural Safety, 7(1), 57-66.

Cai, C.S. and Chen, S.R. (2004). “Framework of vehicle-bridge-wind dynamic analysis.” Journal of Wind Engineering & Industrial Aerodynamics, 92 (7-8), 579-607.

Caprani, C.C., O’Brien, E.J. (2006). “Statistical computation for extreme bridge traffic load effects.” Civil-Comp Press, Proceedings of the Eighth International Conference on Computational Structures Technology, Paper 139.

Catbas, F.N., Susoy, M., Frangopol, D.M. (2008). “Structural health monitoring and reliability estimation: Long span truss bridge application with environmental monitoring data.” Engineering Structures, 30, 2347-2359.

Chen, S. R. and Cai, C. S. (2004). “Accident assessment of vehicles on long-span bridges in windy environments.” Journal of Wind Engineering and Industrial Aerodynamics, 92(12), 991-1024.

Chen, S. R., Cai C. S. (2006). “Unified approach to predict the dynamic performance of transportation system considering wind effects.” Structural Engineering and Mechanics, 23(3), 279-292.

Chen, S. R., Cai, C. S. (2007). “Equivalent wheel load approach for slender cable-stayed bridge fatigue assessment under traffic and wind: feasibility study.” Journal of Bridge Engineering, 12(6), 755-764.

Chen, S. R., Cai, C. S., Levitan, M. (2007). “Understand and improve dynamic performance of transportation system- a case study of Luling Bridge.” Engineering Structures, 29, 1043-1051.

Cheng, J., Cai, C. S., Xiao, R. C., Chen, S. R. (2005). “Flutter reliability analysis of suspension bridges.” Journal of Wind Engineering and Industrial Aerodynamics, 93, 757-775.

Cheybani, S., Kertesz, J. and Schreckenberg, M. (2000). “Stochastic boundary conditions in the deterministic Nagel-Schreckenberg traffic model.” Phys.l Rev. E, 63, 016107.

Coleman, S. A. and Baker, C. J. (1990). “High sided road vehicles in cross winds.” Journal of Wind Engineering and Industrial Aerodynamics, 36, 1383-1392.

Cooper, R. K. (1981). “The effect of cross-winds on trains.” Journal of Fluid Mechanics, 103, 170-178.

Czarnecki, A.A., Nowak, A.S. (2008). “Time-variant reliability profiles for steel girder bridges.” Structural Safety, 30, 49-64.

Fisher, J.W., et al. (1980). “Fatigue behavior of full-scale welded bridge attachments.” NCHRP Report 227, National Academy Press, Washington DC.

Fisher, J.W., et al. (1983). “Steel bridge members under variable amplitude long life fatigue loading.” NCHRP Report 267, National Academy Press, Washington DC.

Frangopol, D. M. (1999). Bridge safety and reliability, ASCE.

Frangopol, D. M., Imai, K. (2004). “Reliability of long span bridges based on design experience with the Honshu-Shikoku bridges.” Journal of Constructional Steel Research, 60, 373-392.

Frangopol, D., Strauss, M. A., Kim, S.Y. (2008). “Use of monitoring extreme data for the performance prediction of structures: general approach.” Engineering Structures, 30, 3644-3653.

Ge, Y. J., Xiang, H. F., Tanaka, H. (2000). “Application of a reliability analysis model to bridge flutter under extreme winds.” Journal of Wind Engineering and Industrial Aerodynamics, 86, 155-167.

Gu, M., Xu, Y. L., Chen, L. Z., Xiang, H. F. (1999). “Fatigue life estimation of steel girder of Yangpu cable-stayed Bridge due to buffeting.” Journal of Wind Engineering and Industrial Aerodynamics, 80, 383-400.

Guo, W. H., Xu, Y. L. (2001). “Fully computerized approach to study cable-stayed bridge-vehicle interaction.” Journal of Sound and Vibration, 248(4), 745-761.

Guo, W. H. and Xu, Y. L. (2006). “Safety analysis of moving road vehicles on a long bridge under crosswind.” Journal of Engineering Mechanics, 132 (4), 438-446.

Imai, K., Frangopol, D. M. (2002). “System reliability of suspension bridges.” Structural Safety, 24, 219-259.

Jakobsen, J. B., Tanaka, H. (2003). “Modeling uncertainties in prediction of aeroelastic bridge behaviour.” Journal of Wind Engineering and Industrial Aerodynamics, 91, 1485-1498.

Kim, C. W., Kawatani, M., Kim, K. B. (2005). “Three-dimensional dynamic analysis for bridge-vehicle interaction with roadway roughness.” Computers and Structures, 83, 1627-1645.

Laman, J. A. (1995). “Fatigue load models for girder bridges.” Dissertation, University of Michigan, Ann Arbor (MI).

Li, Z. X., Chan, T. H. T. (2006). “Fatigue criteria for integrity assessment of long-span steel bridge with health monitoring.” Theoretical and applied fracture mechanics, 46, 114-127.

Moses, F., Schilling, C.G., et al. (1986). Fatigue evaluation procedures for steel bridges, NCHRP report 299, National Academy Press, Washington D.C.

Nagel, K., Schreckenberg, M. (1992). “A cellular automaton model for freeway traffic.” J. Phys. I France, 2(12), 2221-2229.

Olsson, M. (1985). “Finite element model co-ordinate analysis of structures subjected to moving loads.” Journal of Sound and Vibration, 99, 1-12.

Pines, D., Aktan, A.E. (2002). “Status of structural health monitoring of long-span bridges in the United States.” Progress in Structural Engineering and Materials, 4(4), 372-380.

Pourzeynali, S., Datta, T. K. (2002). “Reliability analysis of suspension bridges against flutter.” Journal of Sound and Vibration, 254(1), 143-162.

Pourzeynali, S. and Datta, T.K. (2005). “Reliability analysis of suspension bridges against fatigue failure from the gusting of wind.” Journal of Bridge Engineering, 10(3), 262-271.

Rao, V. G., Talukdar, S. (2003). “Prediction of fatigue life of a continuous bridge girder based on vehicle induced stress history.” Shock and Vibration, 10, 325-338.

Sadiku, S., Leipholz, H. H. E. (1987). “On the dynamics of elastic systems with moving concentrated masses.” Ingenieur-Archiv, 57, 223–242.

Schadschneider, A. (2006). “Cellular automata models of highway traffic.” Physica A, 372, 142–150.

Schilling, C.G., et al., (1978). “Fatigue of welded steel bridge members under variable-amplitude loadings.” NCHRP Report 188, National Academy Press, Washington D.C.

Stephens, R. I., Fatemi, A., Stephens, R. R., Fuchs, H. O. (2001). Metal fatigue in engineering, 2nd edition, John Wiley & Sons, Inc.

Torres, M. A., Ruiz, S. E. (2007). “Structural reliability evaluation considering capacity degradation over time.” Engineering Structures, 29, 2183-2192.

Traffic-Information-System autobahn. NRW, <http://www.autobahn.nrw.de./>, accessed on April 4th 2008.

TRANSIMS Travelogues, Transportation analysis and simulation system, Los Alamos National Laboratory, Los Alamos, <http://www-transims.tsasa.lanl.gov/travel.shtml>, lastly accessed on April 30th 2008.

Virlogeux, M. (1992). “Wind design and analysis for the Normandy Bridge.” In: Larson A, editor. Aerodynamics of large bridges. Rotterdam, The Netherlands: Balkema, 183-216.

White,K. R., Minor, J. and Derucher, K. N. (1992). Bridge maintenance inspection and evaluation, 2nd edition. Marcel Dekker, Inc.

Xu, Y. L., Guo, W. H. (2003). “Dynamic analysis of coupled road vehicle and cable-stayed bridge systems under turbulent wind.” Engineering Mechanics, 25, 473-486.

Xu, Y. L., Liu, T. T., Zhang, W. S. (2009). “Buffeting-induced fatigue damage assessment of a long suspension bridge.” International Journal of Fatigue, 31, 575-586.

CHAPTER 2: PROBABILISTIC TRAFFIC FLOW SIMULATION FOR BRIDGE

2.1 Introduction

Long-span bridges are usually the key linkages of the transportation network in normal conditions as well as critical evacuation paths in emergency conditions. As critical infrastructures experiencing frequent and complex interactions with passing traffic, bridges exhibit unique characteristics which distinguish themselves from traditional civil structures (e.g. buildings). A long-span bridge experiences time-dependent live loads from traffic, which may vary significantly due to the stochastic nature of the traffic flow and its interactions with the bridge, approaching roadways and various incidents. The rational quantification of the traffic load in both normal and extreme conditions becomes very crucial in structural analysis and design of these critical bridges.

Traffic loads have been traditionally evaluated with the data from weight-in-motion (WIM) or traffic spectrum collected from the site (Oh et al. 2007; Broquet et al. 2004; Mullard and Stewart 2009). Neither of these approaches, however, provides instantaneous information of individual vehicles such as velocity and position at any time, which is essential to the assessment of dynamic loads for long-span bridges. Due to the historical gap existing between traditional structural and traffic engineering, little work has been conducted on simulating the bridge, roadways and traffic flow in a systematic context. During the past decades, most existent studies about bridge's dynamic performance under traffic have considered only one or several vehicles distributed in an assumed (usually uniform) pattern on long-span bridges with a focus on demonstrating the methodology (Xu and Guo 2003; Cai and Chen 2004; Chen et al. 2007; Chen

and Cai 2007). Some researchers adopted white noise fields (Ditlevsen 1994; Ditlevsen and Madsen 1995), Poisson distribution (Chen and Feng 2006) and Monte Carlo approach (Nowak 1993, Moses 2001, O'Connor and Obrien 2005) to simulate the traffic flow to obtain the characteristic load effects primarily on short- and medium-span bridges. In those studies, realistic traffic rules or the incidental conditions were not considered. Besides, the detailed information (e.g. instantaneous velocity and location) in the scale of individual vehicles was not available.

Traffic flow simulation techniques have gained rapid development in the field of traffic engineering during the past decades, which provides some useful tool to model traffic loads. Generally speaking, traffic flow can be simulated with three scales: macroscopic, mesoscopic and microscopic (TRB 2000). The former two scales are based on continuous time and space, which are suitable for traffic studies focusing on physical characteristics of the whole traffic flow in a large scale (e.g. meta-stable state, the relationship between traffic occupancy and flow, traffic occupancy and average velocity) (Nagel et al. 1998, Barlovic et al. 1998, Cheybani et al. 2000). Microscopic scale traffic simulation is, however, based on discrete time and space which can provide detailed time-variant information of individual vehicles.

In this chapter, a general framework to model the stochastic traffic load for a long-span bridge will be developed based on the microscopic traffic flow simulation. The Cellular Automaton (CA) traffic flow simulation technique will be adopted to develop the analytical basis of the framework. Based on the traffic flow simulation results, the live load on the bridge from the stochastic traffic will be also studied with a focus on the static component. Some discussions about the static traffic load as compared to the current AASHTO LRFD traffic loads will be made. Finally, parametric studies of major variables, such as the length of the connecting roadways, the speed limit, and the vehicle combination, will be conducted.

2.2 Theoretical Formulations

2.2.1 Background of Cellular Automaton (CA) traffic flow simulation

Cellular Automaton (CA), a microscopic scale traffic flow simulation model, can generate probabilistic traffic information by simulating individual vehicle's behavior. The CA traffic model has been widely used in the transportation field since it was firstly proposed by Nagel and Schreckenberg (1992). After the model was initially introduced, various studies have been conducted on improving the models for more realistic traffic flow simulations (Benjamin et al. 1996; Barlovic et al. 1998; Chowdhury et al. 2000). The CA simulation technique has been adopted in some actual transportation management around the world. For example, TRANSIMS, a commercial software developed by Las Alamos National Laboratory, is based on the concept of the CA model (TRANSIMS Travelogue 2008). In Germany, the CA traffic model is used for online traffic simulation in North Rhein Westphalia (Schadschneider 2006). The CA model is able to provide detailed instantaneous information of each vehicle through replicating major traffic phenomena on highways. Thus it becomes an ideal technology to be integrated into the advanced bridge analysis considering live load in a more accurate manner. In the following sections, the theoretical basis of the proposed simulation framework for long-span bridges with the CA traffic simulation technology will be briefly introduced.

2.2.2 Rules of CA traffic flow

The CA traffic model is based on the assumption that both time and space are discrete and each lane is divided into cells with an equal length as shown in Fig. 2.1 (a). Each cell can be empty or occupied by at most one vehicle at a time. The velocity of a vehicle can be decided by the number of cells a vehicle can move in one time step. The maximum velocity a vehicle can achieve is defined based on the actual speed limit on the road. At each time step, a vehicle moves, accelerates, decelerates or changes lanes based on some predefined rules. The rules are typically

established according to the actual traffic rules with some reasonable assumptions of the driver behavior (Nagel and Schreckenberg 1992). With all the predefined rules which are illustrated as follows, the CA traffic models can thus be used for both *normal* and *incidental* conditions.

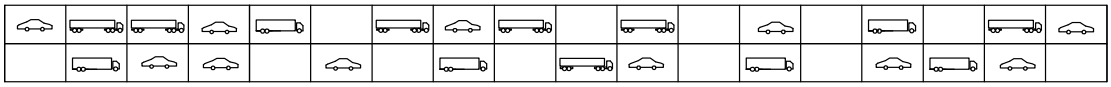

a. CA traffic model

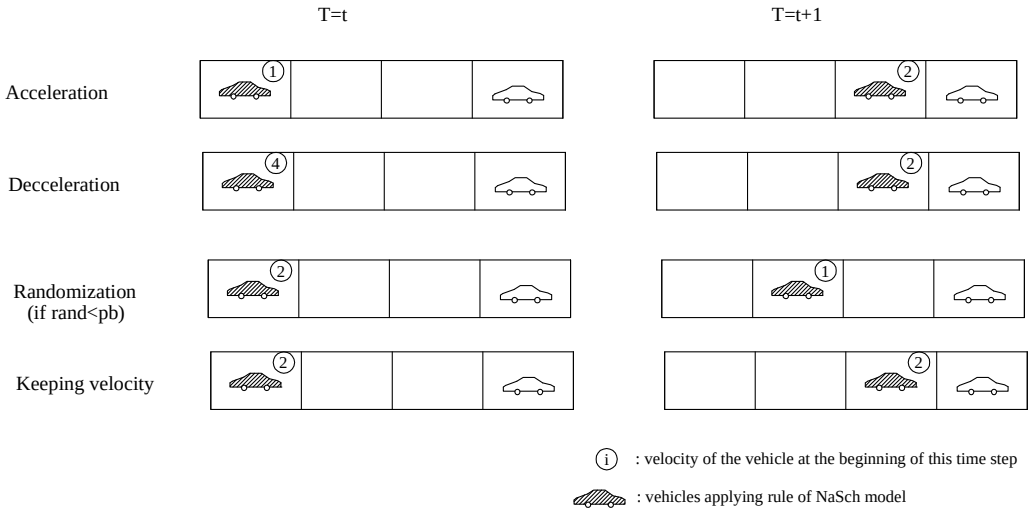

b. NaSch Model rules ($v_{\max} = 5$)

Fig. 2.1 CA-based traffic model

The rules of a typical CA traffic model include: 1) rules for vehicles moving forward on the original lane, i.e. single-lane CA model; and 2) rules for changing lane, i.e. multiple-lane CA model.

The rules of the single-lane CA model (Fig. 2.1(b)) include (Nagel and Schreckenberg 1992):
(1) Acceleration: *if the velocity of Vehicle v is smaller than* v_{max} *(maximum velocity a vehicle is allowed to achieve) and if the distance to the next vehicle ahead is larger than v+1, the velocity is advanced by one*; (2) Deceleration: *if the vehicle at site i finds the next vehicle at site i + j with* $j \leq$

v, it reduces its velocity to j−1; (3) Randomization: *with the probability of pb, the velocity of each vehicle is decreased by one if the velocity is greater than zero;* (4) Vehicle motion: *each vehicle advances v sites.*

The conditions for lane changing (Fig. 2.2 (a)) are shown as follows (Rickert et al. 1996; Li et al., 2006):

(1) The distance (described as "gap") between one vehicle and the vehicle right ahead on the same lane is less than v+1, i.e. the vehicle cannot accelerate in the current lane; (2) The distance (described as "gap_o") between one vehicle and the vehicle ahead on the target lane (i.e. the neighboring lane) is more than v+1, i.e. the vehicle can accelerate if it changes lane; (3) The distance (described as "$gap_{o,\,back}$") between the vehicle and the behind vehicle on the target lane is more than v_{max}, i.e. the vehicle will not crash with the vehicle on the target lane; (4) With the probability of *pch*, a vehicle changes lane if all the three above conditions are satisfied.

To fulfill the lane-changing simulation, the location and the velocity of Vehicle *i* will be updated through two sub-steps: 1) Vehicle *i* moves to the target lane transversely without moving forward; and 2) Vehicle *i* moves forward obeying the single-lane rule as introduced above after moving into the target lane.

When there is ongoing construction or a serious accident happening on the bridge or on the approaching roadway, one lane of the bridge or one portion of a lane of the approaching roadway may be closed for a certain period of time. As a result, the bridge and the approaching roadways may have different numbers of available lanes. Fig. 2.2(b) shows a general case that a portion of the highway (either bridge or approaching roadway) has fewer lanes than the remaining portions. As shown in Fig. 2.2(b), the head vehicle on Lane 1 can simply regard Lane 3 as the extension of lane 1, so vehicles on Lane 1 do not need to consider the variation of available lanes. But the head

vehicle on Lane 2 will be affected by the difference of the lane numbers. The head vehicle intending to enter Lane 3 at next time step should obey the corresponding rules. More details about the traffic rules of these incidental conditions can be found in Refs (Xiao et al. 2005; Wu and Chen 2010).

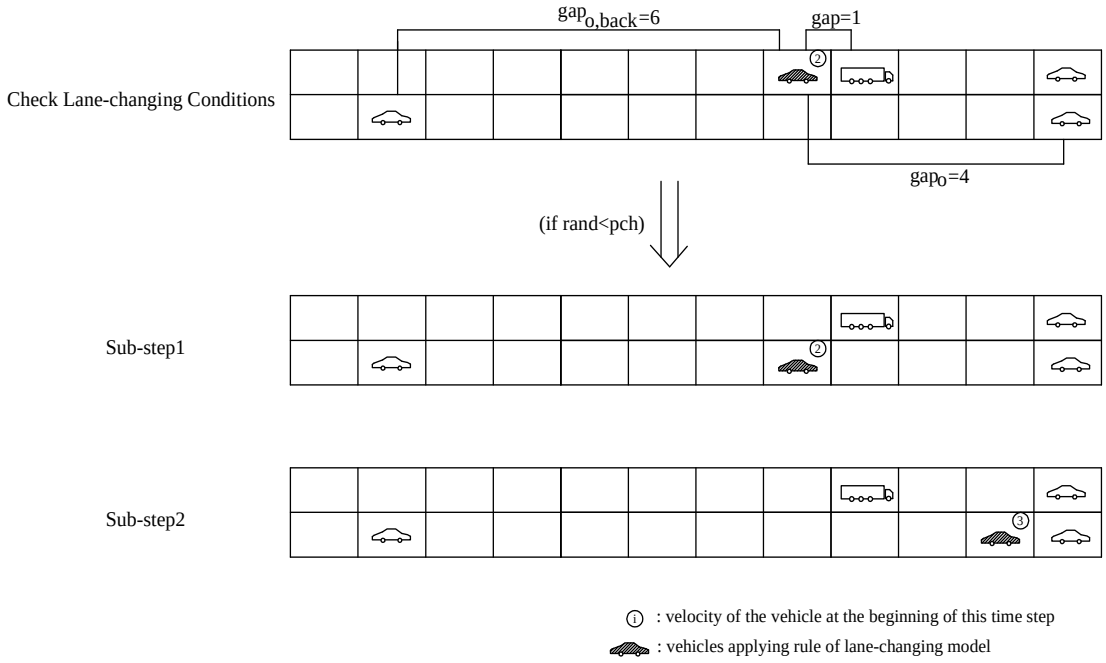

a. Lane-changing rules ($v_{\max} = 5$)

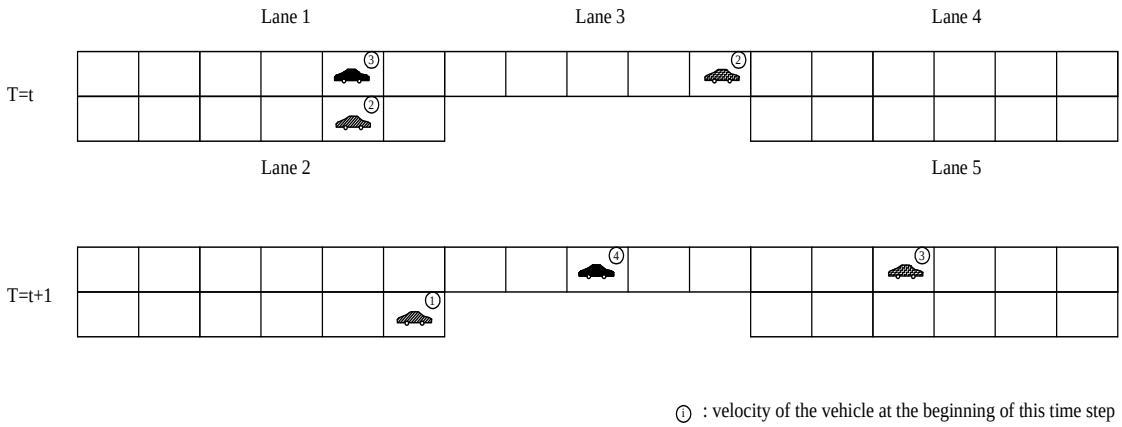

b. Road bottleneck situation ($v_{\max} = 5$)

Fig. 2.2 Lane-changing and road bottleneck rules

2.3 Traffic Load Modeling of Long-Span Bridge

2.3.1 A long-span bridge infrastructure system (BIS)

As interrelated components of a whole transportation network, the actual traffic flow through a long-span bridge is also affected by the traffic on the connecting roadways. Therefore, a bridge infrastructure system (BIS), consisting of a long-span bridge and two stretches of approaching roadways, is to be studied rather than the bridge alone. The "roadway-bridge-roadway" setup makes it possible to more realistically capture the major characteristics of the traffic flow. For typical interstate systems in the US, four-lane bridges (i.e. two lanes in each direction) and two-lane bridges (i.e. one direction) are the most popular types. Since the traffic flow on both directions of a bridge is usually independent, the traffic flow simulations on these two types of bridge are essentially the same.

To facilitate the following presentation, a typical four-lane long-span bridge, with approaching roadways connected on both sides, will be chosen as the basic scenario for the study (Fig. 2.3). All the lanes on the bridge and the connecting roadways share the same width on both driving directions (from east to west and from west to east) and each lane is divided into equally-spaced cells. In the present study, the total length of this four-lane prototype bridge (L_B) is 840m and the approaching roadway has the length of 1,005m (L_R=1,005m) at the each end of the bridge. The length of the approaching roadway, too short or too long, will affect the accuracy of the results or the simulation efficiency, respectively. The length of the approaching roadway in the present study was decided based on some preliminary analysis and the validity of the length of the approaching roadway adopted will be discussed in the following parametric study.

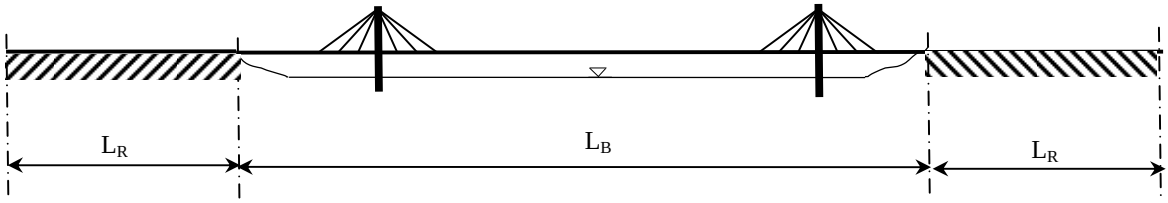

Fig. 2.3 Bridge infrastructure system

The length of each cell is set as 7.5m, which is the typical distance between the centers of two vehicles when the road is in a complete congestion (Nagel and Schreckenberg 1992). The speed limit V_{max} is assumed to be 113km/h (70mph), which is the typical speed limit on interstate highways in the US. So v_{max} in the CA model can be computed accordingly:

$$v_{\max} = \frac{V_{\max}}{L_c} = \frac{113(\text{km/h})}{3600(\text{s/h})} \times \frac{1000(\text{m/km})}{7.5(\text{m/cell})} = 4.19(\text{cell/s}) \approx 4(\text{cell/s}) \tag{2.1}$$

where v_{max} is the maximum vehicle velocity in the unit of cell/s; V_{max} denotes maximum absolute velocity of vehicles (km/h), which is assumed to be the same as the speed limit in the present study; L_c is the size of each cell.

In the CA-based traffic flow simulation, the initial velocities of all the vehicles are typically set to be zero. The CA traffic simulation rules will decide the velocity of each individual vehicle according to the maximum vehicle velocity adaptively. The observation of the traffic flow will start after t_0=10L (L is the number of all cells in one lane, here L=134×2+112=380) when the traffic flow is typically believed to become steady (Nagel and Schreckenberg 1992). Thus, the traffic flow results starting from 3,800s in this study will be presented in the following sections.

Two boundary conditions are often used in the CA simulations. One is the periodic boundary condition which regards the road as a ring. Vehicles move out of one end and come in from

another end in the next time step. The other one is the open boundary condition, which sets two parameters α and β as the probability of vehicles moving in and moving out the simulation boundaries, respectively (Cheybanin et al. 2000). In this study, with the assumption that the traffic occupancy does not fluctuate significantly during the period of time for the simulation, the periodic boundary condition is used. Therefore, the traffic occupancy in the whole system keeps constant for each simulation. Transportation Research Board classifies the Level of Service (LOS) from A to F based on the range of the traffic occupancy in the Highway Capacity Manual (TRB 2000). Three occupancies (ρ) are considered in the present study: 1) "free flow", ρ =0.07 corresponding to level B (9veh/km/lane), 2) "moderate flow", ρ =0.15 corresponding to level D (20veh/km/lane) and 3) "busy flow", ρ =0.24 corresponding to level F (32veh/km/lane). Various vehicles on highways are grouped into three categories of vehicles: v1- heavy multi-axle truck; v2- light truck and bus; v3- light passenger car. The proportions of vehicles in category 1, 2 and 3 among all the vehicles are assumed to be 0.2, 0.3 and 0.5, respectively. All the parameters of the CA traffic model are summarized in Table 2.1. Due to the independent nature of the traffic flow on two driving directions on the bridge, only the results of the two lanes from west to east will be given in the following sections. The traffic flow simulation for both "normal condition" and the "incidental conditions" will be introduced in the following, respectively.

Table 2.1 Parameters of CA traffic model for "roadway-bridge-roadway" system

Parameters	Value	Definition
Lc	7.5m	Length of each cell
dt	1s	The period of each time step
L-road	134(1005m)	Number of cells (absolute length) of one lane of approaching roadway in one end
L-bridge	112(840m)	Number of cells (absolute length) of one lane of bridge
ρ	0.07,0.24	Traffic occupancy of the system(occupied cells/ all cells)
v_{type}	{0.2 0.3 0.5}	Percentage of three types of vehicles(v1, v2 and v3)
v_{max}	4	The maximum cells a vehicle can pass per second
pb	0.5	The probability of braking
pch	0.8	The probability of changing lane

2.3.2 Traffic flow simulation-“normal condition”

Different from the traditional understanding of “normal” and “incidental” traffic, the normal traffic condition in the present study refers to the situation that the bridge and the approaching roadways have the same number of available lanes. For the “normal condition”, both the vehicle-following and lane-changing rules as introduced in the section of “traffic rules” will be applied. The same traffic rules can simulate various traffic conditions, including congestions, as long as the available lanes of the bridge and the approaching roadways are the same. So some unusual traffic events, such as recurrent congestion during rush hours or non-recurrent congestion due to some incidents, are still attributed to the “normal condition” when the available lanes do not change.

The typical two-lane traffic simulation (in one direction) of a “roadway-bridge-roadway” system under the “normal condition” is conducted and the results are shown in Fig. 2.4. As shown in Fig. 2.4, the time versus space information of the simulated traffic on the outer lane (i.e. far from the median barrier) is given. The *x* axis shows the physical location of each vehicle on the BIS (“roadway-bridge-roadway”). The *y* axis shows the time range after 3,800 seconds of simulation have elapsed. At any time instant on the *y* axis, the information of the physical distribution of each vehicle along the spatial simulation region (*x* axis) can be found by drawing a line horizontally. Similarly, at any spatial location on the *x* axis, the time-variant information of vehicles at one particular location can also be retrieved by drawing a line vertically. For the high traffic occupancy (ρ =0.24), the congestion is formed which is evidenced by the black belts in Fig. 2.4 (a). The congestion results are found to be consistent with the phenomenon observed from the real traffic flow photo collected on an American freeway (Fig. 2.4 (b)) (Treiterer et al. 1965).

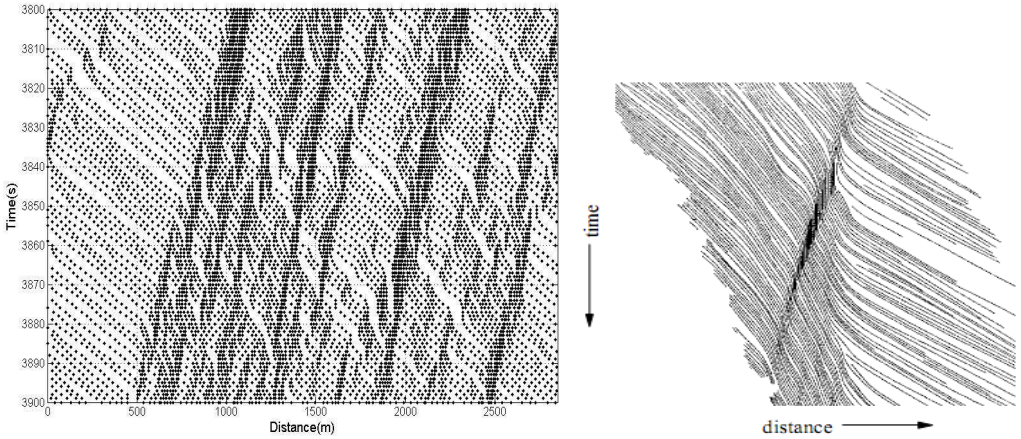

a) CA result

b) Video from an American Freeway (Treiterer et al. 1965)

Fig. 2.4 Comparison of simulated and monitored traffic flow (ρ =0.24)

In addition to the information such as vehicle type and location of each vehicle at any time, the simulated microscopic traffic flow also includes the information of the instantaneous driving velocity of each vehicle at any time. The driving velocities of all the vehicles remaining on both inner and outer lanes of the bridge are statistically analyzed for each time instant, respectively. Due to the probabilistic nature of the traffic flow through the bridge, the mean value of the velocities of all vehicles on the bridge at one moment is different from that at the next moment. The mean velocities versus time in the "free flow" and "busy flow" conditions are plotted in Fig. 2.5a and Fig. 2.5b, respectively. A statistical analysis of the mean velocity curves in Fig. 2.5a shows that the mean values of the two curves are 93.7 km/h and 93.9 km/h and the standard deviations are 4.8 km/h and 4.3 km/h for the inner and outer lanes, respectively for the "free flow" condition. When the traffic occupancy is high (i.e. "busy flow"), the mean values of the two curves in Fig. 2.5b are 55.8 km/h and 56.1 km/h and the standard deviations are 7.1 km/h and 7.4 km/h for the inner and outer lanes, respectively. It is found that in the "normal condition", traffic flow characteristics between the inner and outer lanes are pretty similar under both "free

flow" and "busy flow" conditions. When the traffic occupancy gets higher, slightly more difference between the results on the two lanes were observed.

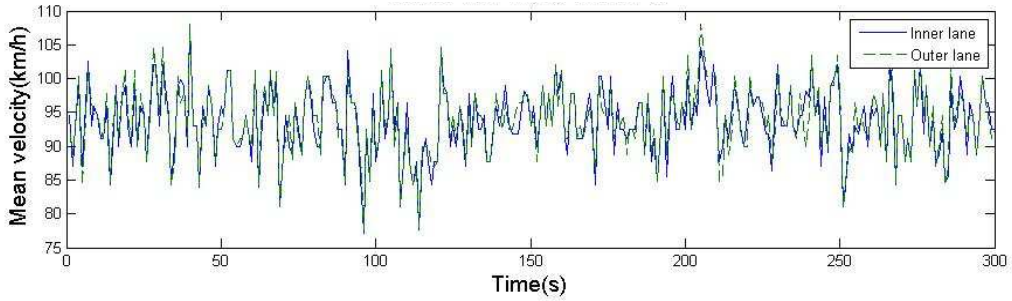

a. Free flow (ρ =0.07)

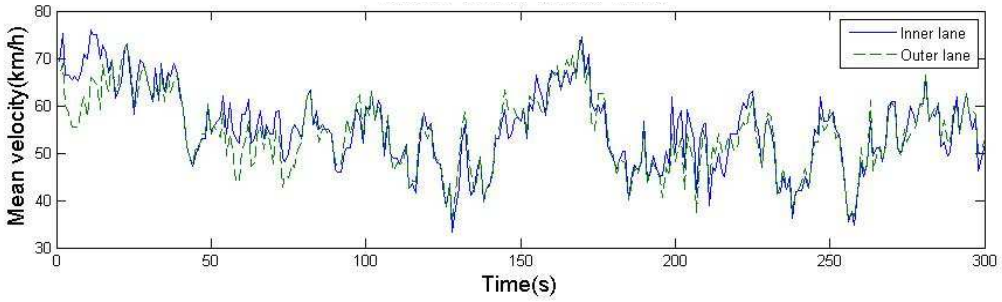

b. Busy flow (ρ =0.24)

Fig. 2.5 Time history of mean velocity for normal condition

Compared to those under the low traffic occupancy ("free flow"), the mean values of the curves of mean velocity vs. time (Fig. 2.5b) under the high traffic occupancy ("busy flow") decrease by 40% and the standard deviations increase by 50%, respectively. When the traffic occupancy is low (Fig. 2.5(a)), sparsely distributed vehicles are able to achieve the optimal velocities through changing lanes with fewer chances to be forced to reduce velocities than congested vehicles. When the traffic occupancy is high (i.e. vehicles are densely populated), the empty space on the two lanes is not as much as that with sparse traffic, which allows for moving forward and lane changing easily. As a result, larger fluctuations of vehicle velocities over time are observed when the traffic occupancy is high. It is known that large fluctuations of the vehicle velocities can cause more variations of the dynamic impacts on the bridge from the traffic, higher risks of rear-end crashes and more chances of accelerating and braking operations (TRB 2000; Chen and Cai

2007). Besides, existing studies also suggested that higher driving velocity will cause more significant dynamic impacts on the bridge from the vehicles (Chen and Wu 2010). So for a critical long-span bridge which often experiences busy traffic, the results confirm that a realistic simulation of traffic flow with appropriate traffic rules is necessary in order to quantify time-dependent live loads on long-span bridges.

2.3.3 Traffic flow simulation-"incidental conditions"

In addition to the normal traffic condition (i.e. bridge and roadway share the same number of available lanes), some incidents, such as work zones or traffic accidents on the bridge or on the approaching roadways, may cause some portion of the lanes, either on the bridge or on the roadways, being closed to traffic. Therefore the "incidental conditions" in the present study refer to the situations that the numbers of the available lanes on the bridge and the approaching roadways are different. Depending on whether the lane on the bridge or the roadway is blocked, the incidents are called "bridge block" and "road block", respectively.

The "bridge block" condition may be formed as a result of several possible scenarios, such as a renovation project on the bridge or a serious accident happening on the bridge. As a result, the bridge may become a "bottleneck" due to the difference between the numbers of available lanes on the bridge and approaching roadways. On the other hand, the "road block" condition may represent two typical scenarios: there is a work zone or an accident happening on the connecting roadway either downstream or upstream of the bridge. Based on the preliminary analysis, it is found that the situation that one lane of approaching roadways upstream of the bridge is closed is not critical to the traffic loads on the bridge. So in the following section, it is only assumed that one lane of the roadway downstream of the bridge (from west to east) is closed for the "road block" condition. For the incidental conditions, the corresponding simulation rules for different

available lanes as introduced in the previous section will be applied in addition to those used in the "normal condition".

The mean velocities for both incidents (i.e. "bridge block" and "road block") under two different occupancies are shown in Fig. 2.6 (a-b). It is found that the mean value of the mean velocity curves for the "bridge block" condition is around 75.1 km/h (ρ =0.07) and 24.9 km/h (ρ =0.24), which are significantly lower than 93.7 km/h (ρ =0.07) and 55.8 km/h (ρ =0.24) in the "normal condition" (Fig. 2.5), respectively. The standard deviations of the mean velocity curves under the low and high traffic occupancies are 7.7 km/h and 7.0 km/h, respectively. It is found that the standard deviation of the mean velocities in the "bridge block" condition is much higher than that in the "normal condition" when the traffic occupancy is low. In fact, the fluctuation of mean velocities of the traffic flow (as indicated by the standard deviation) under the low traffic occupancy is larger than that under the high traffic occupancy, which suggests more fluctuations of the dynamic impacts from vehicles.

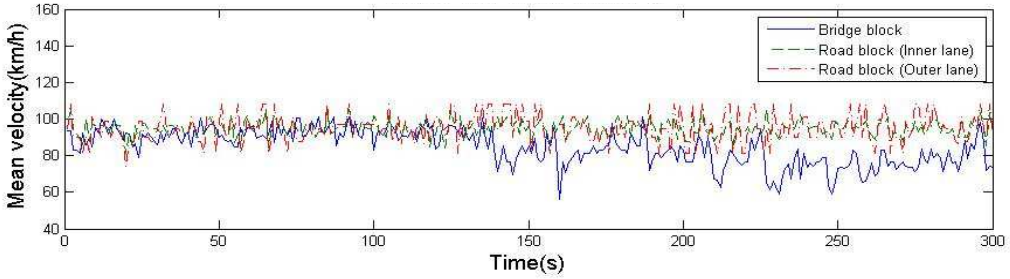

a. Free flow (ρ =0.07)

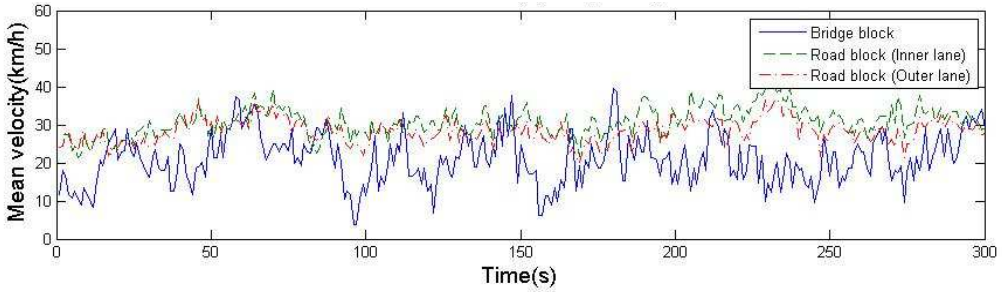

b. Busy flow (ρ =0.24)

Fig. 2.6 Mean velocity of traffic on bridge versus time for incidental conditions

For the “free flow” condition (ρ =0.07) (Fig. 2.6a), the mean values of the mean velocity curves for the “road block” condition are 94.5 km/h and 94.1 km/h and the standard deviations of the curves are 4.5 km/h and 4.9 km/h for both inner and outer lanes, respectively. Compared to the “bridge block” condition, the mean values of the mean velocity curves of the “road block” condition under the low traffic occupancy are much higher, which are close to those in the “normal condition”. The high mean velocities suggest high mobility and relatively larger dynamic impacts of vehicles on the bridge in the “road block” condition when the traffic occupancy is low. When the traffic occupancy is low, the standard deviations of the vehicle velocities in the “road block” condition on both lanes are close to those in the “normal condition”, which are much lower than those in the “bridge block” condition.

For the “busy flow” with the higher traffic occupancy (ρ =0.24) (Fig. 2.6b), the mean values of the mean velocity curves for the “road block” condition are 35.2 km/h and 29.1 km/h and the standard deviations of the curves are 4.9 km/h and 3.7 km/h for both the inner and outer lanes, respectively. When the traffic occupancy gets higher, the mean velocities of the vehicles on the bridge for the “road block” condition significantly decrease, but are still slightly higher than those in the “bridge block” condition. However, the standard deviations are much smaller than those for both the “bridge block” and the “normal condition”. The high standard deviation of the velocities of the vehicles on the bridge suggests high velocity fluctuations. As discussed earlier, the high velocity fluctuations may cause more variations of the dynamic impacts of the traffic load and more chances of accelerating and braking operations on the bridge. The observations from both Figs. 2.6(a-b) suggest that the “road block” condition has less impact on the traffic flow in terms of velocity fluctuations than the “bridge block” condition.

2.3.4 Traffic loads on the bridge

From the perspective of a bridge engineer, the actual traffic loads applying on the bridge is of the most concern. Based on the stochastic traffic flow simulated for normal and incidental conditions, the cumulative static loads from all the vehicles on the bridge for the (a) normal, (b) "bridge block", and (c) "road block" conditions can be calculated for any instant. The time-history results for the three traffic conditions are shown in Figs. 2.7 (a-c), respectively. The *x*-axis shows the time period starting after 3,800 seconds have elapsed. It can be found that the total static load (weight) from the traffic on the bridge generally has some variations over time due to the stochastic nature of the traffic flow. Among the three different traffic conditions, the "bridge block" condition (Fig. 2.7 (b)) is found to cause the minimum mean static traffic loads on the bridge, while the "road block" condition causes the largest mean static traffic loads.

Comparatively, the total static traffic load has larger variations when the traffic occupancy gets higher in the normal and "bridge block" conditions. For the "road block" condition, the total static traffic load has the least fluctuations over time, which is likely because of the limited mobility due to serious congestions (Wu and Chen 2010). Due to the significantly lower static loads for the "bridge block" condition, the "bridge block" condition will not be further discussed in this chapter.

The statistical results on the time histories of the static traffic load can provide useful information to evaluate the actual traffic loads. Before rational statistics of any time-history results are conducted, the required time duration in order to get the converged statistical result has to be studied. Therefore, the convergence analysis is conducted on the time history of the total static load of the traffic. The mean value of the total static load from the beginning up to the current instant was calculated for different traffic conditions and occupancies. Fig. 2.8 shows the mean values versus time for both the normal and "road block" conditions with different traffic

occupancies. It is found from the results that 300-second simulation currently used can lead to stable results. The results also suggest that the statistical results of the time history of the static load are not very sensitive to the length of the simulation time period.

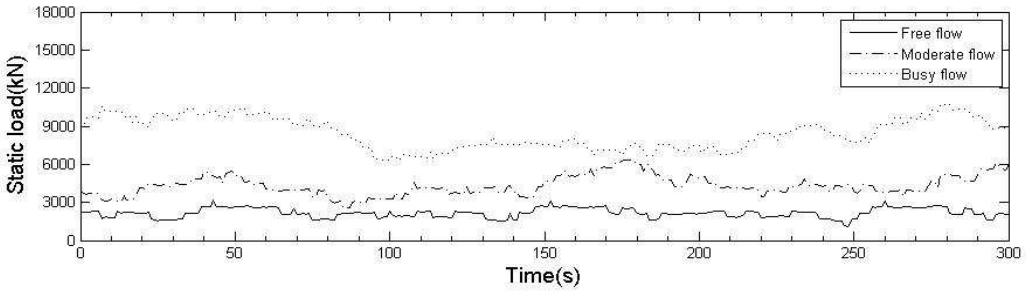

a. Normal condition

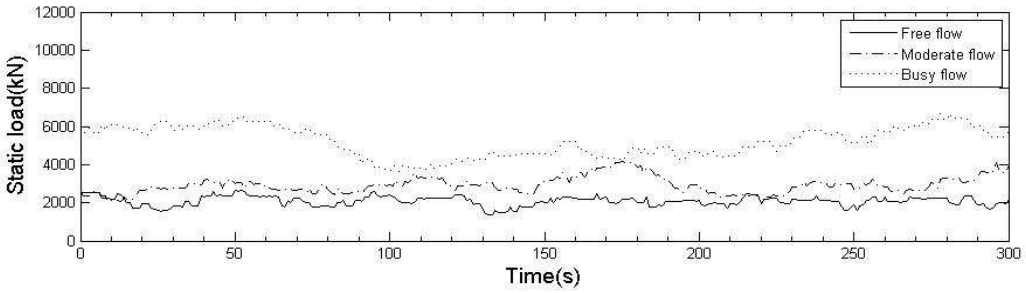

b. Bridge block

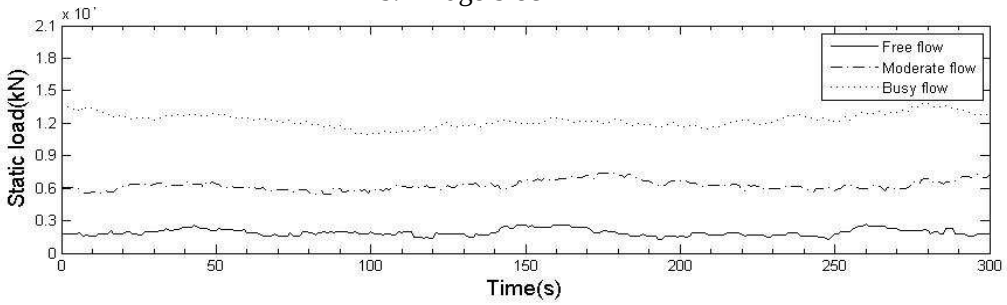

c. Road block

Fig. 2.7 Time history of static load

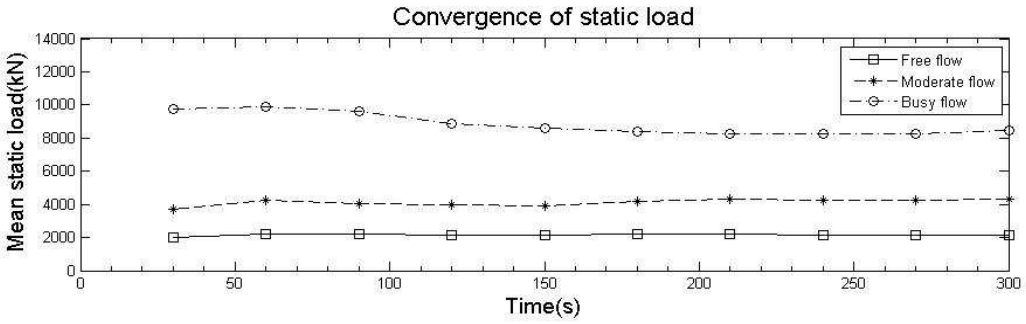

a. Normal case

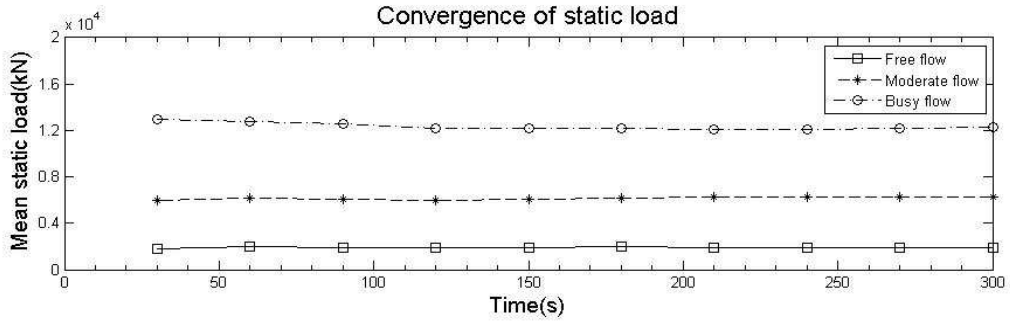

b. Road block

Fig. 2.8 Convergence of mean static load vs. time

AASHTO LRFD specification uses HL-93 live load for both short and medium-span bridges. In AASHTO LRFD specification (AASHTO 2007), the HL-93 live load includes the uniform lane load 0.64 kip/ft (9.3 kN/m) and the HS-20 design truck load or the tandem load for most limit states. Since the design truck load is more common to control the design, the following discussion will only consider the truck loads. For the purpose of a preliminary comparison, the static traffic load derived from the present study is compared with the equivalent HL-93 live loads. The lane load will be applied as the uniformly distributed load all through the bridge. The number of the equivalent design trucks can be estimated which, along with the lane load, will lead to the same total static load as that obtained from the stochastic traffic flow simulation in the present study. It is found that the lane load alone has provided sufficient static load for the “free flow” and “moderate flow” situations. When the traffic occupancy is high (“busy flow”), there will be

equivalently 2-3 design trucks in each direction along with the lane load which can generate the same total static load as the simulated traffic load on the bridge.

2.4 Parametric Studies

Parametric studies are conducted to further investigate the sensitivity of several parameters on the simulation results. Three parameters include: length of approaching roadway, driving speed limit and vehicle combination.

2.4.1 Approaching roadway length

For the traffic simulation of the "roadway-bridge-roadway" system, the approaching roadways are actually the extended boundaries of the bridge within the system. Taking the long-span bridge analyzed in the previous section as the example, the parametric studies are carried out with various lengths of approaching roadways (L_R). Fig. 2.9 shows mean velocities of the vehicles on the BIS with different lengths of approaching roadways. The dimensionless length ratio is defined as the ratio of the approaching roadway length (L_R) to the length of the bridge (L_B) (Fig. 2.3). Fig. 2.9 suggests that L_R/L_B does not have significant impact on the mean velocities of the vehicles on the bridge for the "free flow" condition. For higher traffic occupancies ("moderate flow" and "busy flow"), the fluctuations of the mean velocities of the traffic on the bridge over different approaching roadway lengths become larger as compared to those under the low traffic occupancy ("free flow"). The results suggest that when the traffic occupancy is low, the details of the approaching roadways (e.g. length) are not very critical to the results of the simulated traffic on the bridge. When the traffic occupancy is high, however, an accurate description of the actual boundary conditions of the bridge (i.e. the approaching roadways) is critical in order to accurately simulate the traffic flow. As discussed earlier, it is known that larger variations of the velocities usually will cause more variations of the dynamic impacts of the traffic load on the bridge.

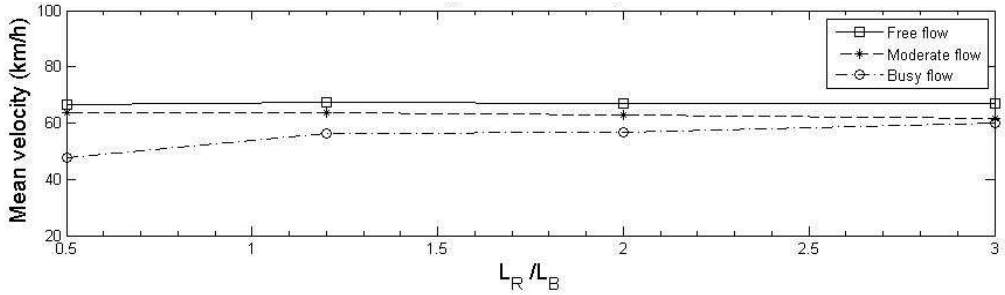

a. V_{max}=81 km/h

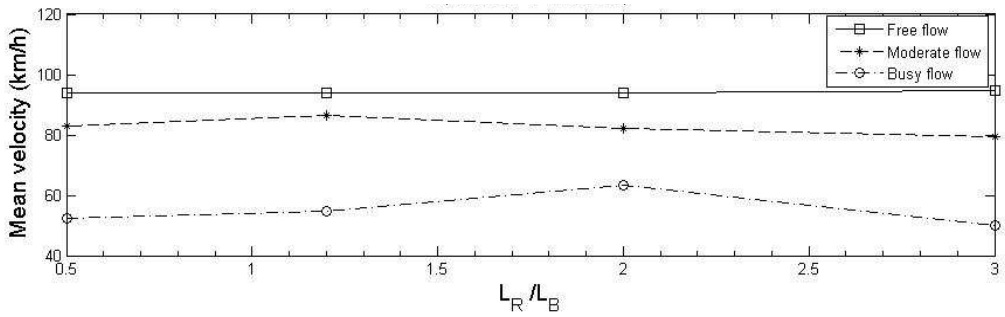

b. V_{max}=108 km/h

Fig. 2.9 Mean velocity vs. length ratio

Fig. 2.10 gives the results of the mean value of the total static load under different length ratios (L_R/L_B). Fig. 2.10(a) and Fig. 2.10(b) show the results when the speed limit equals to 81 km/h and 108 km/h, respectively. In each subplot, the results for the three different traffic occupancies are plotted together. Similar to the impacts on the mean velocity as shown in Fig. 2.9, it is found from Fig. 2.10 that the mean static load is not sensitive to the length ratio L_R/L_B when the traffic occupancy is low or moderate. When the traffic occupancy becomes high (i.e. "busy flow"), the mean static load has limited fluctuations around the mean value over the different length ratios. The results show that the "roadway-bridge-roadway" system with L_R/L_B =0.5 or above is normally sufficient to provide stable static load of the traffic flow as long as the traffic occupancy is not very high. For the "busy flow", longer approaching roadways in the BIS may help on further improving the accuracy.

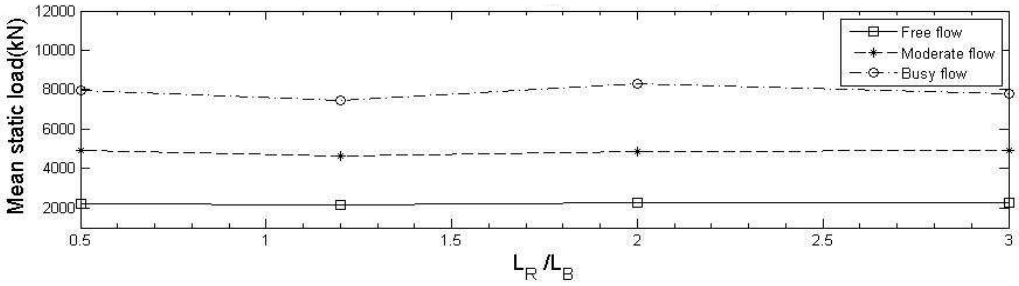

a. V_{max}=81km/h

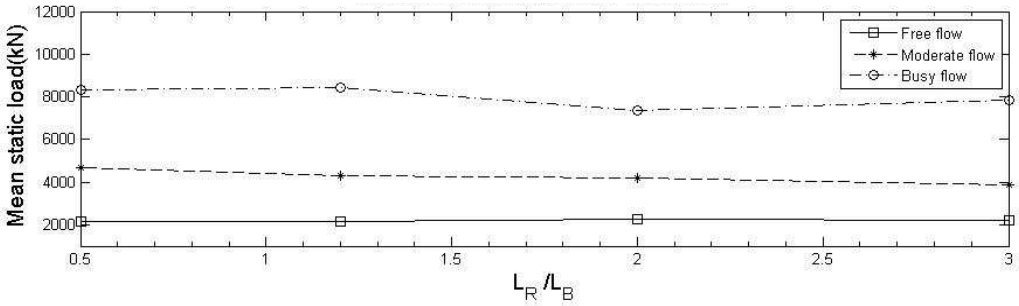

b. V_{max}=108km/h

Fig. 2.10 Mean static load vs. length ratio

2.4.2 Speed limits

The relationship between the mean velocity and the speed limit is studied under various traffic occupancies (Fig. 2.11). For “free flow” condition, the mean velocity increases in a nearly linear way with the increase of the speed limit for two different length ratios (Fig. 2.11a and Fig. 2.11b). When the traffic occupancy is high (“busy flow”), the mean velocity increases in a nonlinear way and may even decrease when the speed limit is around 110 km/h for both length ratios of the approaching roadway (Fig. 2.11(a-b)). It is known that vehicles cannot move faster when traffic congestion exists even with a higher posted speed limit. The results numerically confirm a common observation that densely distributed vehicles may move slowly on the bridge during rush hours regardless of the posted speed limit. Therefore, to avoid heavy traffic remaining on the bridge for extended time, some traffic control measures in addition to the speed limits should be applied during rush hours.

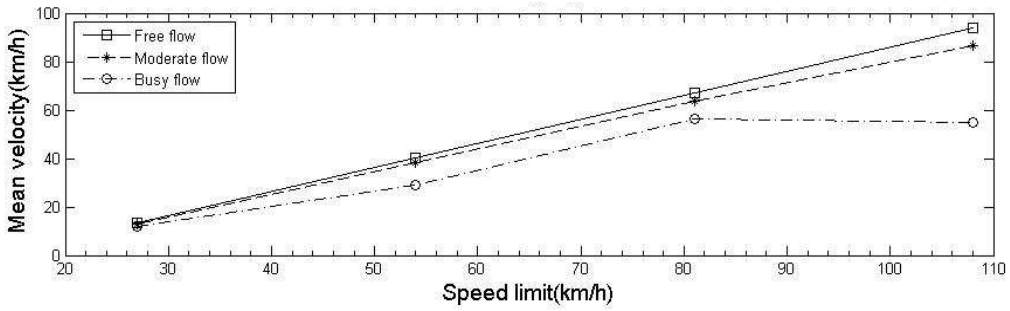

a. L_R/L_B =1.2

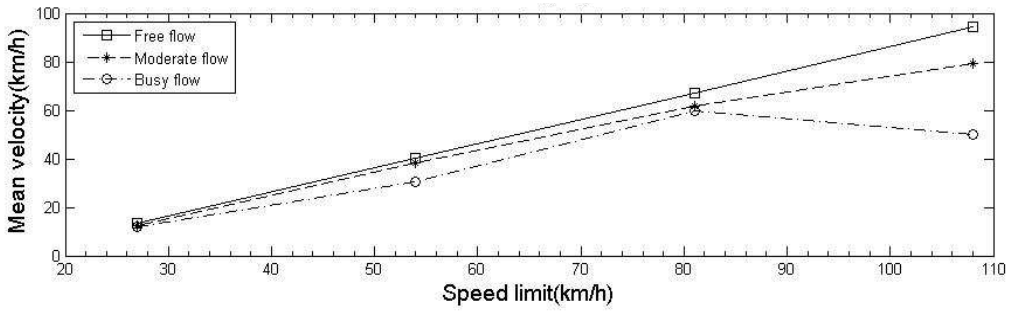

b. L_R/L_B =3

Fig. 2.11 Mean velocity vs. speed limit

The mean static load of traffic under different speed limits was also studied. As shown in Fig. 2.12, the mean static load remains almost the same for different speed limits when the traffic occupancies are low or moderate. When the traffic occupancy becomes high ("busy flow"), the mean static load has some fluctuations with the speed limits. For the typical range of speed limits of long-span bridges, the impact from the speed limit on the static traffic load is found to be very limited. Since the mean velocity of the traffic has pretty significant change over the different speed limits (Fig. 2.11), the dynamic impacts of the traffic, however, can be considerably affected by the speed limits. The detailed quantification of the dynamic loads considering interactions needs to be studied separately.

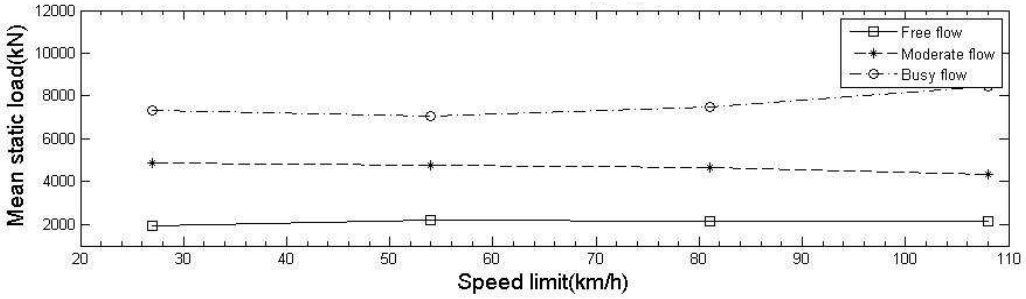

a. L_R/L_B =1.2

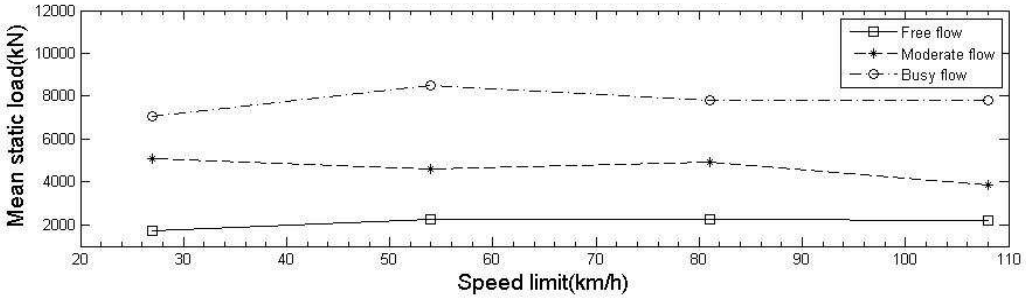

b. L_R/L_B =3

Fig. 2.12 Mean static load vs. speed limit

2.4.3 Vehicle combination

In the present study, the combination ratio of different types of vehicles is assumed to be v_{type} ={0.2 0.3 0.5} for the three categories of vehicles: "heavy multi-axle truck", "light truck and bus" and "light passenger cars", respectively. In order to study the impact of the different vehicle combinations, another vehicle combination ratio v_{type} ={0.2 0.2 0.6} is also studied and the results are shown in Fig. 2.13. "Combination I" and "Combination II" in Fig. 2.13 refer to v_{type} ={0.2 0.3 0.5} and {0.2 0.2 0.6}, respectively. The mean static load of the vehicles for the "free flow" and "moderate flow" seem to simply increase with the increase of the percentage of heavier vehicles. The mean static load of all the vehicles for the "busy flow" condition shows a complicated trend. This is probably due to the congestion and more turbulent traffic flow when the traffic occupancy gets high. For various traffic occupancies, the mean static load of all the vehicles on the bridge

seems to be pretty sensitive to different vehicle combinations. So for an accurate traffic load characterization, the specific vehicle classification information should be used, if available.

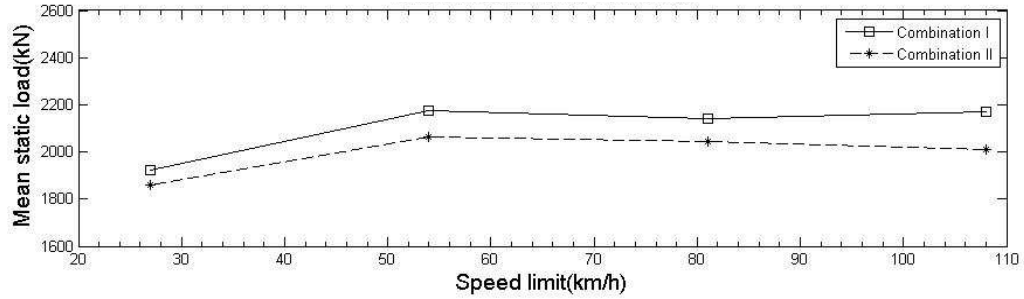

a. Free flow

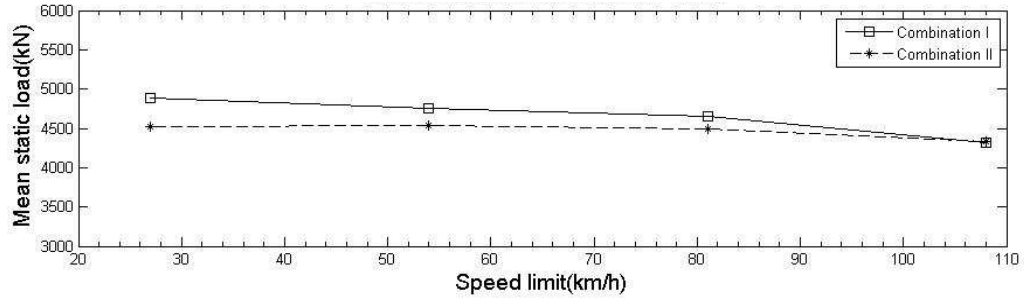

b. Moderate flow

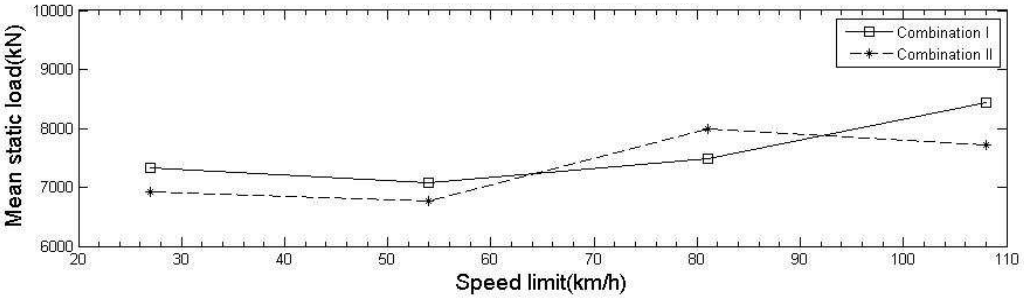

c. Busy flow

Fig. 2.13 Mean static load vs. vehicle combination (L_R/L_B =1.2)

2.5 Conclusions

A general framework of modeling the stochastic live load from traffic for a long-span bridge was developed. Depending on the site-specific information of the bridge, different approaching roadway lengths, traffic occupancies, speed limits and combinations of vehicle types for both the normal and incidental conditions can be considered. Following the development of the

methodology, parametric studies were conducted for several critical parameters used in the simulation. Major findings are summarized as follows:

(1) Larger fluctuations of vehicle velocities over time were observed when the traffic occupancy is high for both normal and incidental conditions. For a critical long-span bridge which often experiences busy traffic, a rational simulation of the traffic flow with realistic traffic rules was confirmed to be necessary in order to quantify time-dependent traffic load on the bridge.

(2) The "road block" traffic condition has less impact on the traffic flow in terms of the velocity fluctuations than the "bridge block" or normal traffic conditions. Large fluctuations of the vehicle velocities can cause more variations of the dynamic impacts of the traffic load, higher risks of rear-end crashes and more chances of accelerating and braking operations.

(3) Among the three different traffic conditions, the "bridge block" condition is found to cause the minimum mean static traffic load on the bridge, while the "road block" condition causes the largest mean static traffic load, but with the least fluctuations of the static traffic load over time.

(3) When the traffic occupancy is low, the boundary conditions of the bridge (i.e. details of approaching roadways) are not very critical to the simulated traffic. The "roadway-bridge-roadway" system with $L_R/L_B = 0.5$ or above is normally sufficient to provide stable static load of the traffic flow as long as the traffic occupancy is not very high. When the traffic occupancy on a bridge is high, an accurate description of the site-specific details of the approaching roadways connecting the bridge becomes critical in order to accurately quantify the traffic load on the bridge.

(4) For the typical range of speed limits of long-span bridges, the impact from the speed limit on the static traffic load from the stochastic traffic is found to be very limited. Since the mean velocity of the traffic has pretty significant change over the different speed limits, the dynamic traffic load, however, could be considerably affected by the speed limits.

(5) The mean static load of all the vehicles on the bridge is pretty sensitive to different vehicle combinations. For an accurate load characterization, the site-specific vehicle classification information should be used, if available.

(6) A simple comparison between the simulated static traffic load and the AASHTO LRFD HL-93 design load was made. It was found that the lane load of HL-93 can provide sufficient static load for the "free flow" and "moderate flow" conditions. When the traffic occupancy is high ("busy flow"), there will be equivalently 2-3 design trucks along with the lane load which can generate the same total static load as the simulated traffic loads. Since it was only about the static load, more detailed and rigorous comparison of the live load considering dynamic impacts with AASHTO LRFD design loads, which require extensive interaction analysis, should be conducted in the future.

2.6 References

American Association of State Highway and Transportation Officials (AASHTO) (2007). LRFD bridge design specifications, Washington, D.C.

Benjamin, S. C., Johnson, N. F. and Hui, P. M. (1996). "Cellular automata models of traffic flow along a highway containing a junction." J. Phys. A: Math. Gen., 29, 3119-3127.

Barlovic, R., Santen, L. and Schadschneider,A. and Schreckenberg, M. (1998). "Metastable states in cellular automata for traffic flow." Eur. Phys. J. B, 5, 793-800.

Broquet, C., Bailey, S. F., Fafard, M., and Brühwiler, E. (2004). "Dynamic behavior of deck slabs of concrete road bridges." Journal of Bridge Engineering, 9(2), 137–146.

Cai, C. S., Chen, S. R. (2004). "Framework of vehicle-bridge-wind dynamic analysis." J. Wind. Eng. Ind. Aerodyn., 92 (7-8), 579-607.

Chen, S. R. and Cai, C. S. (2007). "Equivalent wheel load approach for slender cable-stayed bridge fatigue assessment under traffic and wind: Feasibility study." Journal of Bridge Engineering, ASCE, 12(6), 755-764.

Chen, S. R., Cai, C. S. and Levitan, M. (2007). "Understand and improve dynamic performance of transportation system- A case study of Luling Bridge." Engineering Structures, 29, 1043-1051.

Chen, S. R. and Wu, J. (2010). “Dynamic performance simulation of long-span bridge under combined loads of stochastic traffic and wind.” Journal of Bridge Engineering, 15(3), 219-230.

Chen, Y.B. and Feng, M.Q. (2006). “Modeling of traffic excitation for system identification of bridge structures.” Computer-Aided Civil and Infrastructure Engineering, 21, 57-66.

Cheybani, S., Kertesz, J. and Schreckenberg, M. (2000). “Stochastic boundary conditions in the deterministic Nagel-Schreckenberg traffic model.” Phys.l Rev. E, 63, 016107.

Chowdhury, D., Santen, L. and Schadschneider, A. (2000). “Statistical physics of vehicular traffic and some related systems.” Phys. Rep., 329, 199.

Ditlevsen, O. (1994). “Traffic loads on large bridges modeled as white-noise fields.” J Eng Mech, 120(4), 681-694.

Ditlevsen, O, Madsen, H. O. (1995). “Stochastic vehicle-queue-load model for large bridges.” J Eng Mech, 120 (9), 1829-1874.

Li, X. G., Jia, B., Gao,Z.Y. and Jiang, R. (2006). “A realistic two-lane cellular automata traffic model considering aggressive lane-changing behavior of fast vehicle.” Physica A, 367, 479-486.

Moses, F. (2001). NCHRP Report 454: Calibration of load factors for LRFR Bridge evaluation, TRB, National Research Council, Washington, D.C.

Mullard, J. A. and Stewart, M. G. (2009). “Stochastic Assessment of Timing and Efficiency of Maintenance for Corroding RC Structures.” Journal of Structural Engineering, 135(8), 887-895.

Nagel, K., Schreckenberg, M. (1992). “A cellular automaton model for freeway traffic.” J. Phys. I France, 2(12), 2221-2229.

Nagel, K., Wolf, D., Wagner P. and Simon, P. (1998). “Two-lane traffic rules for cellular automata: A systematic approach.” Physical Review E 58 (2): 1425-1437 Part A.

Nowak, A. S. (1993). “Live load model for highway bridges.” Structural Safety, 13, 53- 66.

O'Connor, A. J. and Obrien, E. J. (2005). “Traffic load modeling and factors influencing the accuracy of predicted extremes.” Canadian Journal of Civil Engineering, 32, 270-278.

Oh, B. H., Lew, Y. and Choil, Y. C. (2007). “Realistic assessment for safety and service life of reinforced concrete decks in girder bridges.” Journal of Bridge Engineering, 12(4), 410-418.

Rickert, M., Nagel, K., Schreckenberg, M., Latour, A. (1996). “Two lane traffic simulations using cellular automata.” Physica A, 231, 534-550.

Schadschneider, A. (2006). “Cellular automata models of highway traffic.” Physica A, 372, 142–150.

TRANSIMS Travelogues, Transportation analysis and simulation system, Los Alamos National Laboratory, Los Alamos, <http://www-transims.tsasa.lanl.gov/travel.shtml>, lastly accessed on April 30th 2008.

Transportation Research Board (2000). Highway capacity manual, Washington, D.C.

Treiterer, J. et al. (1965). "Investigation and measurement of traffic dynamics, Appendix IX to Final Report EES 202-2." Ohio State University, Columbus.

Wu, J. and Chen, S. R. (2010). "Probabilistic dynamic behavior of long-span bridge under extreme events." Engineering Structures (under re-review with minor change).

Xiao, S.F., Kong, L.J. and Liu, M., (2005). "A cellular automaton model for a bridge traffic bottleneck." Acta Mech Sinica, 21,305-309.

Xu, Y. L. and Guo, W. H. (2003). "Dynamic analysis of coupled road vehicle and cable-stayed bridge system under turbulent wind." Engineering Structures, 25, 473-486.

CHAPTER 3: DYNAMIC PERFORMANCE SIMULATION OF LONG-SPAN BRIDGES UNDER COMBINED LOADS OF STOCHASTIC TRAFFIC AND WIND

3.1 Introduction

Slender long-span bridges exhibit unique features not present in short-span bridges, such as simultaneous presence of multiple trucks, and significant sensitivity to wind. The performance assessment under service loads has been primarily focused on traffic and wind loads for slender long-span bridges. Wind-induced buffeting analysis is the common approach to estimate the dynamic behavior of slender long-span cable-stayed or suspension bridges under turbulent wind excitations. No traffic load was typically considered simultaneously with wind (Simiu and Scanlan 1996; Jain et al. 1996), assuming that the bridges will be closed to traffic at relatively high wind speeds or the excitations from vehicles are negligible. However, recent studies of Bridge/Vehicle/Wind interaction analyses showed that there is a considerable difference in the predicted bridge response between the case where several trucks were considered and the case where no vehicle was considered (Xu and Guo 2003; Cai and Chen 2004; Chen et al. 2007), and such a difference exists over a wide range of wind speeds. Furthermore, long-span bridges are rarely closed even when wind speeds exceed the commonly-quoted criterion for long-span bridge closure [e.g. 55 mph (AASHTO 2004)]. For slender long-span bridges, the governing (most severe) case of stress and potential damage is when the collective effects from wind and the real traffic loadings are the largest, not necessarily when wind is the strongest or when the traffic volume is the highest.

Even for conventional long-span bridges which are not sensitive to wind excitations, such as those with slab & beam girder, arch and truss (Huang 2005; Calcada et al. 2005; Shafizadeh and Mannering 2006), wind dynamic effects on fast-moving vehicles are still significant. The results from the preliminary study suggested that the wheel load applied by one standard truck on a long-span bridge without considering wind dynamic impacts on the vehicle will be underestimated by about 6% to 11% compared to the case considering wind impacts on the vehicle when wind speed is between 10 m/s to 20 m/s. With busy traffic flow and moderate wind on a long-span bridge, the cumulative dynamic impacts on the bridge transferred from wind through many vehicles can be significant and some critical scenarios with excessive stress or response for the bridge may not be captured appropriately by ignoring the dynamic wind effects on vehicles.

In recognizing the significance of dynamic interactions of a long-span bridge, vehicles and wind as a coupled system, people have recently started working on dynamic behavior of Bridge/Vehicle/Wind coupled system (Xu and Guo 2003; Cai and Chen 2004; Chen and Cai 2006; Chen et al. 2007). As a first step to demonstrate the methodology, these studies have considered only one or several vehicles distributed in an assumed (usually uniform) pattern on a bridge. For a bridge with a long span, there is a high probability of the simultaneous presence of multiple vehicles including several heavy trucks on the bridge. Such an assumed pattern obviously differs from reality that vehicles actually move probabilistically through the bridge following some traffic rules. Although white noise fields (Ditlevsen 1994; Ditlevsen and Madsen 1995), Poisson distribution (Chen and Feng 2006) and Monte Carlo approach (Nowak 1993, Moses 2001, O'Connor and Obrien 2005) have been used to simulate the traffic flow to obtain the characteristic load effects for short- and medium-span bridges, these approaches have not been used on long-span bridges to address relatively complicated traffic loading, especially with wind load simultaneously. For example, the traffic flow is more complicated in terms of vehicle number, vehicle type combination and drivers' operation such as lane-changing, acceleration or

deceleration on long-span bridges compared to short-span bridges. In Chapter 2, a framework of probabilistic bridge dynamic analysis is introduced which considers the dynamic interactions between bridge, stochastic traffic and wind. The stochastic traffic flow on the bridge is simulated with the Cellular Automata (CA) traffic flow model. The equivalent dynamic wheel load (EDWL) approach (Chen and Cai 2007) is incorporated into the model to make the simulation of the coupled system in time domain practically possible. A case study of a slender cable-stayed bridge is conducted based on the proposed methodology.

3.2 Theoretical Basis of Bridge/Traffic/Wind Interaction Analysis

As illustrated in Fig. 3.1, the proposed analytical model has three parts: the first one is to simulate the stochastic traffic flow; the second one is to obtain time-dependent equivalent dynamic wheel load (EDWL) information for each vehicle from the developed EDWL database; and the third one is the interactive simulation framework in the time domain to obtain statistical results of the bridge performance. The theoretical basis of these three parts is introduced in the following.

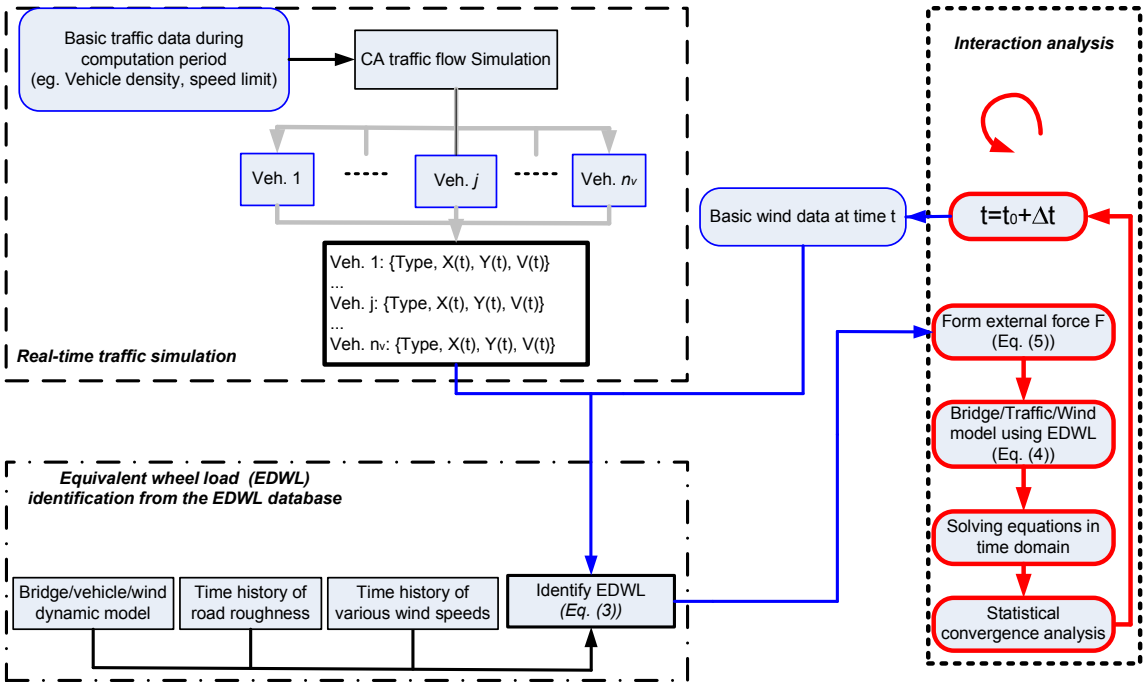

Fig. 3.1 Flow chart of the analytical method

3.2.1 Probabilistic traffic flow simulation with CA model

As introduced in Chapter 2, the Cellular Automaton (CA) traffic simulation model, a type of microscopic traffic flow simulation techniques, is based on the assumption that both time and space are discrete and each lane is divided into cells with an equal length (Nagel and Schreckenberg 1992). Each cell can be empty or occupied by at most one vehicle at a time. The instantaneous speed of a vehicle is determined by the number of cells a vehicle can advance within one time step. The maximum speed a vehicle can achieve is decided by the legal speed limit of the highway. For each time step, operations such as accelerating, decelerating or lane-changing of any vehicle are automatically decided based on some algorithms established according to some actual traffic rules as well as some reasonable assumptions of the driver behavior. For instance, it is assumed that drivers intend to achieve the maximally allowable driving speed without having traffic conflicts with other vehicles or breaking any traffic rule.

The rules of a typical multi-lane CA traffic model include: (1) those for vehicles moving forward on the original lane, i.e. single-lane CA model (Nagel and Schreckenberg, 1992); and (2) those of lane-changing. For any vehicle *i*, lane-changing will happen if the following conditions are all met (Rickert et al. 1996; Li et al., 2006). A detailed introduction of the CA-based traffic simulation model and the simulation results on a long-span bridge can be found in Ref. (Wu and Chen 2008).

3.2.2 Equivalent dynamic wheel load (EDWL)

Beginning with the finite element modeling of a bridge, the bridge dynamic model is developed. Each vehicle is modeled as a multi-degree-of-freedom, and mass-spring-damper system. Once the road roughness and wind loading acting on a bridge as well as on the vehicles are simulated in the

time domain, the general Bridge/Vehicle/Wind interaction model can be expressed as (Chen 2004; Cai and Chen 2004):

$$\begin{bmatrix} \mathbf{M}_V & \mathbf{0} \\ \mathbf{0} & \mathbf{M}_B \end{bmatrix} \begin{Bmatrix} \ddot{\boldsymbol{\gamma}}_V \\ \ddot{\boldsymbol{\gamma}}_B \end{Bmatrix} + \begin{bmatrix} \mathbf{C}_V & \mathbf{C}_{VB} \\ \mathbf{C}_{BV} & \mathbf{C}_B^S + \mathbf{C}_B^V \end{bmatrix} \begin{Bmatrix} \dot{\boldsymbol{\gamma}}_V \\ \dot{\boldsymbol{\gamma}}_B \end{Bmatrix} + \begin{bmatrix} \mathbf{K}_V & \mathbf{K}_{VB} \\ \mathbf{K}_{BV} & \mathbf{K}_B^S + \mathbf{K}_B^V \end{bmatrix} \begin{Bmatrix} \boldsymbol{\gamma}_V \\ \boldsymbol{\gamma}_B \end{Bmatrix} = \begin{Bmatrix} \{\mathbf{F}\}_R^V + \{\mathbf{F}\}_W^V \\ \{\mathbf{F}\}_R^B + \{\mathbf{F}\}_W^B + \{\mathbf{F}\}_G^B \end{Bmatrix} \quad (3.1)$$

where **M**, **C** and **K** are the matrices of mass, damping and stiffness, respectively; **γ** is the displacement; the subscripts and superscripts *B* and *V* refer to the bridge and vehicles, respectively; **F** is the force vectors; subscripts *R*, *W* and *G* refer to the forces induced by road roughness, wind and the gravity of the vehicles on the right hand side of equations, respectively.

The vehicle models in Eq. (3.1) can be used to simulate various types and numbers of vehicles at any location on the bridge. By removing wind-related terms in Eq. (3.1), the coupled equations will reduce to the traditional Bridge/Vehicle interaction model without considering wind for conventional long-span bridges (Huang 2005; Calcada et al. 2005). Theoretically, when real traffic flow is considered, each vehicle dynamic model with corresponding actual vehicle properties (e.g. driving speed and location) of the traffic flow can be brought into Eq. (3.1) to formulate a "fully-coupled" Bridge/Traffic/Wind dynamic interaction analysis with detailed vehicle dynamic models with Eq. (3.1). The "fully-coupled" analysis in an "exact" manner obviously can provide the most accurate simulation results, but requires extremely high computational costs as the number of degree-of-freedom of the matrices in Eq. (3.1) increases proportionally with the number of vehicles remaining on the bridge at any time. When the bridge span is long, traffic is busy or an extended simulation time is required, a "fully-coupled" interaction analysis of a Bridge/Traffic/Wind system increases the number of degree-of-freedom too dramatically to be realistic for practical simulations (Chen and Cai 2007).

In order to provide a more computationally practical option for engineering analyses, the equivalent dynamic wheel load (EDWL) approach has been proposed by Chen and Cai (2007) to significantly improve the efficiency of the analysis by avoiding solving the "fully-coupled" Bridge/Multi-vehicle/Wind interaction equations. Each EDWL, which is obtained from the dynamic interaction analysis of the Bridge/Single-vehicle/Wind system in the time domain, is essentially a time-variant moving force representing the actual wheel loading applied by each moving vehicle on the bridge deck considering essential dynamic interactions. The EDWL varies with time and is specific to vehicle type, driving speed and other environmental conditions.

The EDWL and the dimensionless variable EDWL ratio R for the j^{th} vehicle are defined in Eq. (3.2) and Eq. (3.3), respectively (Chen and Cai 2007).

$$EDWL_j(t) = \sum_{i=1}^{n_a} \left(K_{vl}^i \bar{Y}_{vl}^i + C_{vl}^i \dot{\bar{Y}}_{vl}^i \right) \tag{3.2}$$

where K_{vl}^i and C_{vl}^i are the spring stiffness and damping terms of the suspension system of vehicle, respectively. $\bar{Y}_{vl}^i$ and $\dot{\bar{Y}}_{vl}^i$ are the relative displacement and velocity of the suspension system to the bridge in vertical direction, respectively. n_a is the axle number of the j^{th} vehicle model. Since the vehicle moves in a constant speed, any specific time after the vehicle gets on the bridge corresponds to a spatial location along the bridge. As a result, the time-variant $EDWL_j(t)$ can be easily translated to spatially-variant $EDWL_j(x)$ by using a simple relationship ($x(t) = x(t-1) + \int_{t-1}^{t} V(t)\,dt$), where x is the longitudinal position along the bridge, $V(t)$ is the instantaneous driving speed of the vehicle at time t.

The equivalent dynamic wheel load ratio (R) for the j^{th} vehicle can be defined as (Chen and Cai 2007):

$$R_j(t) = EDWL_j(t)/G_j \tag{3.3}$$

where G_j is the weight of the j^{th} vehicle.

3.2.3 Bridge/Traffic/Wind interaction model using EDWL

By introducing EDWL to replace physical moving vehicles on the bridge, the "fully-coupled" equations (Eq. (3.1)) can be simplified to Bridge/Wind coupled model under excitations of many moving forces- EDWLs, at the corresponding locations of the physical vehicles on the bridge (Chen and Cai 2007). Accordingly, the "fully-coupled" Bridge/Traffic/Wind model as shown in Eq. (3.1) will be simplified to:

$$\mathbf{M_b}\{\ddot{\gamma}_\mathbf{b}\} + \mathbf{C_b^s}\{\dot{\gamma}_\mathbf{b}\} + \mathbf{K_b^s}\{\gamma_\mathbf{b}\} = \{\mathbf{F}\}_\mathbf{w}^\mathbf{b} + \{\mathbf{F}\}_\mathbf{Eq}^\mathbf{wheel} \tag{3.4}$$

where $\{\mathbf{F}\}_\mathbf{Eq}^\mathbf{wheel}$ is the cumulative equivalent dynamic wheel load (EDWL) of all the vehicles existing on the bridge at a time, as defined in Eq. (3.5); matrices $\mathbf{C_b^s}$ and $\mathbf{K_b^s}$ are the damping and stiffness matrices of the bridge which have included the wind-induced aeroelastic damping and stiffness components, respectively (Simiu and Scanlan 1996); $\{\mathbf{F}\}_\mathbf{w}^\mathbf{b}$ denotes the wind-induced buffeting force acting on the bridge. It is easy to find Eq. (3.4) will be reduced to the traditional wind-induced buffeting analysis equations after removing the $\{\mathbf{F}\}_\mathbf{Eq}^\mathbf{wheel}$ term.

The cumulative EDWL $\{\mathbf{F}\}_\mathbf{Eq}^\mathbf{wheel}$ acting on the bridge in Eq. (3.4) can be defined as:

$$\{\mathbf{F}(\mathbf{t})\}_\mathbf{Eq}^\mathbf{wheel} = \sum_{j=1}^{n_v}\left\{\left(1-R_j(t)\right)G_j \bullet \sum_{k=1}^{n}\left[h_k\left(x_j(t)\right) + \alpha_k\left(x_j(t)\right)d_j(t)\right]\right\} \tag{3.5}$$

where R_j, G_j, x_j, and d_j are the dynamic wheel load ratio, self-weight of the j^{th} vehicle, longitudinal location, and transverse location of the gravity center of the j^{th} vehicle on the bridge, respectively. h_k, and α_k are the vertical and torsion mode shapes for the k^{th} mode of the bridge model. n_v is the total number of vehicles on the bridge at a time. Since there may be different numbers of vehicles

on the bridge at different time, n_v changes with time depending on the simulation results of the stochastic traffic flow.

The feasibility study conducted by Chen and Cai (2007) compared the bridge response estimations using EDWL and the "fully-coupled" bridge/multi-vehicle/wind interaction analysis. Very close results of both displacement and acceleration responses can be obtained with the EDWL approach and the computational errors compared to the "fully-coupled" analysis results were around 1-7%. As shown in Eq. (3.4), the degrees of freedom of Eq. (3.4) equal to those of the bridge model, and thus do not change with the number of vehicles on the bridge. As a result, the computation efficiency of busy traffic flow moving through a long-span bridge with the EDWL approach by using Eq. (3.4) , even for an extended time period, can be significantly improved compared to the "fully-coupled" equations (Eq. (3.1)).

3.3 "Semi-deterministic" Bridge/Traffic/Wind Interaction Analysis

Fig. 3.1 gives the flowchart of the simulation process in the time domain: based on the input data of simulation at any time step, the corresponding EDWL value of each vehicle of the simulated traffic will be obtained from the EDWL database. The dynamic interaction analysis of the Bridge/Traffic/Wind system is then carried out, based on which the statistical assessment of bridge performance can be conducted. Details of the whole simulation process in Fig.3.1 are illustrated in the following sections.

3.3.1 Input data of simulation

After the theoretical basis of the traffic flow simulation and the equivalent dynamic wheel load approach have been introduced in the above section, the probabilistic simulation of the bridge dynamic behavior in the time domain will be conducted with following basic input data:

Bridge – basic geometric and material parameters; bridge finite element model and critical modes selected for the interaction analysis; surface roughness of bridge deck, which can be the actual measurements or from simulations based on the spectrum of surface roughness profiles (Huang and Wang 1992; Xu and Guo 2003).

Traffic – vehicle occupancy (or traffic density); vehicle classifications (i.e. percentage of each category of vehicles) and speed limit.

Wind – wind speed; static wind force coefficients and flutter derivatives of the bridge; static wind force coefficients of various high-sided vehicles which are typically obtained from wind tunnel testing (Baker 1991).

With all the required data, the EDWL database associated with a particular bridge will be developed which will be introduced in detail in the following "EDWL database".

3.3.2 EDWL database

A comprehensive EDWL database is to provide EDWL for any possible combination of vehicle properties (e.g. vehicle type, driving speed), wind speed and road surface roughness condition. Existing studies have already identified some key factors affecting the values of EDWL (Chen and Cai 2007) such as wind speed, vehicle type, vehicle driving speed, vehicle instantaneous position on the bridge and surface roughness profiles of the bridge deck. For a particular bridge, all common vehicles of the traffic flow on the bridge can be classified into several categories. For each category of vehicles, some typical variables are selected such as mass, stiffness, damping and wind force coefficients. Wind speeds, vehicle driving speeds and road roughness are also described with some typical discrete values with reasonable intervals (e.g. 5m/s interval of wind and driving speeds). Comprehensive collections of possible combinations of variables, such as vehicle variables, wind speed, vehicle driving speed and road roughness level, are made. Under each combination of variables, Bridge/Single-vehicle/Wind interaction analysis is conducted and

the corresponding EDWL(t) and EDWL(x) in both time and spatial domains respectively, are obtained (Chen and Cai 2007). Depending on the intervals of discrete values for each input variable, appropriate interpolation techniques may be applied when the actual input value is between two predefined discrete values for each variable. In the present study, a simple linear interpolation is adopted due to pretty dense intervals adopted.

3.3.3 Statistical assessment of bridge dynamic performance

Since the objective of the present study is to develop the framework of Bridge/Traffic/Wind interaction analysis, uncertainties of variables about bridge, wind, and roughness excitations will not be considered in this study. The only randomness is from the stochastic nature of the traffic flow which is simulated based on the CA model. So the proposed Bridge/Traffic/Wind simulation model is actually a type of "semi-deterministic approach" as the instantaneous distributions of positions and speeds of the vehicles of the CA-based traffic flow at any time are probabilistic, but the basic traffic input (e.g. vehicle occupancy (or traffic density) and vehicle classifications) for the CA simulation is still deterministic. Because of the "semi-deterministic" nature of the proposed model, a convergence analysis of the time-history results over time will be necessary in order to get stable statistical descriptions over time (e.g. mean and standard deviation) of bridge responses under stochastic traffic. The basic traffic input varies in a typical day (e.g. rush hour and normal hours) and a typical week (e.g. weekdays and weekend). These uncertainties, along with uncertainties associated with other variables of bridge, wind and vehicle models, will be considered in a comprehensive reliability-based lifetime analysis model in Chapter 6 based on the present model.

The whole simulation process, as shown in the flowchart in Fig. 3.1, is summarized as the following steps:

(1) With the deterministic values of the basic traffic input (e.g. traffic density and vehicle classifications), the CA traffic flow simulation model will be used to simulate the stochastic traffic flow, among which each vehicle carries detailed time-variant (or spatially-variant) information such as instantaneous driving speed and position at each time step as well as time-invariant information (e.g. vehicle type);

(2) The information of each vehicle, along with the instantaneous wind data and roughness profile data, will be fed into the EDWL database to obtain the corresponding instantaneous EDWL(t) value at each time step based on the corresponding instantaneous spatial position identified for each vehicle. EDWLs of all the vehicles of the traffic flow will be articulated to form the external loading term $\{\mathbf{F}\}_{\mathbf{Eq}}^{\mathbf{wheel}}$ on the right-hand side of Eq. (3.4) at the moment;

(3) The differential equations of Eq. (3.4) will be solved at each time step with the external loading term $\{\mathbf{F}\}_{\mathbf{Eq}}^{\mathbf{wheel}}$ updated. Time-dependent response, such as dynamic displacement, shear force, moment and stress, of each member of the bridge can be obtained;

(4) Repeat steps (1)-(3) for each time step, time-history of response/shear-force/moment/stress at any point on the girders along the bridge can be obtained;

(5) Due to the stochastic nature of the traffic loads carried over from the simulated traffic flow, a convergence analysis is required in order to get a rational estimation of the statistical performance of the bridge. For any point of interests along the bridge, statistical analyses over the time period from the starting time of the simulation to the current time will be conducted repeatedly with the increase of time steps until the mean and standard deviation of the interested bridge response both converge. The converged mean and standard deviation of the bridge response will become the final statistical descriptions of the bridge behavior (e.g. mean and standard deviation) under stochastic traffic flow and wind for a specific traffic density and vehicle classification.

3.4 Case Study

A case study will be made to demonstrate the proposed approach on the bridge behavior study of a slender long-span cable-stayed bridge.

3.4.1 Bridge and vehicle model

The long-span cable-stayed bridge (Fig. 3.2) with a total length of 836.9m is adopted as the prototype bridge. The same bridge has been selected as the prototype bridge in several previous studies (e.g. Chen et al. 2007). The approaching roadway at each end of the bridge is assumed to be 1005m. The speed limit of the highway system is 70 mph which is converted to v_{max}=4 in the CA model as shown in Eq. (3.6).

$$v_{\max} = \frac{V_{\max}}{L_c} = \frac{113(\mathrm{km/h})}{3600(\mathrm{s/h})} \times \frac{1000(\mathrm{m/km})}{7.5(\mathrm{m/cell})} = 4.19(\mathrm{cell/s}) \approx 4(\mathrm{cell/s}) \tag{3.6}$$

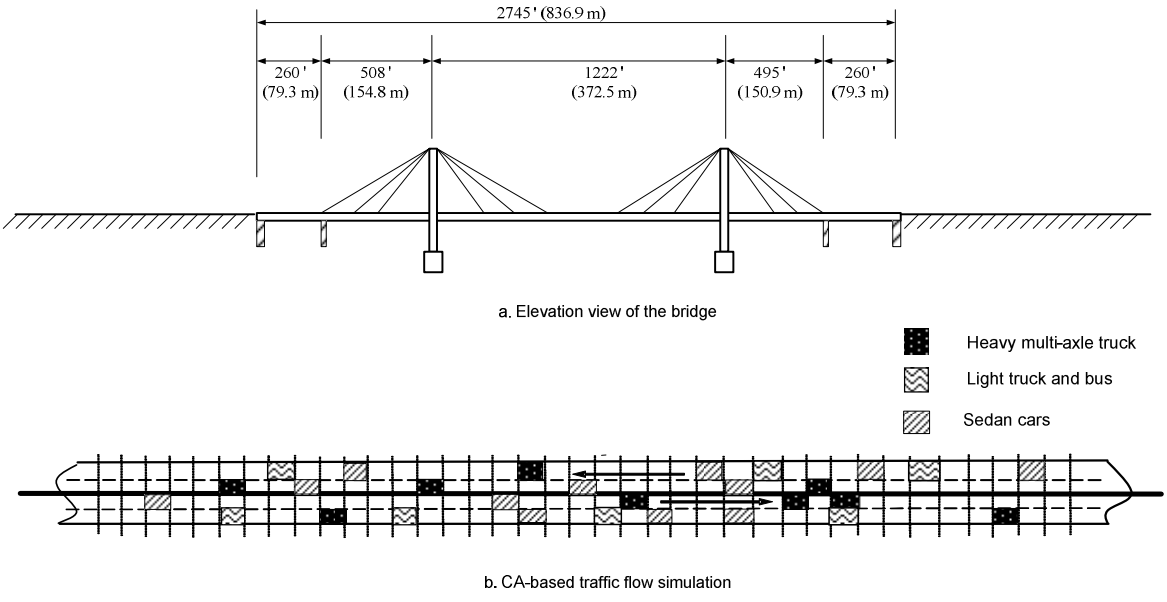

Fig. 3.2 Cable-stayed bridge and CA-based traffic flow simulation on the bridge

In order to develop the EDWL database, all the vehicles are classified as three types: 1) v1-heavy multi-axle trucks 2) v2-light trucks & buses and 3) v3-sedan car. Please be noted different

categories may be classified based on the specific vehicle classification characteristics of traffic on other bridges. According to the existing studies (Xu and Guo 2003; Cai and Chen 2004), heavy trucks, which are critical to bridge dynamic behavior, require more detailed vehicle dynamic modeling. It was also found in the feasibility study (Chen and Cai 2007) that the quarter vehicle models can give reasonable estimations of EDWL for light trucks. Therefore, in present study, only heavy trucks are modeled with the detailed vehicle dynamic model and light trucks and sedan cars use the quarter vehicle model to be computationally efficient. Both the detailed vehicle dynamic model and the quarter vehicle model are shown in Fig. 3.3 and the parameters of the vehicle models are summarized in Tables 3.1 and 3.2. The vehicle classifications (i.e. percentage of each type of vehicles) are defined in Table 3.3 as the variable v_{type}. The Transportation Research Board classifies the "Level of Service (LOS)" from A to F which ranges from driving operation under desirable condition to operation under forced or breakdown conditions (NRC 2000). Three traffic occupancies (ρ) are computed: 1) ρ =0.07 (9 veh/km/lane) corresponding to level B, 2) ρ =0.15 (20 veh/km/lane) corresponding to level D and 3) ρ =0.24 (32 veh/km/lane) corresponding to level F. Also based on the existing studies, wind loadings on vehicles are considered for heavy and light trucks, but are ignored for sedan cars due to the insignificance of dynamic impacts from wind. In this chapter, in order to study the normal service condition of long-span bridges, only two wind speeds are considered in this study: breeze (wind speed =2.7 m/s) and moderate wind (wind speed =17.6 m/s).

Table 3.1 Parameters of vehicle model (quarter-model)

Parameters	Unit	Sedan car	Light truck
Sprung mass (m1)	kg	1460	4450
Unsprung mass (m2)	kg	151	420
Stiffness of suspension system (k)	N/m	434920	5e5
Stiffness of tire (kt)	N/m	7.02e5	1.95e6
Damping (c)	N/(m/s)	5820	2e4

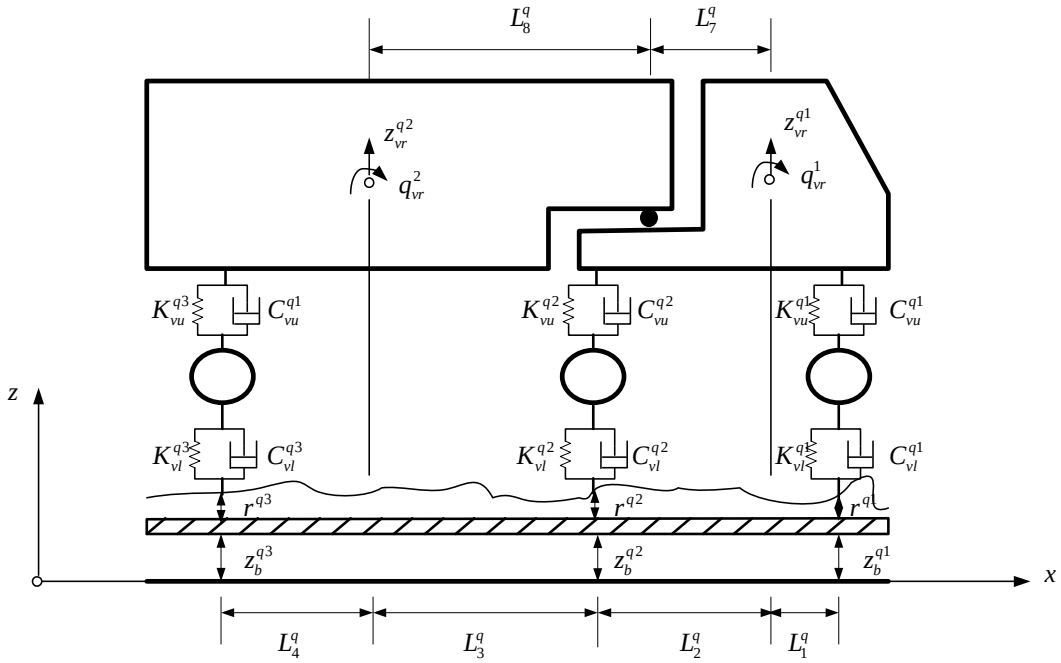

a. Full vehicle model

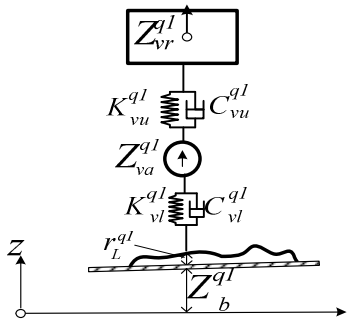

b. Quarter vehicle model

Fig. 3.3 Vehicle models

Table 3.2 Parameters of vehicle model (full-model)

Parameters	Unit	Heavy truck
Mass of each rigid body (M_v_i)	kg	[3930,15700]
Inertial moment of each rigid body in zy plane (I_v_i)	m4	[17395,29219]
Inertial moment of each rigid body in xz plane (J_v_i)	m4	[10500,147000]
Mass of each axle (M_a_L or M_a_R)	kg	[220,1500,1000]
Coefficient of upper vertical spring for each axle (K_u_L or K_u_R)	N/m	[2e6 4.6e6 5e6]

Coefficient of upper vertical damping for each axle (C_u_L or C_u_R)	N/(m/s)	[5e3 3e4 4e4]
Coefficient of lower vertical spring for each axle (K_l_L or K_l_R)	N/m	[1.73e6 3.74e6 4.6e6]
Coefficient of lower vertical damping for each axle (C_l_L or C_l_R)	N/(m/s)	[2e4 2e4 2e4]

Table 3.3 Parameters of CA model

Parameters	Value	Definition
Lc	7.5m	Length of each cell
dt	1s	The period of each time step
L-road	134 cells (1005m)	Number of cells (absolute length) of one lane of approaching roadway in one end
L-bridge	112 cells (840m)	Number of cells (absolute length) of one lane of bridge
ρ	0.07,0.15,0.24	Occupancy of the system(occupied cells/ all cells)
v_{type}	{0.2 0.3 0.5}	Percentage of three types of vehicles(v1, v2 and v3)
v_{max}	4	The maximum cells a vehicle can pass per second
pb	0.5	The probability of braking
pch	0.8	The probability of changing lane

3.4.2 Traffic flow simulation results

The traffic flow simulation results with CA technique usually become stable after a continuous simulation with a period which equals to 10 times the cell numbers (380 cells totally) of the highway system (Nagel and Schreckenberg 1992). Accordingly, in the present study, only the traffic flow simulation results between the range of 3,800 seconds and 4,100 seconds (totally 5 minutes) are used. The periodic boundary condition is applied which assumes the vehicle occupancy is constant for the highway system throughout the 5-minute period of simulation. For a comparison purpose, three different vehicle occupancies are considered: smooth traffic (vehicle occupancy ρ =0.07), median traffic (vehicle occupancy ρ =0.15) and busy traffic flow (vehicle occupancy ρ =0.24). All the basic parameters of the traffic flow simulation are summarized in Table 3.3.

Due to the symmetric nature of traffic flow, only the traffic flow results in the direction from west (left) to east (right) of the bridge are displayed. Fig. 3.4(a-b) shows the simulated traffic flow on

both the inner and outer lanes of the bridge when vehicle occupancies equal to 0.07 and 0.24. It can be found that the simulated traffic flow on both the inner and outer lanes under the same vehicle occupancy is similar. The *x*-axis and *y*-axis represent the coordinates in both spatial (along the bridge) and time domains, respectively. Each dot on the figure represents a vehicle (Fig.3.4). By picking any time (*y* value) and drawing a horizontal line, one can get a snapshot of the spatial distribution of vehicles along the bridge at that moment. Similarly, by picking any location on the bridge and drawing a vertical line, the time history of different vehicles passing the same spot on the bridge can be obtained. For the low traffic occupancy, the traffic flow is like laminar flow. With the increase of the traffic occupancy, local congestions may be formed at some locations as indicated by black belts in Fig. 3.4. Detailed statistical properties of the traffic flow on the bridge are presented in Table 3.3. It is easily found from Table 3.4 that the mean speed of the traffic flow decreases while the standard deviation of the vehicle speeds increases with the increase of the vehicle occupancy. In reality, with more vehicles moving on the same road, available spaces for vehicles to accelerate or decelerate are decreased and the mean speed of the whole traffic flow will decrease accordingly. A higher standard deviation of the vehicle driving speeds suggests higher speed variations among vehicles, which imply relatively higher potentials of traffic congestion and possible traffic conflicts (TRB 2007).

Table 3.4 Statistical property of traffic flow on bridge

Occupancy	Lane	Average speed μ (km/h)	Standard deviation σ (km/h)
0.07	Inner lane	93.89	14.04
	Outer lane	93.89	14.05
0.15	Inner lane	86.58	22.07
	Outer lane	86.70	22.09
0.24	Inner lane	55.14	36.84
	Outer lane	54.23	36.80

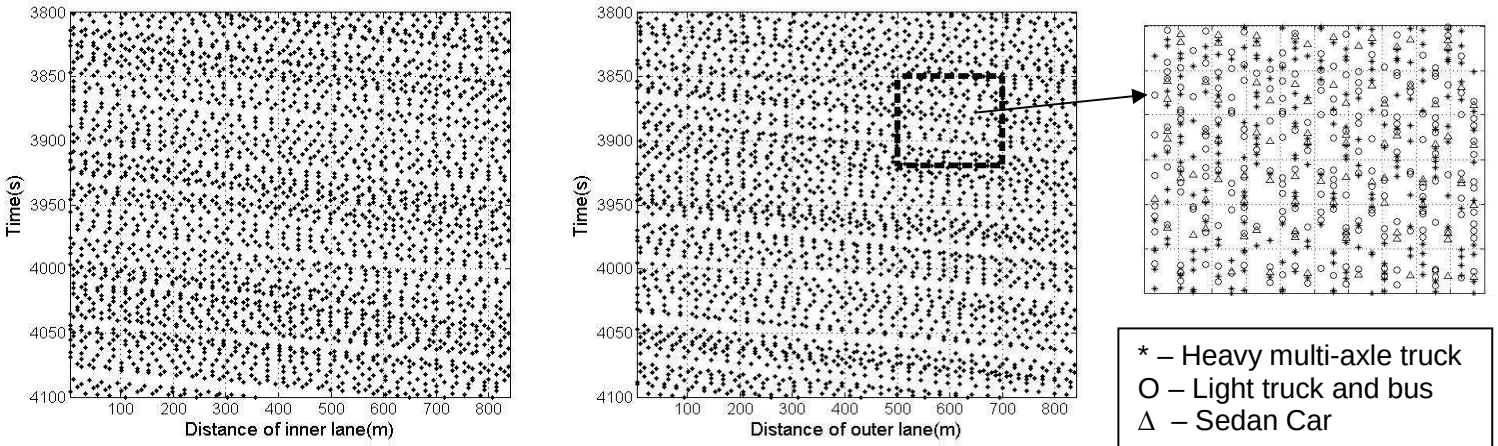

a. Occupancy ρ =0.07

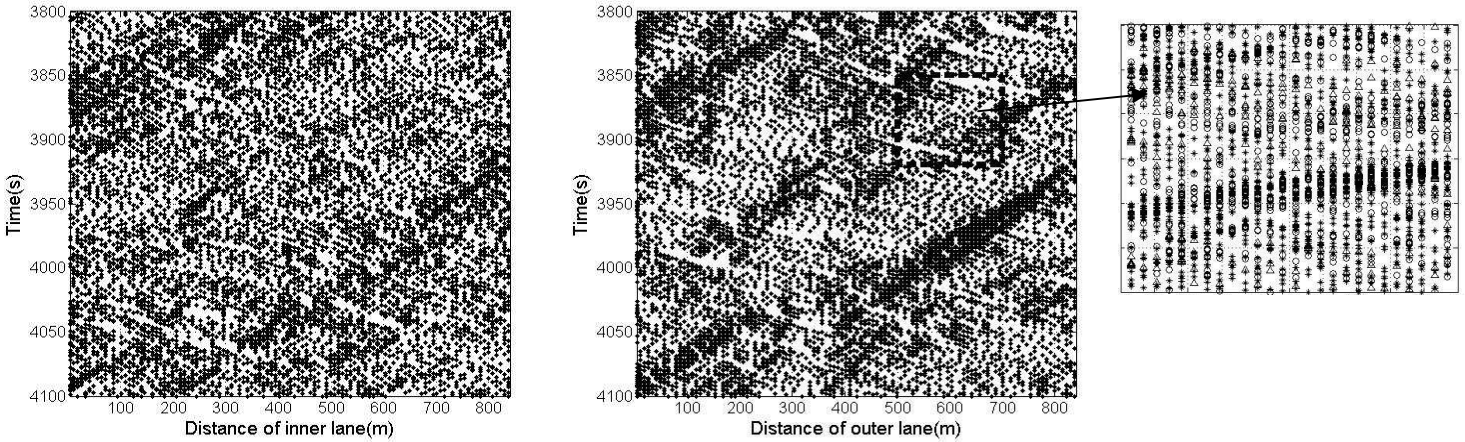

b. Occupancy ρ =0.24

Fig. 3.4 Simulated traffic flow on bridge with CA model

3.4.3 Equivalent dynamic wheel load factor (R)

Three types of different representative vehicle models: heavy truck, light truck and bus and sedan car (Tables 3.1 and 3.2) are considered to investigate respective equivalent dynamic wheel load factors (R). Fig. 3.5 gives the time history of the equivalent dynamic wheel load factor R on the inner lane when the wind speed U equals to 2.7m/s and 17.6 m/s, respectively. The vehicle travels with a speed of 7.5m/s from west (left) to east (right). Labels of "on bridge" and "on road" show the spatial locations of the vehicle corresponding to time in the *x* axis. Under both wind velocities, when a vehicle is on the road and heading to the bridge, R is very small as the vibration is primarily caused by the excitation of the pavement surface roughness. Much higher equivalent dynamic wheel loads are observed when the vehicles are on the bridge due to the dynamic interactions. After the vehicle leaves the bridge, R decreases slowly as the vibration excited by the bridge requires some time to be damped out. The comparisons of the results for the heavy trucks and light trucks under both weak and moderate wind speeds suggest that heavy trucks will cause much larger R than the light trucks. For heavy trucks, R is considerably amplified when the trucks are close to the middle point of the bridge compared to those at other locations on the bridge. It is understandable that the strongest dynamic interactions of large trucks have been observed at the middle point region of long-span bridges in previous studies (Xu and Guo 2003; Chen et al. 2007). The increase of the wind speed from 2.7 m/s to 17.6 m/s will increase R for the heavy truck considerably and will also increase R mildly for the light truck.

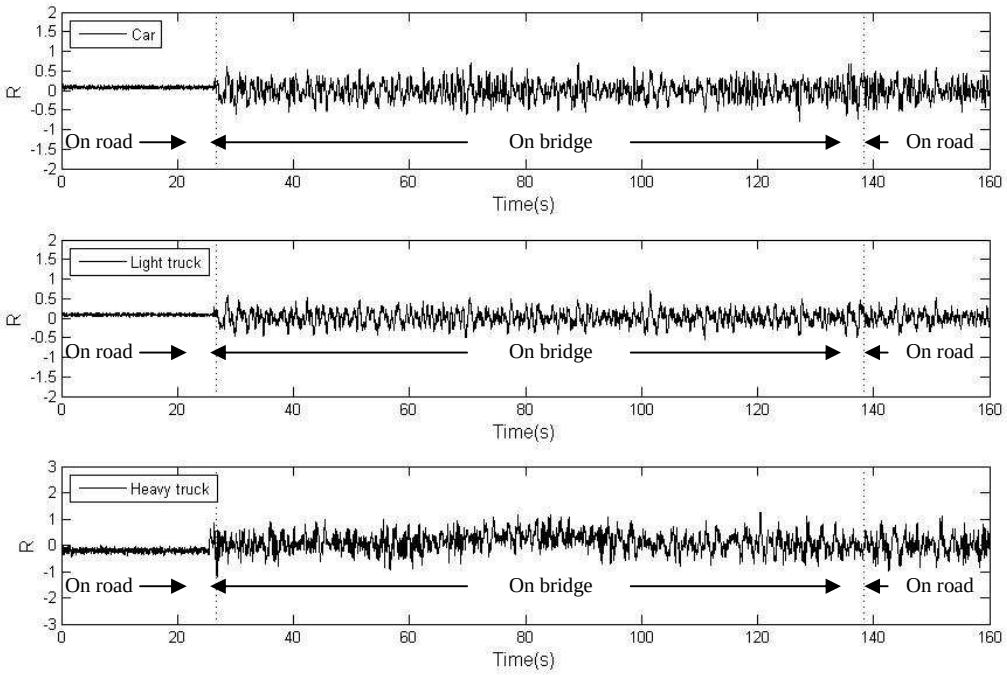

a. U=2.7m/s

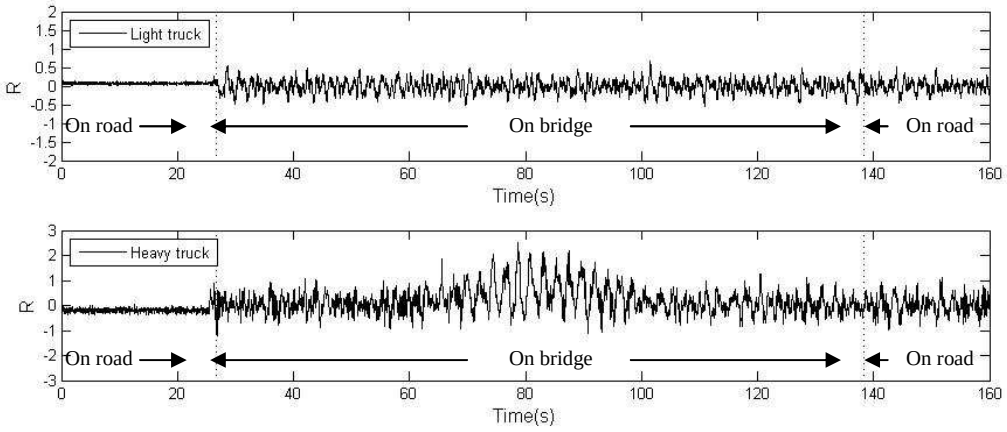

b. U=17.6 m/s

Fig. 3.5 Time history of R on inner lane under different wind speeds

The mean values of R for different types of vehicles with different driving speeds on the bridge under both breeze and moderate wind conditions are presented in Fig. 3.6. When the wind is very weak (U=2.7m/s), R for all the three types of vehicles are pretty close under a low vehicle driving speed (V < 15 m/s). The differences of R among different types of vehicles become larger when

the vehicle driving speed gets higher. The heavy truck has the largest R among all types of vehicles under the same driving and wind speeds. When the wind is moderate (U=17.6 m/s), the comparison of R between those of the light truck and the heavy truck shows that the heavy truck has a considerably larger mean value of R than that of the light trucks under the same wind and driving speeds. With the increase of the driving speed when the wind is moderate, the heavy truck also shows higher sensitivity to different driving speeds than the light truck. For both breeze and moderate wind conditions, with the increase of vehicle driving speeds, R of all types of vehicles has a "jump" when the vehicle driving speed increases from 15m/s to 22.5m/s. It suggests that although the EDWL factor R generally increases with the vehicle driving speed, the driving speed of 22.5m/s seems to be a critical threshold which will trigger a substantial increase of wheel loading on the bridge when the driving speed further increases in the present example. This critical value is probably related to the specific dynamic properties of the bridge and more insightful studies of different bridges may be needed in the future.

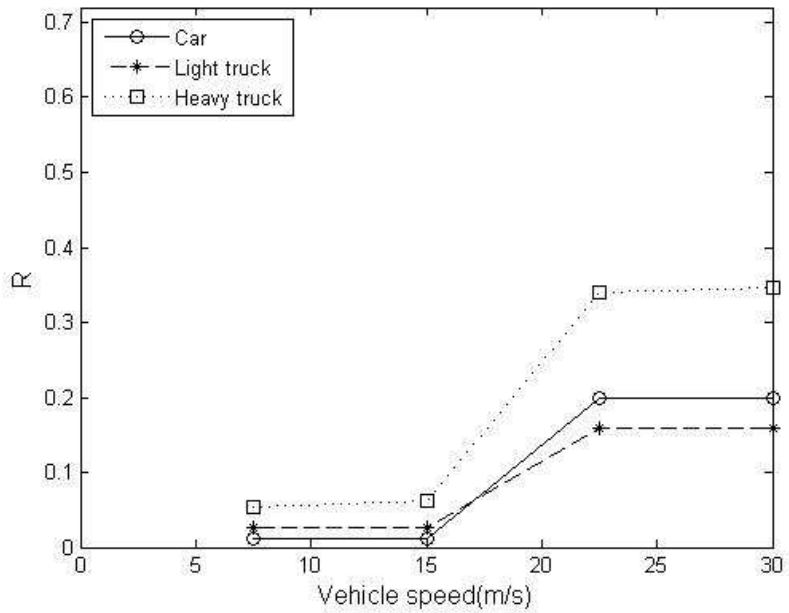

a. U=2.7 m/s

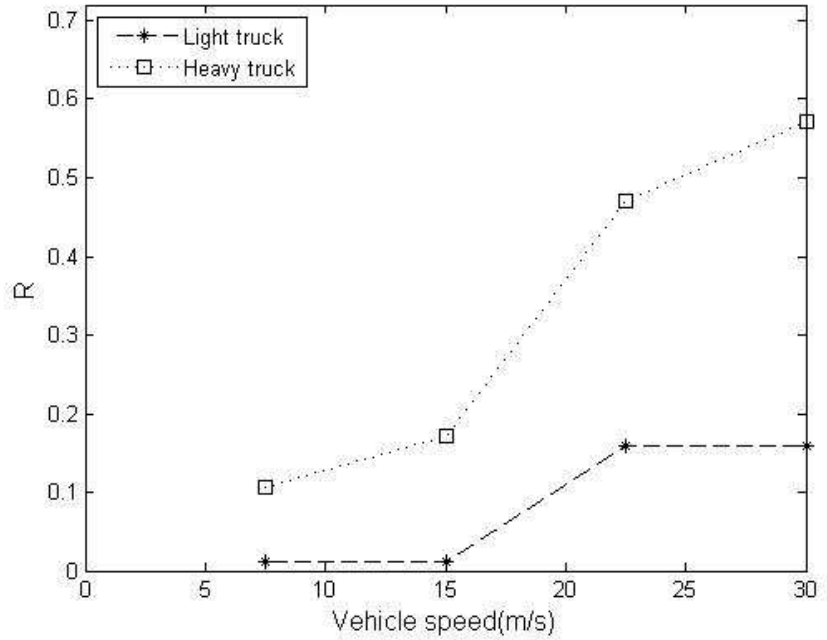

b. U=17.6 m/s

Fig. 3.6 Comparison of mean value of *R* under different wind speeds

3.4.4 Statistical bridge dynamic behavior

With the equivalent dynamic wheel load (EDWL) approach, time histories of displacement at any point along the bridge can be obtained by solving Eq. (3.4). As discussed above, statistical analyses of the bridge response are required in order to obtain converged statistical predictions of the bridge behavior. Statistical analyses of the time-history response after the simulation starts are conducted continuously to check the convergence. Fig.3.7 shows the mean values of bridge displacement and stress at the middle point of the main span under different averaging time when the wind speed is 17.6m/s. It is found that both the displacement and the stress results can gradually converge when the simulation time increases. In the present study, the 5-minute (300 seconds) simulation time is enough to generate stable results of the bridge response (e.g. displacement and stress) as the relative difference is constantly lower than 4% beyond the 5-minute averaging time. Under breeze, it has been found it takes even shorter time for the bridge

response to converge (results not shown here). Therefore, in following sections, all the statistical results are those obtained from a convergence analysis with a time period of 5 minutes (300 seconds).

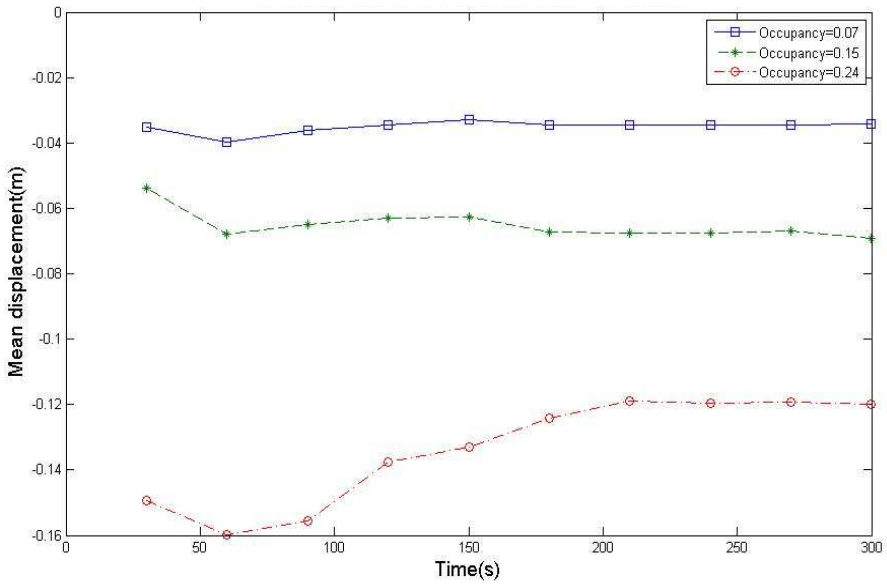

a. Mean displacement

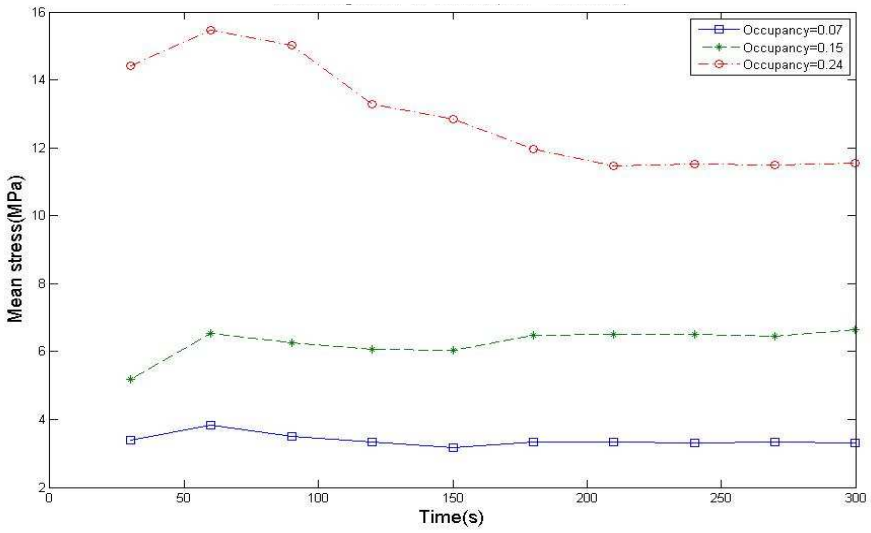

b. Mean stress

Fig. 3.7 Convergence analysis results of displacement and stress

The midpoint of the main span of a long-span bridge is usually the critical location which typically has the largest bridge response. Time histories of the vertical response at the midpoint of

the bridge under different traffic flow occupancies (ρ =0.07, 0.15, 0.24) and wind speeds (U=2.7, 17.6m/s) are presented in Fig. 3.8. The mean value as well as the absolute value of coefficient of variance |COV| of the vertical displacement is given in Fig.3.9 under different combinations of traffic occupancy and wind speed. It is found that the mean value of the bridge displacement at the midpoint generally increases with wind speed and vehicle occupancy (Fig. 3.9(a)). Under both breeze and moderate wind conditions, the vehicle occupancy plays a more significant role than the wind speed on the bridge displacement. For example, the mean value of the bridge displacement increases from 0.04 m to 0.11 m when the vehicle occupancy increases from 0.07 to 0.24 (wind speed is 17.6 m/s). This phenomenon, for one more time, justifies the importance of including traffic load into the bridge buffeting analysis especially when the wind speed is not very high. The |COV| increases with the increase of wind speeds, while decreases with the increase of vehicle occupancy (Fig. 3.9(b)). It is found that the |COV| becomes the maximum when the occupancy is 0 (i.e. no traffic flow on the bridge). When the road is densely occupied by vehicles, as indicated by higher values of the vehicle occupancy, the randomness level of the traffic flow (e.g. variations of speeds) on the bridge is reduced as reflected by lower |COV| of the bridge displacement.

Mean stress values at the bottom and top fibers of the girder along the whole bridge are presented in Fig. 3.10 and the *x* axis is the spatial position along the bridge. It can be found the largest stress level happens at the midpoint of the bridge. The mean stress shows a slight increase when wind speed increases from 2.7 m/s to 17.6 m/s. Under the same wind speed, the mean stress value increases with the increase of vehicle occupancy considerably. The extreme tension stress on both the bottom and the top of the fibers of the girders during the 5-minute simulation are displayed in Fig. 3.11. It is obvious that the largest tension stress happens on the bottom fiber of the girder at the midpoint of the bridge. The top fiber of the girder may experience tension stress in some situations with much lower amplitudes compared to the bottom fibers. Significant increase of

stress can be observed at the higher wind speed and higher vehicle occupancies compared to that under breeze and under low vehicle occupancy, respectively.

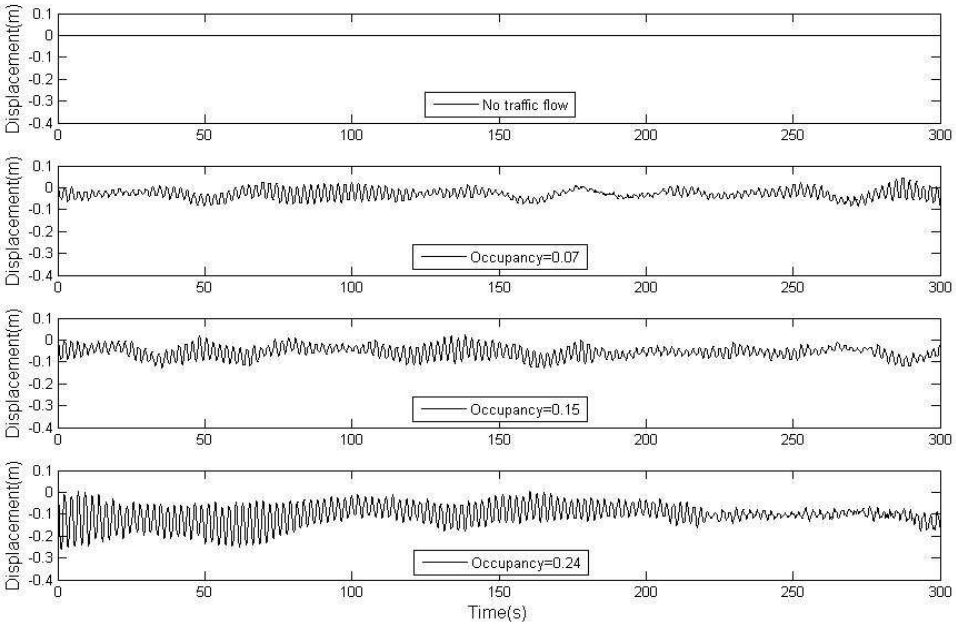

a. Wind speed =2.7m/s

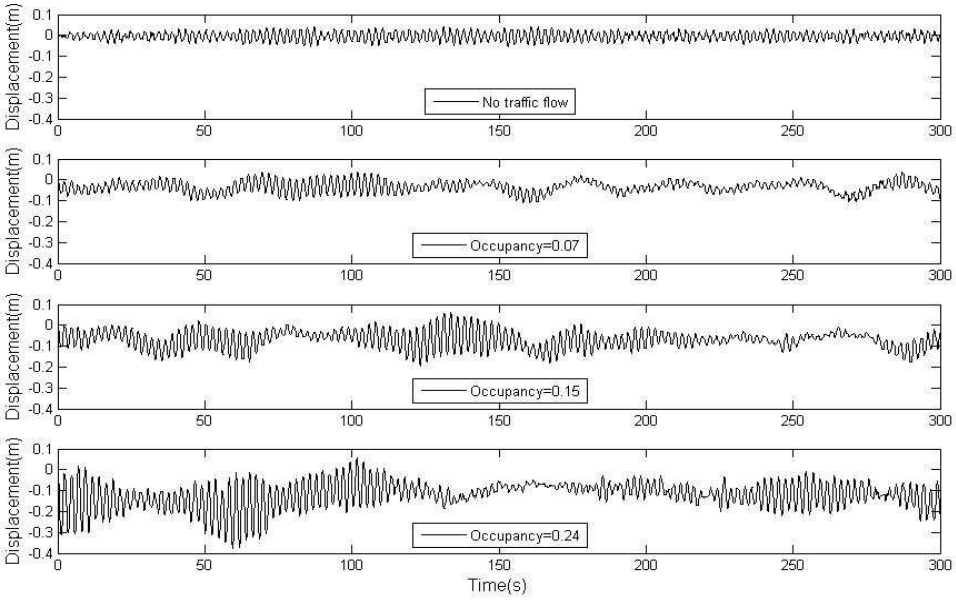

b. Wind speed =17.6m/s

Fig. 3.8 Time history of vertical displacement at midpoint

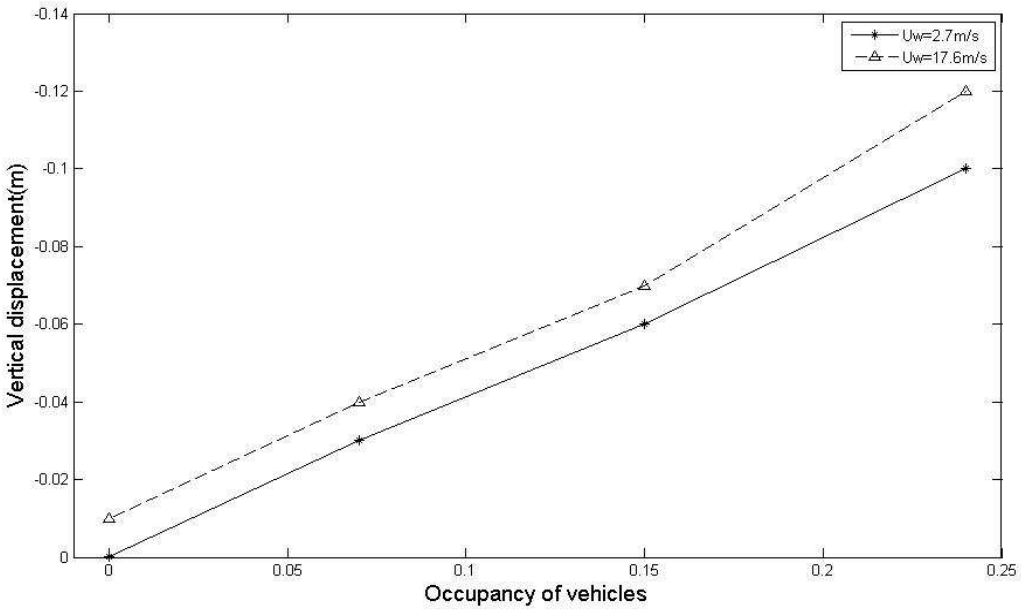

a. Mean value comparison

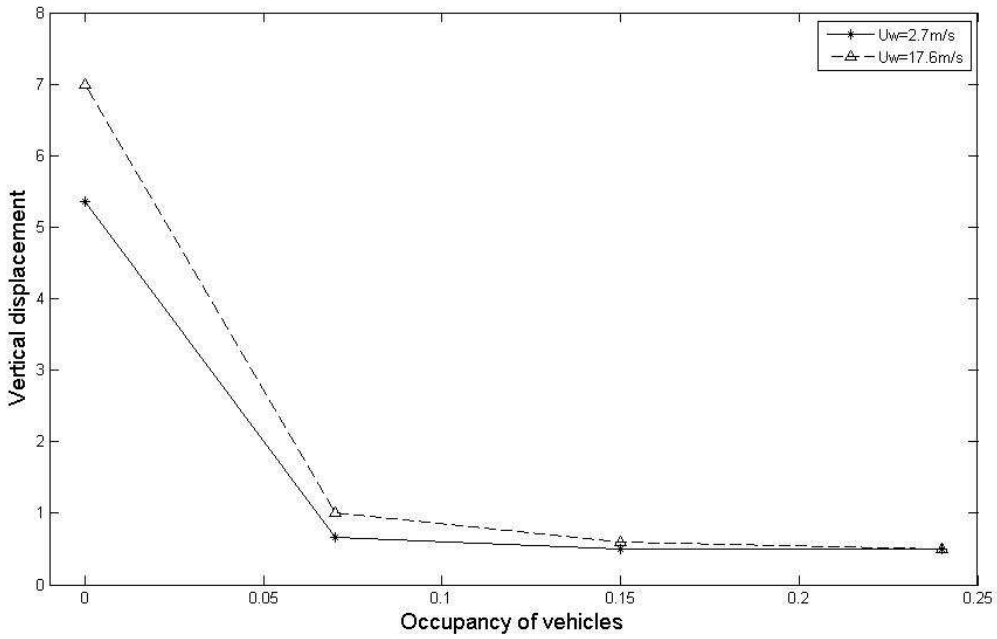

b. |COV| comparison

Fig. 3.9 Statistical results of vertical displacement at midpoint of the bridge

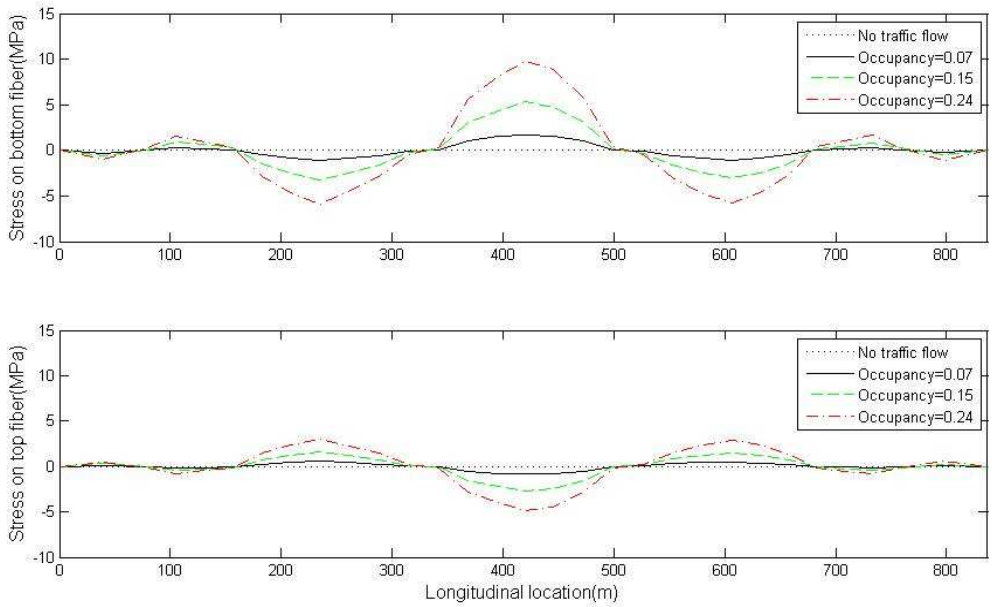

a. Wind speed =2.7m/s

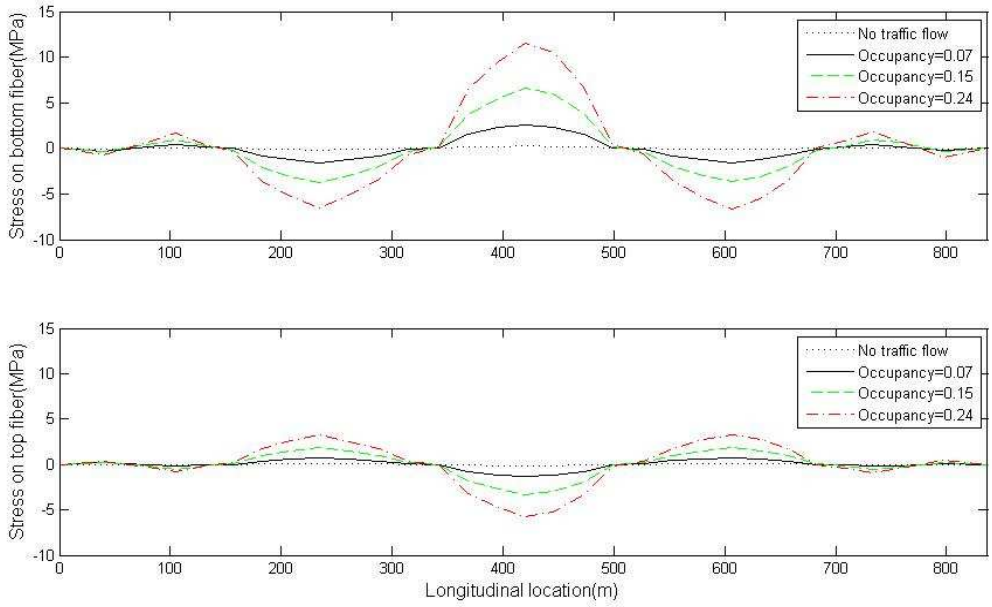

b. Wind speed =17.6m/s

Fig. 3.10 Mean stress contour along the bridge

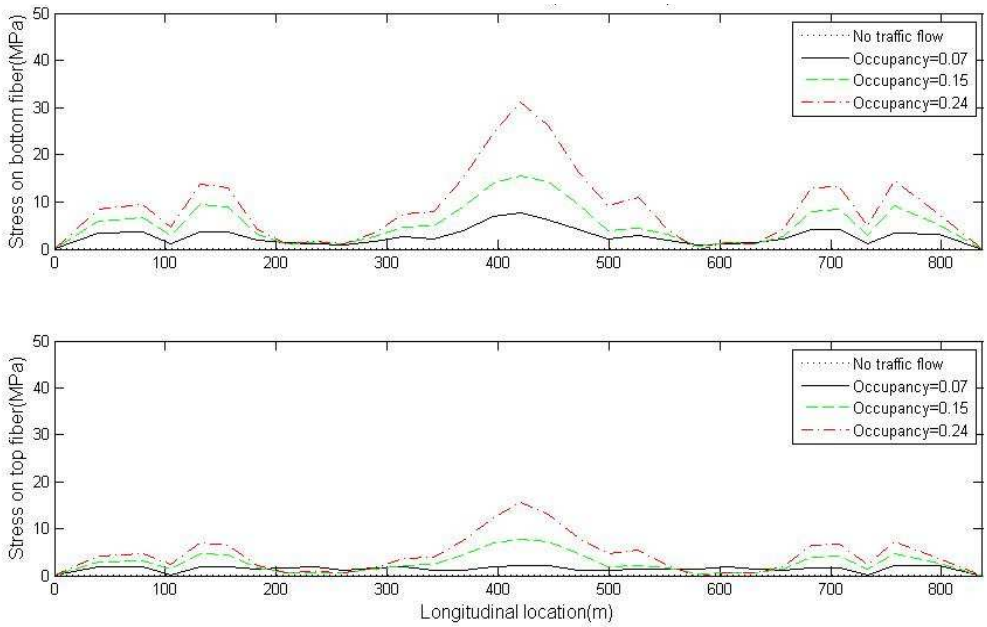

a. Wind speed =2.7m/s

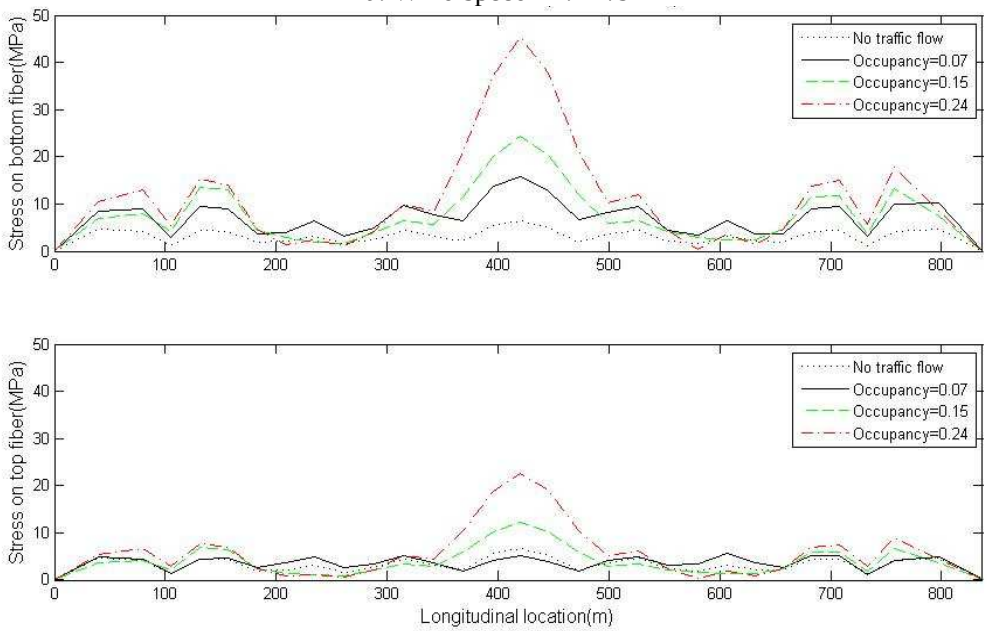

b. Wind speed =17.6m/s

Fig. 3.11 Extreme tension stress contour along the bridge

Since the tension stress at the midpoint of the bridge is the highest along the whole bridge, the mean value, COV and extreme value of the tension stress at the bottom fiber of the midpoint of the bridge are further studied under different vehicle occupancies (Fig. 3.12). The mean stress at

the midpoint of the bridge increases almost linearly with the vehicle occupancy under the same wind speed (Fig. 3.12(a)). It is found the vehicle occupancy has larger impacts than the variation of wind speeds (i.e. from breeze to moderate wind) has on the mean stress level. For example, when the vehicle occupancy is 0.07, the mean stress under the 17.6m/s wind speed is about 0.83 MPa larger than that under the 2.7 m/s wind speed. When the vehicle occupancy is 0.24 and other conditions remain the same, the difference of mean stress levels increases to 1.74 MPa. As shown in Fig. 3.12(b), the coefficient of variation (COV) of stress decreases with the increase of vehicle occupancy under both wind speeds. It is probably because more densely occupied road will have limited flexibility for vehicles to change lanes or accelerating. As a result, the fluctuations of spatial distributions of the vehicles on the bridge are reduced, which in turn reduce the fluctuations of stress on the bridge under both wind and traffic. It is also found that the COV under moderate wind is larger than that under breeze, which suggests that stronger wind may reinforce the fluctuations of stress along with impacts from traffic (Fig. 3.12 (b)). Fig. 3.12(c) gives the results of extreme stress and it suggests that higher wind speeds will cause larger extreme stress on the bridge. When the vehicle occupancy is 0.24 and the wind speed is 17.6 m/s, the extreme stress can be around 45.32 MPa at some time instances.

3.5 Discussion and Conclusion

An innovative “semi-deterministic” Bridge/Traffic/Wind interaction analysis model considering stochastic traffic flow and wind was developed. The approach adopts the cellular automaton (CA) traffic flow simulation technique and the equivalent dynamic wheel load approach (EDWL) to consider the stochastic traffic flow and dynamic interactions, respectively. As a result of adopting the proposed model, the performance of long-span bridges can be predicted in a more realistic way by considering the combined load of stochastic traffic and wind integrally. A case study with a prototype cable-stayed bridge was conducted with the proposed analytical approach. Although the proposed approach was demonstrated through a slender long-span bridge, it actually can also

be applied to other conventional long-span bridges which are not sensitive to wind and even pavement-traffic-wind interactions. The detailed applications on conventional long-span bridges and pavement-traffic interaction analysis, however, are beyond the scope of the present study and will be investigated separately. The proposed "semi-deterministic" interaction analysis model will also serve an important basis to develop a reliability-based model to consider uncertainties of many variables associated with bridge, traffic and wind.

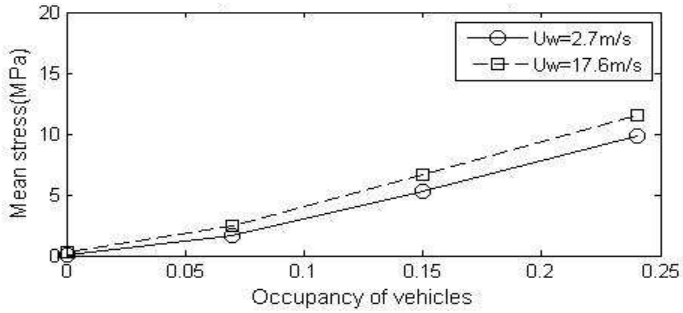

a. Mean stress

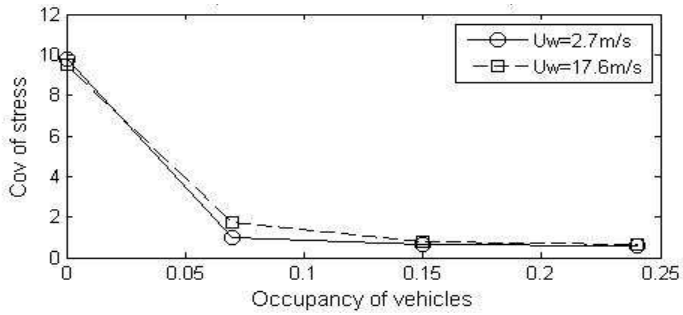

b. Coefficient of variation (COV)

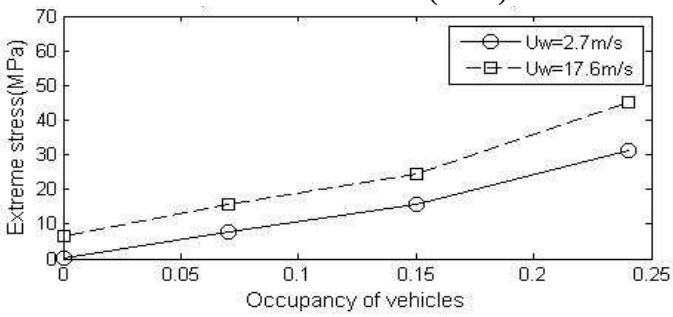

c. Extreme stress

Fig. 3.12 Comparison of statistical value of stress at bottom fiber at midpoint of the bridge

In the case study, the traffic flow on the bridge as well as the approaching roadways with four lanes was simulated. Based on the simulated traffic flow, the statistical dynamic responses such as displacement and stress of the bridge under both the low and moderate wind speeds in normal service conditions were studied. In the present study, it took a common personal computer about 2 hours to conduct the Bridge/Traffic/Wind interaction analysis after the EDWL database was developed. The reasonable efficiency of the proposed model allows for the adoption into typical engineering analyses.

The developed approach in the present study has been partially validated on the EDWL approach by comparing the results considering several vehicles (Chen and Cai 2007). A full validation of the proposed model considering stochastic busy traffic, however, still remains a challenge as a comparison of statistical results, other than deterministic results, should be made. Due to the extremely time consuming nature of "fully-coupled" analysis, to get a converged statistical result (e.g. 5 minutes in the case study using EDWL) will be extremely hard, if not impossible at all. It is expected that the developed model can be validated and calibrated by comparing the predictions with actual bridge response measured by health monitoring techniques in the future.

3.6 References

ASCE (2003). Assessment of performance of vital long-span bridges in the United States, ASCE Sub-committee on performance of Bridges, edited by Richard J. Kratky.

Baker, C. J. (1991). "Ground vehicles in high cross winds. Part I: Unsteady aerodynamic forces." Journal of fluids and structures, 5, 91–111.

Cai, C. S. and Chen, S. R. (2004). "Framework of vehicle-bridge-wind dynamic analysis." Journal of Wind Engineering & Industrial Aerodynamics, 92 (7-8), 579-607.

Calcada, R., Cunha, A., Delgado, R. (2005). "Analysis of traffic-induced vibrations in a cable-stayed bridge. Part II: Numerical modeling and stochastic simulation." Journal of Bridge Engineering, 10 (4), 386–397.

Chen, S. R. (2004). "Dynamic performance of bridges and vehicles under strong wind." Ph. D. Dissertation. Louisiana State University, Baton Rouge, USA, 2004.

Chen, S. R. and Cai, C. S. (2006). "Unified approach to predict the dynamic performance of transportation system considering wind effects." Structural Engineering & Mechanics, 23(3), 279-292.

Chen, S. R., Cai, C. S. and Levitan, M. (2007). "Understand and improve dynamic performance of transportation system- A case study of Luling Bridge." Engineering Structures, 29, 1043-1051.

Chen, S.R. and Cai, C.S. (2007). "Equivalent wheel load approach for slender cable-stayed bridge fatigue assessment under traffic and wind: feasibility study." Journal of Bridge Engineering, 12(6), 755-764.

Chen, Y.B. and Feng, M.Q. (2006). "Modeling of traffic excitation for system identification of bridge structures." Computer-Aided Civil and Infrastructure Engineering, 21, 57-66.

Ditlevsen, O (1994). "Traffic loads on large bridges modeled as white-noise fields." Journal of Engineering Mechanics, 120(4), 681-694.

Ditlevsen, O and Madsen, H. O. (1995). "Stochastic vehicle-queue-load model for large bridges." Journal of Engineering Mechanics, 120 (9), 1829-1874.

National Research Council (2000). Highway Capacity Manual, Washington, D.C.

Huang, D. (2005). "Dynamic and impact behavior of half-through arch bridges." Journal of Bridge Engineering, 10(2), 133-141.

Huang, D. Z. and Wang, T. L. (1992). "Impact analysis of cable-stayed bridges." Computers & Structures, 31, 175-183.

Jain, A., Jones, N. P. and Scanlan, R. H. (1996), "Coupled aeroelastic and aerodynamic response analysis of long-span bridges." Journal of Wind Engineering and Industrial Aerodynamics, 60 (1–3), 69–80.

Li, X.G., Jia, B., Gao, Z.Y. and Jiang, R. (2006). "A realistic two-lane cellular automata traffic model considering aggressive lane-changing behavior of fast vehicle." Physica A, 367, 479-486.

Moses, F. (2001). Calibration of load factors for LRFR bridge, Transportation Research Board, NCHRP Report, No. 454.

Nagel, K. and Schreckenberg, M. (1992). "A cellular automaton model for freeway traffic." Journal de Physique I France, 2(12), 2221-2229.

Nowak, A.S. (1993). "Live load models for highway bridges." Structural Safety, 13, 53-66.

O'Connor, A. and O'Brien, E. (2005). "Mathematical traffic load modeling and factors influencing the accuracy of predicted extremes." Canadian Journal of Civil Engineering, 32(1), 270–278.

Pines, D. and Aktan, A. E. (2002). “Status of structural health monitoring of long-span bridges in the United States.” Progress in Structural Engineering and Materials, 4(4), 372-380.

Rickert, M., Nagel, K., Schreckenberg, M. and Latour, A. (1996). “Two lane traffic simulations using cellular automata.” Physica A, 231, 534-550.

Schadschneider, A. (2006). “Cellular automata models of highway traffic.” Physica A, 372, 142–150.

Shafizadeh, K. and Mannering, F. (2006). “Statistical modeling of user perceptions of infrastructure condition: Application to the case of highway roughness.” Journal of Transportation Engineering, 132(2), 133-140.

Simiu, E. and Scanlan, R. H. (1996). Wind Effects on Structures - Fundamentals and Applications to Design, 3rd Edition, Wiley, New York.

TRANSIMS Travelogues, Transportation analysis and simulation system, Los Alamos National Laboratory, Los Alamos, <http://www-transims.tsasa.lanl.gov/travel.shtml>, lastly accessed on April 30th 2008.

Transportation Research Board (TRB) (2007). “The domain of truck and bus safety research.” Transportation Research Circular, Number E-C117, May 2007.

Wu, J. and Chen, S. R. (2008). “Traffic flow simulation based on cellular automaton model for interaction analysis between long-span bridge and traffic.” Inaugural International Conference of the Engineering Mechanics Institute (EM08), May 18-21, 2008.

Xu, Y. L., Guo, W. H. (2003). “Dynamic analysis of coupled road vehicle and cable-stayed bridge system under turbulent wind.” Engineering Structures, 25, 473-486.

CHAPTER 4: PROBABILISTIC DYNAMIC BEHAVIOR OF LONG-SPAN BRIDGES UNDER EXTREME EVENTS

4.1 Introduction

Long-span bridges usually support a large volume of traffic and locate on oceans, grand rivers or valleys where the wind speed at the typical height of the bridge decks can be considerably high. In addition to moderate wind and normal traffic scenarios, it is known that some extreme (or adverse) events may also occur. These extreme events may include complex traffic congestion on the bridge, coupled with moderate or even strong wind. For example, severe traffic congestions may be formed on the bridge or connecting roadways as a result of an evacuation or a partial blockage of driving lanes due to traffic accidents, construction or maintenance. For hurricane evacuations, there is usually a lot of traffic passing through the bridge before the landfall while the wind speed may become pretty high already (Chen et al. 2009).

It is known that the excessive dynamic response and stress level of the bridge under these rare but critical scenarios, even for a very short period, may cause critical damage initiation or accumulation on some local bridge members. In addition to accelerating damage, the extreme events (e.g. heavy traffic) may even trigger the hazardous collapse of a whole bridge by breaking the "weakest link" in some rare cases, especially when some hidden damage or design flaw has not been detected. One recent example is the Minnesota bridge failure which occurred during rush hours with heavy traffic. For slender long-span bridges, strong wind may also cause threats by working interactively with heavy traffic loads. Therefore, even though the extreme cases associated with congested traffic and/or windy weather may be relatively rare and the durations

could be short, it is still important for bridge engineers to appropriately look into these unusual extreme events during structural design and life-time management of these critical infrastructures.

In the AASHTO LRFD specification (2007), the only limit state similar to the scenarios discussed above is “Strength V”, which is descriptively defined as “a load combination relating to normal vehicular use of the bridge with wind of 55 mph velocity.” No detailed information about how the “normal vehicle use” has been defined in the specification, except for adopting the standard design vehicles as live loads. It is usually understandable as the specification was developed from and also primarily for short and medium-span bridges. For long-span bridges, it is known that multiple presence of heavy vehicles are very likely on long-span bridges and the simple assumption of single design truck plus lane load, or two trucks spaced at 50 ft, used in the LRFD specification (AASHTO 2007), may not capture the worst case scenarios of long-span bridges (Chen and Cai 2007; Wu and Chen 2009). As a result, it is not clear to which extent the worst-case scenarios of long-span bridges are actually representative from the perspective of identifying critical dynamic response and stress. To understand and further capture the worst case scenarios of dynamic response, strength and serviceability for a long-span bridge, an analytical platform, which is able to be used to appropriately replicate the extreme situations and further investigate the performance of long-span bridges, is desirable. However, to the knowledge of the writer, little study about critical scenarios of long-span bridges under extreme events can be found in literatures.

By applying the general Bridge/Traffic/Wind coupled analysis methodology developed in Chapter 3, the present study focuses on (1) conducting the CA-based traffic flow simulation of a long-span bridge and connecting roadways under incidental situations; (2) defining representative scenarios for the extreme events, and (3) numerically studying the bridge performance under these possible extreme events. Through conducting studies of a comprehensive set of typical

scenarios, it is anticipated that better understanding of extreme events of long-span bridges from the design perspectives of strength and serviceability can be achieved, which may eventually contribute to the future design specification for long-span bridges. The methodology introduced here will also offer a general methodology for researchers and engineers to define probabilistic traffic flow, characterize dynamic interaction and assess structural performance in those rare but critical situations for long-span bridges.

4.2 Bridge Performance under Extreme Events

4.2.1 Bridge/Traffic/Wind interaction analysis using CA model and EDWL approach

The analytical framework on Bridge/traffic/Wind interaction integrated Cellular Automaton (CA) traffic model and equivalent dynamic wheel loading approach has been already described in detail in Chapter 3. Thus, the basic information of the interaction model is briefly introduced for the sake of completeness.

The cellular automaton (CA)-based traffic flow model of the “roadway-bridge-roadway” system was introduced in Chapter 2. The normal situation in this chapter refers to the scenarios when the lane numbers of the approaching roadways and the bridge are the same. In reality, the typical incidental cases for traffic flow simulation is that part of a lane may be closed either on the bridge or on the approaching roadway due to traffic accidents, regular maintenance or construction. As a result, one lane of the bridge or one portion of a lane of the approaching roadway may be closed for a certain period of time. Accordingly, the bridge and the approaching roadways will have different numbers of available lanes. In contrast to the normal situation, these scenarios are referred as the “blockage situation”. The specific CA traffic rule for both “normal” and “blockage” situation can be referred to Chapter 2.

When the traffic flow information is obtained, the EDWL approach is applied. Firstly, the fully-coupled bridge/single-vehicle/wind analysis considering road roughness is conducted to find the equivalent dynamic wheel loadings for each specific type of vehicle with certain speed under the concerned wind speed. Then, the collective dynamic wheel loadings on bridge induced by vehicle, wind on vehicle and road roughness at any moment combining the traffic information from CA model can be obtained. The Bridge/Traffic/Wind analysis is thus converted into the problem of bridge under moving loads and wind speed which can be solved quickly as the dimension of mass, stiffness, damping and force matrices has been largely reduced.

4.2.2 Prototype bridge and extreme events

A four-lane highway system consisting of a long cable-stayed bridge with the length of around 840 m and the approaching roadway of 1008 m at each end of bridge is studied as an example. Two typical scenarios of road incidents are defined. Incident I is that one lane of the approaching way on the downstream side of the bridge is blocked (hereafter refer to “road blockage”) and Incident II is that one lane of the bridge is closed (hereafter refer to “bridge blockage”) (Fig.4.1). The reason to select the downstream side of roadways is due to the relatively larger impacts on the traffic congestion on the bridge than those of the upstream side based on a preliminary analysis. These two incidents represent the lane closure due to work zone or serious accidents happening on the bridge or on the approaching roadways, respectively. Two wind speeds, including “normal wind” (U= 2.7 m/s) and “strong wind” (U=32.8 m/s), are selected to represent the breeze situation and the strong wind situation, such as a severe wind storm or before the landfall of hurricane.

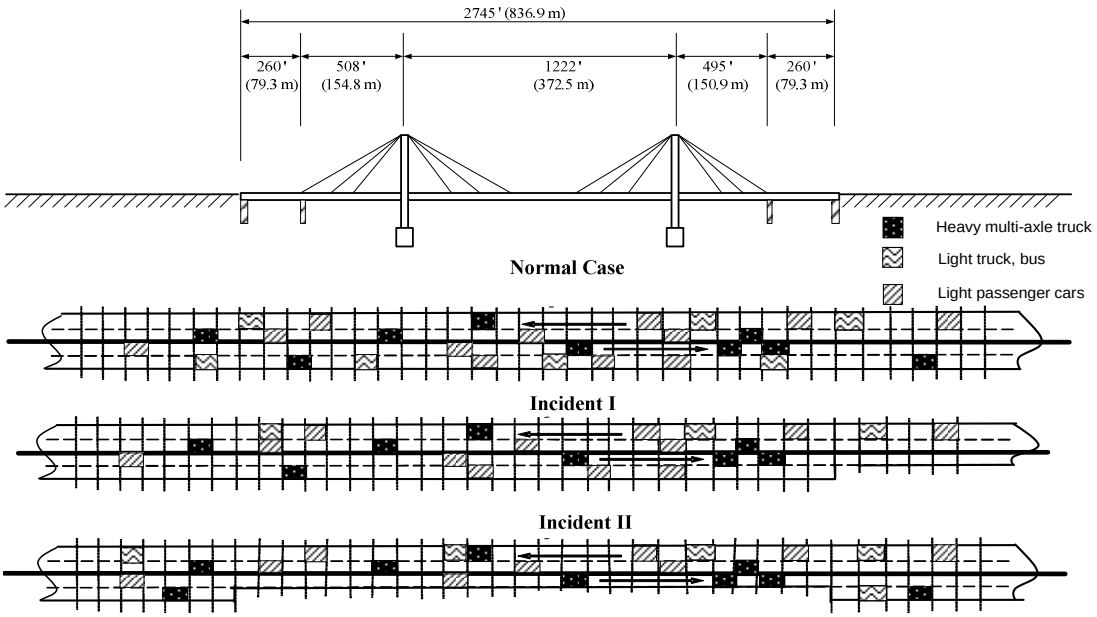

Fig. 4.1 Bridge elevation and roadway layout

The different combinations of possible scenarios include (1) normal wind and "road blockage"; (2) normal wind and "bridge blockage"; (3) normal wind and bumper-to-bumper traffic; (4) strong wind and normal traffic; (5) strong wind and "road blockage"; (6) strong wind and "bridge blockage"; and (7) strong wind and bumper-to-bumper traffic. The first two extreme events (1) and (2) are to simulate the case when the lane-blockage occurs along with normal wind condition. The extreme event (3) is to study the general evacuation scenario for any emergency or the early evacuation stage of hurricane when the wind speed is still normal. The extreme event (4) is to simulate the case with a severe wind storm, but no evacuation. The extreme events (5-7) represent several rare cases in the late evacuation stage of hurricane when wind speed is already pretty high and the blockage or serious traffic jam may occur simultaneously.

4.2.3 Stochastic traffic flow and live loads on bridge under extreme events

For different long-span bridges, the traffic volumes as well as the composition of vehicle types on the bridge vary from one place to another. In order to provide some general insights in the present study, the representative values of traffic density and vehicle type composition will be adopted.

According to the Highway Capacity Manual (2000), the traffic densities of 9, 20 and 32 vehicle/km/lane, represent comfortable, medium and severe driving conditions, respectively. The percentages of heavy trucks, light trucks and sedan cars among all the vehicles in the traffic flow are chosen as 0.5, 0.3 and 0.2, respectively. The speed limit is set as 4 cells/s which is equivalent to 113 km/h (Chen and Wu 2009). The probabilities for braking and lane changing are assumed to be 0.5 (*pb*) and 0.8 (*pch*), respectively.

The difference between the inner lane and the outer lane for one driving direction is typically insignificant for the normal condition as the lane-changing rule decrease the difference between the traffic flow on the two lanes (Wu and Chen 2008). So only the results of the inner-lane traffic flow in the normal condition will be used to compare with the results of traffic flow on the available lane for the incidental situations, as shown in Fig. 4.2. The subplots on the left, middle and right side stand for the “normal” case, the “road blockage” case and the “bridge blockage” case, respectively. The 5-mininute simulation period is sufficient to consider the randomness of the traffic flow in order to obtain stable mean stress and displacement results of the bridge for one specific traffic density as well as vehicle composition (Chen and Wu 2009). With the increase of the traffic density, it can be found in Fig. 4.2 that traffic congestion gradually becomes severer (shown as thick black belts) under the “road blockage” case compared with the “normal” case. In a contrast, the congestion is moderate for the “bridge blockage” case even with the increase of the vehicle density. This is due to the fact that severe congestion has already been formed on the approaching roadway before the vehicles enter the bridge. As a result, there is only limited number of vehicles which are able to actually move onto the bridge (Wu and Chen 2008).

Normal condition Road blockage Bridge blockage

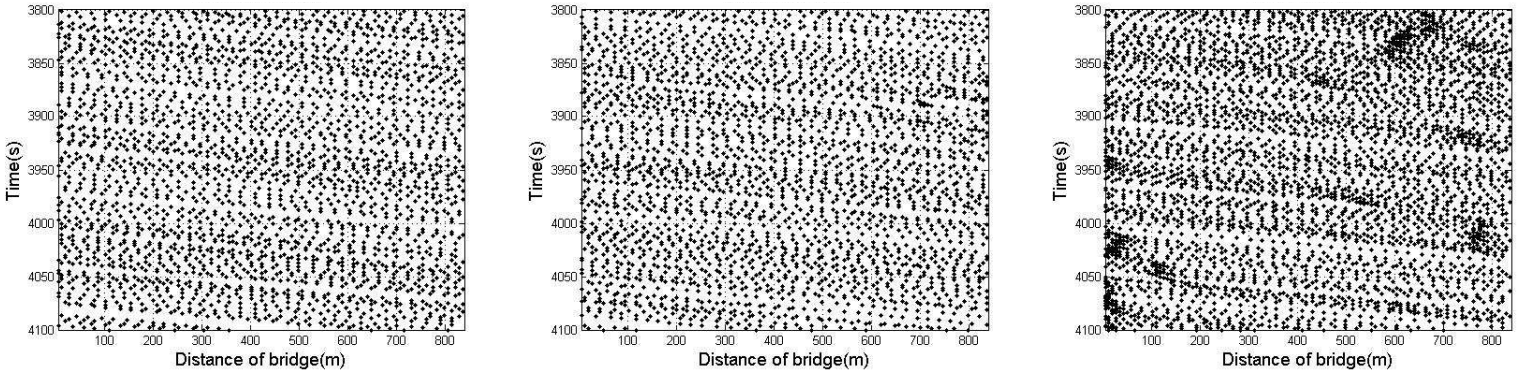

a. Vehicle density=9 veh/km/lane

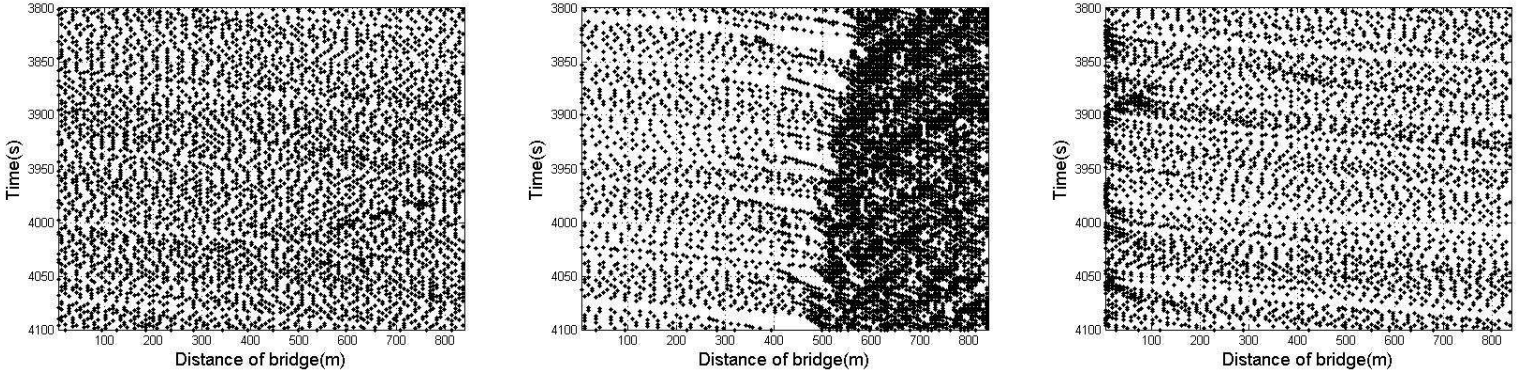

b. Vehicle density=20 veh/km/lane

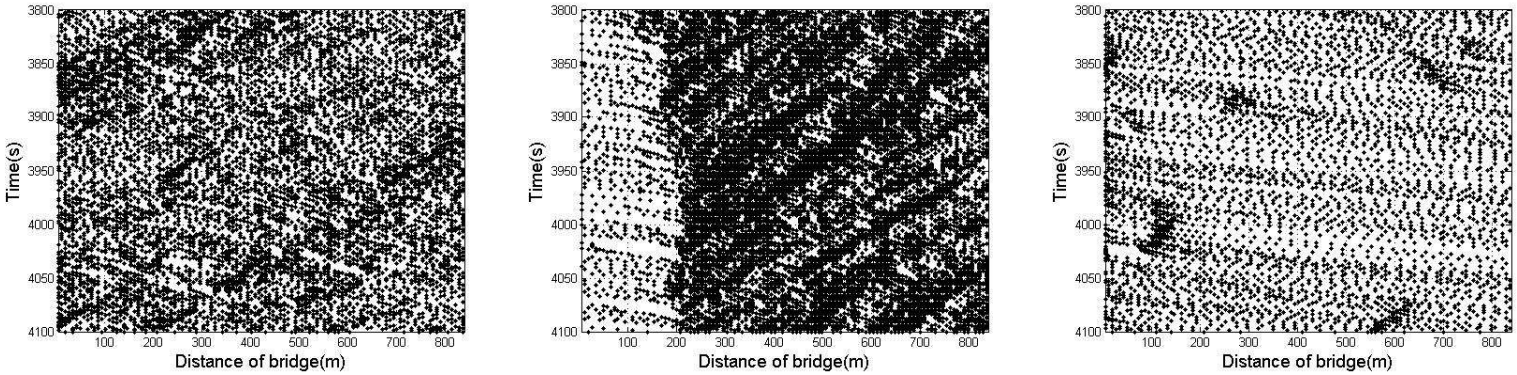

c. Vehicle density=32 veh/km/lane

Fig. 4.2 Comparison of traffic flow for each road condition

It has been found that the vehicle density has significant impacts on the overall velocity of the traffic flow, which is closely related to the dynamic impacts on bridges (Chen and Wu 2009). From Fig. 4.3, it can be observed that the mean velocity drops dramatically with the increase of the vehicle density. For the normal road condition, the mean velocity decreases from 93.89 km/h to 55.14 km/h when the traffic density varies from 9 vehicle/km/lane to 32 vehicle/km/lane. The mean velocity decreases from 94.93 km/h to 30.78 km/h for the "road blockage" condition and from 85.24 km/h to 21 km/h under the "bridge blockage" condition. Thus, the mean velocity under the "bridge blockage" condition is the minimum among all the cases and the normal road conditions is the maximum when vehicle density is medium and large.

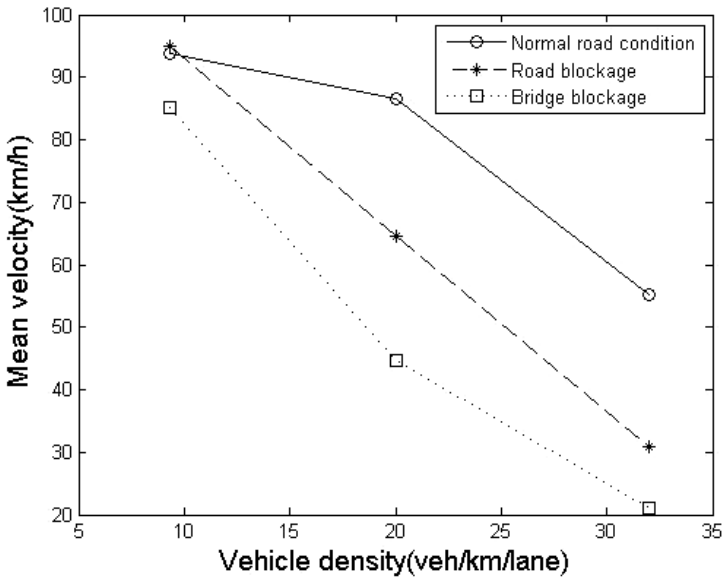

Fig. 4.3 Mean velocity vs. vehicle density

In contrast, the coefficient of variation (COV) of the driving speeds increases with the increase of the vehicle density (Fig. 4.4). It is because that the traffic flow becomes smoother when the vehicle density is small as more space is available to enable relatively constant speed with fewer stops or lane-changing maneuvers. The COV of the mean speed is the largest under the "bridge blockage" condition and is the smallest under the normal road condition. Fig. 4.5 gives the mean

values of the total static weight of all the vehicles on the two lanes of the bridge over time under different road conditions (i.e. “normal”, “road blockage” and “bridge blockage”). When the traffic density is low, there is little difference of the cumulative weight of the vehicles remaining on the bridge for all the three cases. It is found that the “road blockage” scenario becomes more critical among all the three cases with the increase of the traffic density. Comparatively, the “bridge blockage” is found to be the least critical one among all the three cases when the traffic density is high.

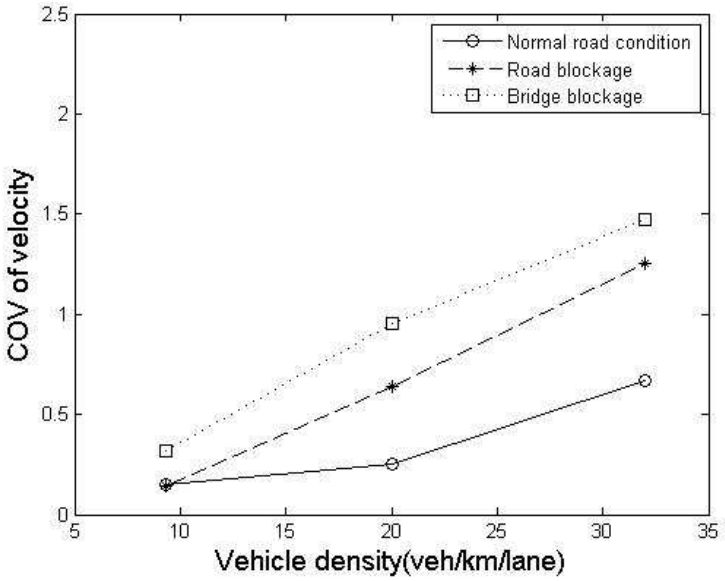

Fig. 4.4 COV of velocity vs. vehicle density

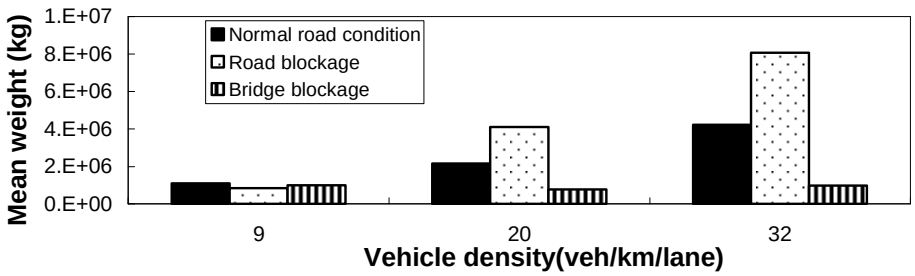

Fig. 4.5 Mean static weight of all vehicles moving through bridge over time

4.2.4 Bridge dynamic response under extreme events

Once the traffic flow in time history is simulated, the equivalent dynamic wheel loading (EDWL) approach can be applied to predict the bridge response. The EDWL ratio for each type of vehicles with specific driving speeds is calculated firstly through fully-coupled Bridge/Vehicle/Wind analysis. The properties of each type of vehicle are listed in Table 3.1-3.2 (Chapter 3). Subsequently, the bridge response is calculated by incorporating the CA traffic flow information and the corresponding EDWL ratios.

4.2.4.1 Bridge dynamic displacement

The time history of displacement and stress can be obtained by incorporating the results of traffic flow and the database of EDWL ratio into the interaction analysis of the bridge. Due to the limitation of space, only the time history of vertical displacement at midpoint of the bridge under the normal situation is displayed in Fig. 4.6. It is found that the displacement varies significantly with vehicle density and wind speed. When the traffic density is low (Fig. 4.6(a)), the dynamic displacement increases significantly while the wind speed increases from 2.7 m/s to 32.8 m/s. This observation is similar to that in traditional buffeting analysis of long-span bridges, for which traffic load were typically not considered. With the increase of the traffic density, the difference between the displacement results under the low and high wind speeds gradually become smaller (Fig. 4.6(b-c)). This phenomenon is obviously due to the growing contribution of traffic to the total displacement as a result of the increase of the traffic density. For the case of “bumper-to-bumper” when the traffic density is as high as 133 vehicle/km/lane, the dynamic response under the low and high wind speeds becomes nearly identical, except for some local difference (Fig. 4.6(d)). So, for the “bumper-to-bumper” situation, it is easy to find the contribution from the heavy traffic to the bridge displacement has considerably outweighed that from wind excitation.

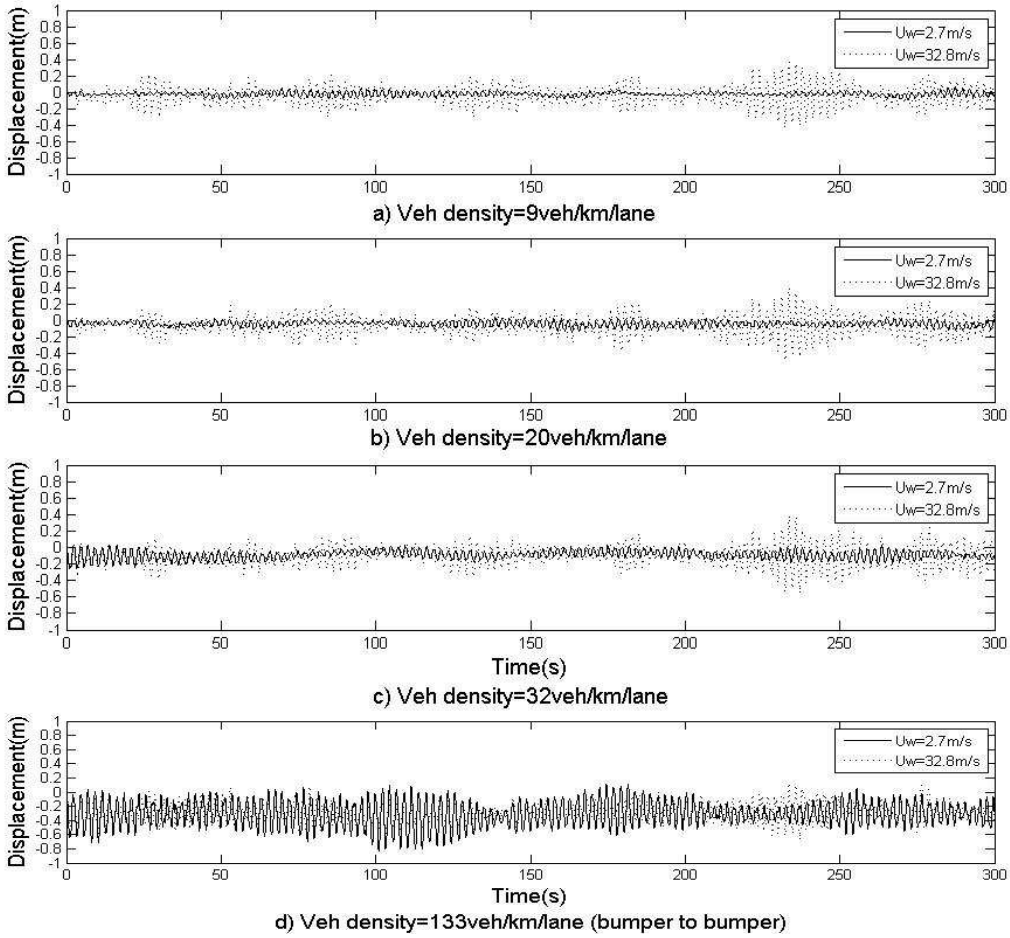

Fig. 4.6 Time history of vertical displacement at midpoint under "normal" road condition

4.2.4.2 Bridge dynamic stress

Bridge dynamic stress provides critical information for evaluating bridge performance, such as strength, fatigue, damage assessment, and remaining service life. Extreme stress values, although not occurring all the time, may cause initiation of cracks which will further propagate under repeating loads or even strength problem for some local members. Fig. 4.7(a) and Fig. 4.7(b) show the extreme stress envelops for different traffic densities along the whole bridge of both the bottom and the top fiber of the bridge girder, respectively. Each profile is to record the maximum values which have ever occurred at each location along the bridge through the time-domain simulation. It can be found that the midpoint of the main span still exhibits the largest extreme

stress levels at both the bottom and top fibers along the bridge. Comparatively, the bottom fiber experiences higher extreme stress level than the top fiber, and the largest tension stress is about 115 MPa in the "bumper-to-bumper" scenario when the wind speed is low (i.e. traffic density=133 veh/km/lane and U=2.7 m/s). The extreme stress levels along the bridge vary considerably. In addition to the largest stress levels at the mid-point of the bridge, several other locations along the bridge also have pretty large stress levels (Fig. 4.7).

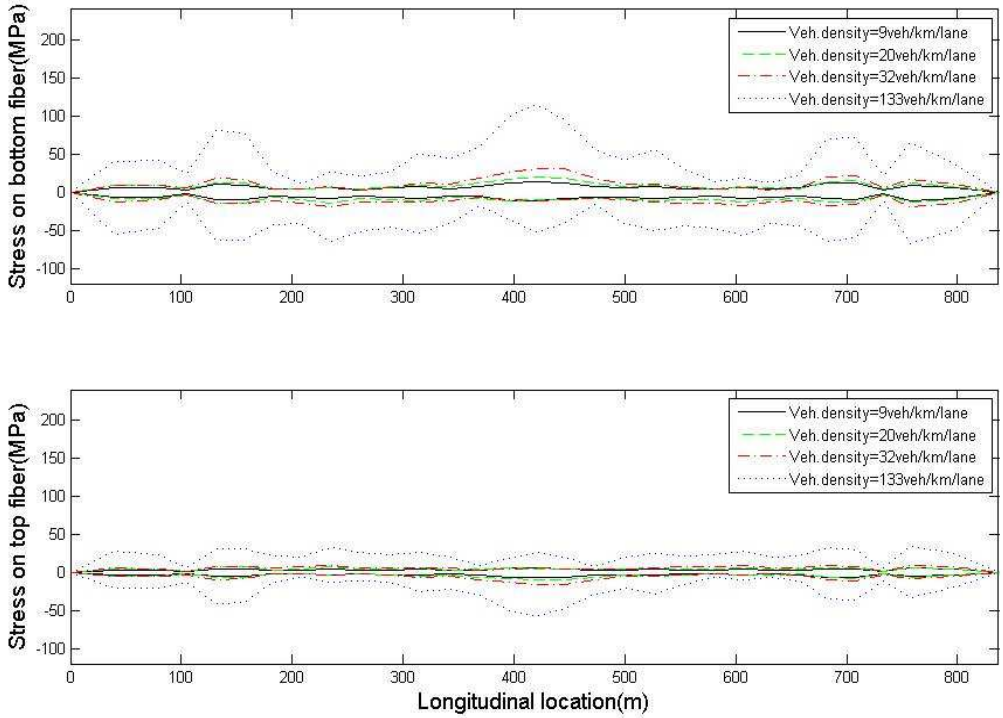

Fig. 4.7 Extreme stress profile of bridge under "normal" road condition (U=2.7 m/s)

Fig. 4.8 shows the results of extreme stress when the wind speed is high. It can be found from Fig. 4.8 that the extreme stress values only increase slightly with the increase of the vehicle density. For the "bumper-to-bumper" case when the wind speed is also high, the largest extreme tension stress is around 130 MPa, which is a just little higher than that under mild wind (Fig. 4.7). This phenomenon confirms again that the interaction effects between the bridge, traffic and wind are more complicated than a linear superposition of stress contributions from individual loads.

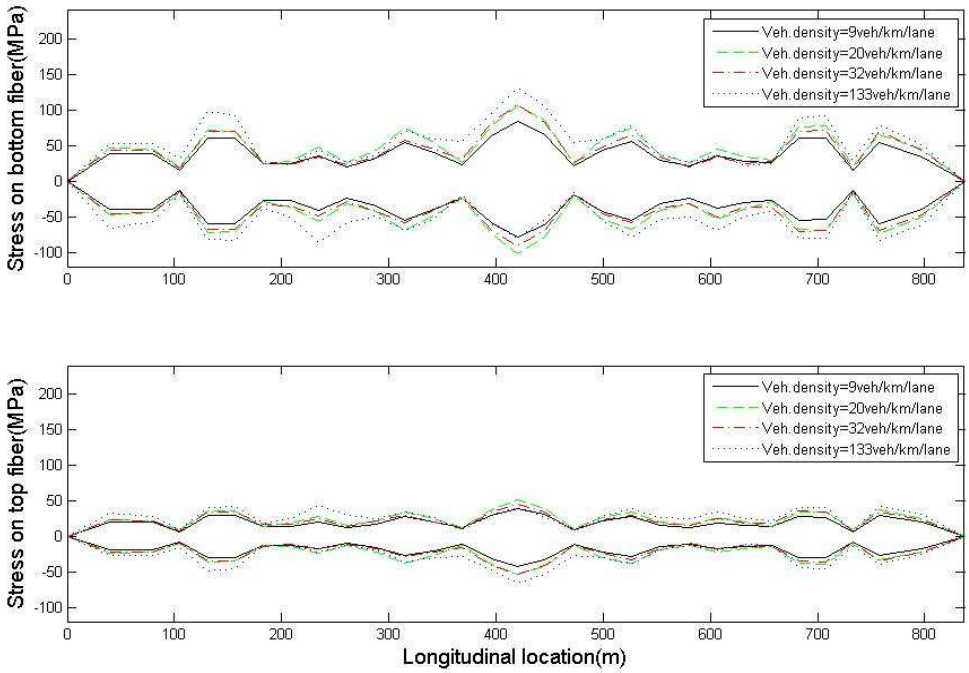

Fig. 4.8 Extreme stress profile of bridge under “normal” road condition (U=32.8 m/s)

Figs. (4.9-4.10) illustrate the mean and COV values of the stress level over time at the midpoint of the main span for different traffic densities. Results of three cases are compared, including the “normal” traffic case, the “road blockage” and the “bridge blockage” cases. In Fig. 4.9, it is found that the mean stress generally increases with the wind speed. Compared to different wind speeds, the increase of the mean stress over different traffic densities seems to be more significant. By comparing the results of the three traffic conditions (i.e. “normal”, “road blockage” and “bridge blockage”) under low traffic density, people can find that the mean stress values for the three cases are similar. With the increase of the traffic density, the “road blockage” case has relatively higher mean stress value. For the “bridge blockage” case, the mean stress levels seem not changing considerably with different traffic densities.

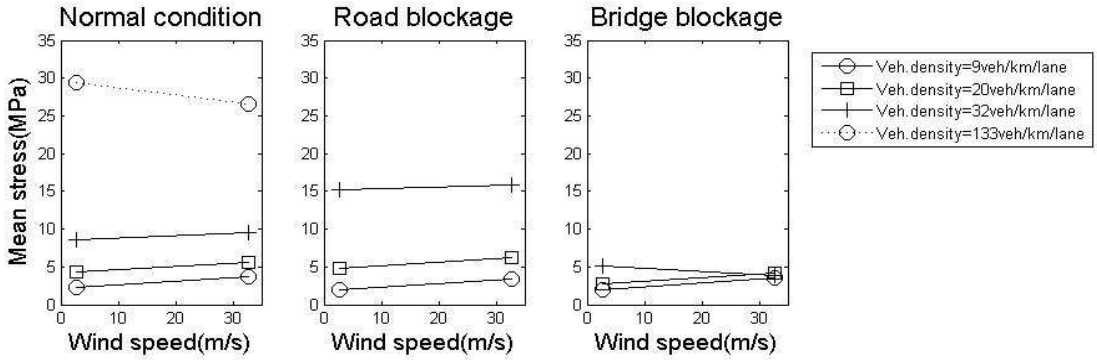

Fig. 4.9 Comparison of mean stress at bottom fiber of midpoint of bridge

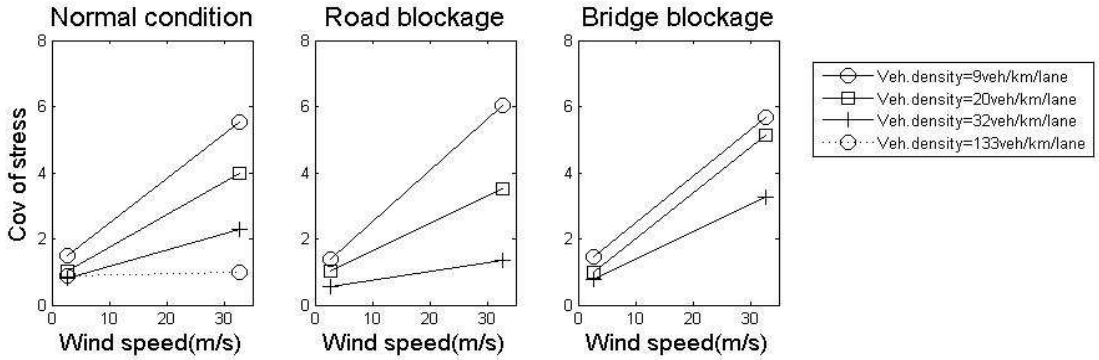

Fig. 4.10 Comparison of COV of stress at bottom fiber of midpoint of bridge

When the traffic density keeps increasing to 133 veh/km/lane for the "normal case" (i.e. "bumper-to-bumper" situation), the mean stress value will become as high as 30 MPa (Fig. 4.9). It is interesting to find that the mean stress value for the "bumper-to-bumper" traffic actually decreases with the increase of the wind speed, which can also be found for the "bridge blockage" case when the traffic density is high. As discussed in several previous studies (Chen and Cai 2007; Chen and Wu 2009), the dynamic interactions between the bridge, traffic and wind exhibit complex manner. For example, the controlling case which causes the highest mean stress may not always be the case when the traffic density and wind speeds are both the highest, as people usually assume.

As shown in Fig. 4.10, for both normal and incidental cases, the COV of dynamic stress increases with wind velocity considerably, but decreases with the traffic density. This is understandable since the variation of vehicle velocities is usually lower for higher traffic density due to fewer chances to freely change lane or accelerate/decelerate (Chen and Wu 2009). When the wind speed is low, the COV values for different traffic densities as well as different traffic situations are all similar. When the wind speed is high, the "road blockage" case with the low traffic density is found to have the relatively higher COV value. But when the wind speed is high and the traffic density is moderate or high, the "bridge blockage" case will have the highest COV value. Different from the observation of the mean stress values for the "bumper-to-bumper" case, the COV value for the "bumper-to-bumper" case is not critical, especially when the wind speed is high.

Fig. 4.11 gives the extreme stress values at the bottom fiber of the midpoint of the span for different cases. The extreme stress values generally increase with the wind speed, but they vary slightly under different traffic density for the same scenario. For both the "normal" and the "road blockage" case, the highest extreme stress occurs when both the wind speed and traffic density are the highest. For the "bridge blockage" case, however, the extreme stress becomes the highest when the traffic density is moderate. This phenomenon suggests that the most critical scenario in terms of extreme dynamic stress exhibits unique and complicated patterns for incidental cases. This interesting observation shows that the most critical scenario of incidental cases is not always straightforward, which may require specific analysis on a case-by-case basis. For the normal case, "bumper-to-bumper" traffic will cause the highest extreme stress levels among all the traffic densities.

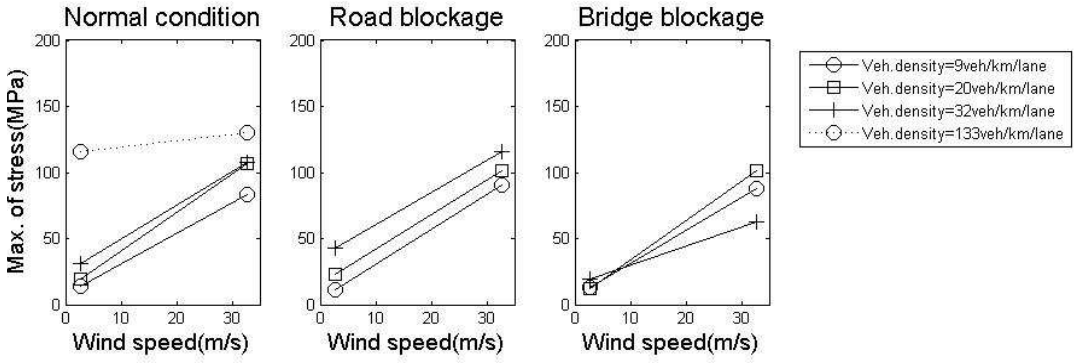

Fig. 4.11 Comparison of max. stress at bottom fiber of midpoint of bridge

4.3 Conclusions

In this chapter, the bridge dynamic performance under extreme cases considering dynamic coupling of the Bridge/Traffic/Wind system was studied by applying the analytical framework integrating the CA traffic model and the EDWL approach. The major findings are summarized in the following:

(1) The bridge dynamic displacement generally increases with the increase of the traffic density and wind speed. With the increase of the traffic density, the dynamic displacement response will be gradually dominated by the component contributed by the traffic load. For the "bumper-to-bumper" case, the dynamic displacement under the low and high wind speeds becomes nearly identical;

(2) The extreme dynamic stress of the bridge in the "bumper-to-bumper" case for both the low and high wind speeds is about 115 MPa and 130 MPa, respectively. This phenomenon of insignificant difference confirms again that the interaction effects among the bridge, traffic and wind are more complicated than linear superposition of stress contributions from individual loads (i.e. traffic and wind);

(3) The mean stress values generally increase with both the wind speed and traffic density. When the traffic density is low, the mean stress values for the "normal", "road blockage" and

"bridge blockage" conditions are all similar. With the increase of the traffic density, the "road blockage" condition has a relatively higher mean stress value;

(4) The COV of stress increases with the wind speed, but decreases with the vehicle density. When the wind speed is low, the COV values for different traffic densities as well as different traffic situations are all similar. When the wind speed is high, the "road blockage" case with the low traffic density is found to have the relatively higher COV value. But when the wind speed is high and the traffic density is moderate or high, the "bridge blockage" case will have the highest COV value;

(5) In terms of extreme stress values, the most critical case is not always at the time when both the wind speed and traffic density become the highest under different road conditions. For both the "normal" and the "road blockage" case, the highest extreme stress occurs when both the wind speed and traffic density are the highest. For the "bridge blockage" case, however, the extreme stress becomes the highest when the traffic density is moderate. Specific analysis is therefore required to identify the most critical scenario of the extreme events for a particular long-span bridge.

4.4 References

AASHTO (2007). AASHTO LRFD Bridge Design Specifications (4th ed.) , American Association of State Highway and Transportation Officials, Washington, D.C.

Cai, C. S. and Chen, S. R. (2004). "Framework of vehicle-bridge-wind dynamic analysis." Journal of Wind Engineering & Industrial Aerodynamics, 92 (7-8), 579-607.

Chen, S. R. and Cai, C. S. (2007). "Equivalent wheel load approach for slender cable-stayed bridge fatigue assessment under traffic and wind: feasibility study." Journal of Bridge Engineering, 12(6), 755-764.

Chen, S. R., Cai, C. S. and Levitan, M. (2007). "Understand and improve dynamic performance of transportation system- A case study of Luling Bridge." Engineering Structures, 29, 1043-1051.

Chen, S. R., Cai, C. S, Wolshon, B. (2009). "From normal operation to evacuation: single-vehicle safety under adverse weather, topographic and operational conditions." Natural Hazards Review, ASCE, 10(2), 68-76.

Chen, Y. B. and Feng, M. Q. (2006). “Modeling of traffic excitation for system identification of bridge structures.” Computer-Aided Civil and Infrastructure Engineering, 21, 57-66.

Chen, S. R., Wu, J. (2010). “Dynamic performance simulation of long-span bridge under combined loads of stochastic traffic and wind.” Journal of Bridge Engineering, ASCE 15(3), 219-230.

Ditlevsen, O. (1994). “Traffic loads on large bridges modeled as white-noise fields.” Journal of Engineering Mechanics, 120(4), 681-694.

Ditlevsen, O. and Madsen, H. O. (1995). “Stochastic vehicle-queue-load model for large bridges.” Journal of Engineering Mechanics, 120 (9), 1829-1874.

Guo, W. H., Xu, Y. L. (2001). “Fully computerized approach to study cable-stayed bridge-vehicle interaction.” Journal of Sound and Vibration 2001, 248(4), 745–61.

National Research Council (2000). Highway Capacity Manual, Washington, D.C.

Nowak, A. S. (1993). “Live load models for highway bridges.” Structural Safety, 13, 53-66.

Nagel, K. and Schreckenberg, M. (1992). “A cellular automaton model for freeway traffic.” Journal de Physique I France, 2(12), 2221-2229.

Rickert, M., Nagel, K., Schreckenberg, M., Latour, A. (1996). “Two lane traffic simulations using cellular automata.” Physica A, 231, 534-550.

Wu, J. and Chen, S. R. (2008). “Traffic flow simulation based on cellular automaton model for interaction analysis between long-span bridge and traffic.” Inaugural International Conference of the Engineering Mechanics Institute (EM08), May 18-21, 2008.

Wu, J. and Chen, S. R. (2009). “Traffic flow simulation on bridge with cellular automaton technique.” 88th Transportation Research Board Annual Meeting, Jan, 13-7.

Xiao, S. F., Kong, L. J., Liu, M.(2005). “A cellular automaton model for a bridge traffic bottleneck.” Acta Mech Sinica, 21: 305-9.

CHAPTER 5: SCENARIO-BASED INVESTIGATION OF FATIGUE DAMAGE OF LONG-SPAN BRIDGES

5.1 Introduction

Fatigue damage, which results from repetitive stress cycles accumulated under dynamic loads over time, is critical for the serviceability as well as safety of any bridge. A slender long-span bridge (e.g. span length > 152.4m or 500 ft) usually experiences complicated dynamic loads from the bridge, stochastic traffic and wind (Guo and Xu 2001; Chen and Cai 2007). The stochastic nature of wind and traffic, as well as the dynamic interactions, makes a realistic assessment of fatigue damage of a long-span bridge over time very challenging (Chen and Cai 2007).

For short- and medium-span bridges, the fatigue design load defined in the AASHTO LRFD (AASHTO 2007) specification includes one design truck per bridge with 15% dynamic allowance. Other than using the single design vehicle from the specification, there are some existing studies that estimated the traffic load with statistical traffic spectrum data, such as truck gross weight on the bridge over a certain period of time (Oh et al. 2007; Broquet et al. 2004; Mullard and Stewart 2009). Traffic spectrum, however, does not provide instantaneous information of individual vehicles such as speed and position at any time, which is essential to the assessment of bridge/vehicle interactions for long-span bridges. In recent years, some researchers adopted white noise fields (Ditlevsen 1994; Ditlevsen and Madsen 1995), Poisson distribution (Chen and Feng 2006) and Monte Carlo approach (Nowak 1993, Moses 2001, O'Connor and Obrien 2005) to simulate the traffic flow to obtain the characteristic load effects primarily on short- and medium-span bridges. These approaches did not provide time-dependent information of individual

vehicles (e.g. instantaneous speed, position) by following realistic traffic rules and driving behavior. Although they may not be critical for short or medium-span bridges, the realistic traffic rules and driving conditions can be significant for long-span bridges accommodating extended length of stochastic traffic flow (Wu and Chen 2008). To solve that problem, Wu and Chen (2008) adopted the cellular-automaton (CA) based traffic flow simulation scheme to simulate the stochastic traffic flow through a long-span bridge. The CA-based model can replicate the actual traffic situations in both normal and incidental conditions by following some realistic traffic rules (Nagel and Schreckenberg 1992). Based on the results of the stochastic traffic as well as the "equivalent dynamic wheel load (EDWL)" approach (Chen and Cai 2007), the "semi-deterministic" analysis model is developed in Chapter 3 and 4 to predict the dynamic performance of long-span bridges under stochastic traffic and wind in both normal and extreme conditions.

In addition to the challenges on simulating stochastic traffic flow on long-span bridges, existing studies on the fatigue performance of slender long-span bridges were limited to those only considering wind load but without traffic load at the same time (Pourzeynali and Datta 2005; Gu et al. 1999). To date, there is no study so far that incorporates the contributions from stochastic traffic, wind and dynamic interactions integrally into the fatigue performance assessment of long-span bridges. It is thus the goal of the present study to develop an analytical basis of fatigue analysis of long-span bridges considering both traffic and wind loads. The proposed scenario-based deterministic fatigue damage assessment of long-span bridges involves improvements over the existing methodologies by integrating the characterization of site-specific loads, advanced bridge dynamic analysis based on representative scenarios, and fatigue damage assessment. Moreover, such a model will also become the critical basis for the reliability-based fatigue life prediction of long-span bridges, which will be introduced in the next chapter.

5.2 Analytical Methodology

As compared to the analytical model of a conventional long-span bridge that is not sensitive to wind, the dynamic model of a slender long-span bridge actually represents a more general situation as it includes the most complicated Bridge/Traffic/Wind interaction (Chen and Cai 2007). The model of a slender long-span bridge can easily be reduced to that of a conventional long-span bridge by simply removing the wind-related loads on the bridges (Chen and Cai 2007). Therefore the methodology for a slender long-span bridge will be developed in this chapter in order to keep the maximum generality. It is thus obvious that although the formulation and the example in this chapter are about a slender long-span bridge, the fatigue analysis of any conventional long-span bridge in the future can also benefit from the proposed methodology easily.

As shown in Fig. 5.1, the proposed scenario-based fatigue analysis framework for Bridge/Traffic/Wind system consists of three components: (1) Defining site-specific traffic and wind conditions; (2) Conducting scenario-based dynamic simulations; and (3) Carrying out the fatigue damage assessment. These three components will be introduced in the following sections, respectively.

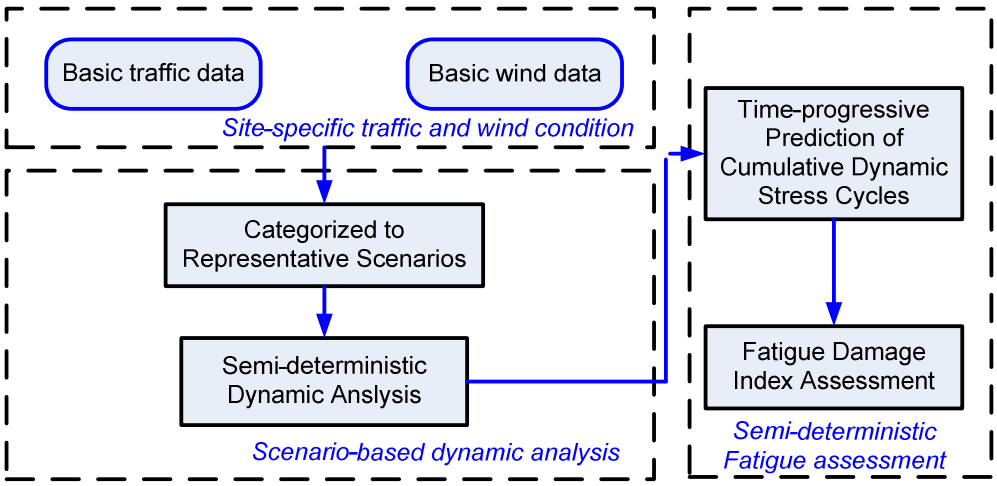

Fig. 5.1 Flowchart of semi-deterministic fatigue analysis methodology

5.2.1 Defining site-specific traffic and wind conditions

5.2.1.1 Basic traffic information

For any long-span bridge connecting roadways in different regions, the vehicle density, speed limit and vehicle classifications (i.e. combinations of different vehicle types) are usually specific to the bridge site. In order to simulate the probabilistic traffic load applied by all vehicles moving simultaneously through the bridge every day, realistic and site-specific information, such as instantaneous speed, vehicle type and position of each vehicle at any time is required. The stochastic traffic flow in the microscopic scale will be simulated using the advanced cellular automaton (CA) traffic flow simulation technique. Cellular Automaton (CA), a microscopic traffic flow simulation model, can generate probabilistic traffic information by simulating individual vehicles' behavior (Nagel and Schreckenberg 1992; Wu and Chen 2008).

In order to conduct the CA-based traffic flow simulation, some basic traffic data specific to the bridge site is needed, such as traffic volume, vehicle classifications and highway data: speed limits and number of lanes etc. Among all the basic data of traffic flow, the traffic volume through a specific bridge (or highway) has the largest variation that usually follows some trend in normal driving conditions, such as rush hours or off-peak hours, weekdays or weekends. The variation of traffic volume over years can also be considered based on the historical data or reasonable predictions. The basic traffic data may be obtained from traffic spectrums or weigh-in-motion data near the bridge site or the connecting roadways that share the similar traffic as the bridge.

In addition to normal traffic conditions, there are some incidental traffic events, which may have impacts on the traffic load applying on the bridge. These incidental events may include (1) lane closure of the bridge or the approaching roadways for construction, maintenance or repair; and (2)

major accidents or evacuation on the bridge or the approaching roadways (Wu and Chen 2010). The durations of these incidental events may be short (from several hours to several months). But serious congestion (e.g. bumper-to-bumper) may be formed on the bridge and/or connecting roadways as a result of these incidents, which will cause excessive dynamic response (e.g. stress levels) and in turn contribute to possible initiation of fatigue cracks or damage accumulation.

5.2.1.2 Wind environments

It is known that wind exists in nature all the time, from breeze to wind storm like hurricane. Similar to basic traffic information, wind environments of a particular slender long-span bridge, such as wind speeds and wind directions, can be typically obtained from historical wind velocity data collected at nearby weather stations. Wind rose maps have been commonly used to define the site-specific wind velocity for bridges, including the probability of combinations of wind speed and direction typically in each month. It is assumed in the present study that wind speed/direction does not change within any hour. Such an assumption is made based on the fact that more refined wind velocity data measurements over the lifetime of a bridge may not always be available. It should be noted, however, that shorter period than 1 hour can be easily adopted within the present framework if more accurate wind velocity data is available for a particular bridge.

In this chapter, the total hours in a month will be randomly assigned with different combinations of wind-speed/direction, which follow the overall statistics from the wind rose map. For conventional long-span bridges that are not sensitive to wind, wind load characterization may still be required in order to consider wind loads on vehicles (Chen and Wu 2008) although the wind loads on the bridge may be trivial enough to be omitted. In addition to common wind conditions, some extreme wind conditions also need to be considered throughout the lifespan of a slender long-span bridge, such as strong wind from hurricane or severe windstorm. These extreme wind

conditions can be considered on a case-by-case basis by estimating possible occurrence within a certain period of service time of the bridge.

5.2.2 Scenario-based dynamic analysis

5.2.2.1 Categorization of representative scenarios

Traffic and wind, as the main service loads for a slender long-span bridge, can be approximated to be mutually independent in the normal traffic condition. Only in some extreme conditions such as under a severe windstorm, the traffic volume and wind speed may have some correlation especially when traffic control is in place (Chen et al. 2009). Different combinations of wind and traffic conditions will generate many different scenarios of service loads on a bridge. According to the existing studies (Chen and Cai 2007; Chen and Wu 2010), the dynamic response of a long-span bridge subjected to traffic and wind loads has to be considered in a coupled way rather than superimposing the respective contributions from individual loads. The number of the representative scenarios should be selected carefully to provide a comprehensive coverage of possible combinations of wind and traffic conditions while maintaining reasonable computational efficiency at the same time. In order to comprehensively capture the most representative scenarios, both normal service conditions and extreme events should be considered.

According to the Highway Capacity Manual (National Research Council 2000), the typical highway traffic has six levels of service (LOS) from A to F, which represent all typical traffic conditions, from “free flow” to “breakdown flow”. Similarly, according to the Beaufort wind scale, the wind speed is typically categorized into scales from 1-12, which correspond to the wind speed increasing from 0 to over 73 mph (hurricane). In reality, the number of the total combinations can be reduced by merging similar categories of traffic and/or wind conditions. The number of total representative scenarios and the categorization process also depend on the required accuracy and the available computational resources.

In addition to normal service conditions, there are some incidental traffic conditions when some lanes of the bridge or approaching roadways may be closed to traffic (Wu and Chen 2010). Therefore, there will be several additional scenarios for extreme events, such as the road-block condition (i.e. one lane on the approaching roadway is closed) or the bridge-block condition (i.e. one lane on bridge is closed). Although these scenarios are usually rare, it has been found that significant stress level may exist on the bridge in these situations (Wu and Chen 2010) and the potential impacts on fatigue damage are not clear.

5.2.2.2 Semi-deterministic dynamic analysis of representative scenarios

In Chapter 3, a semi-deterministic simulation framework has been developed to consider the bridge response subjected to the combined effects from stochastic traffic and wind. Such a semi-deterministic model will predict dynamic displacement and stress level using the basic traffic and wind conditions as inputs. The detailed model can refer to Chapter 3 and Chapter 4.

5.2.3 Deterministic fatigue damage assessment

Although the randomness of traffic flow itself has been partially considered in the CA-based simulation, the uncertainties associated with wind, traffic volume and structural properties of the bridge are not considered in the present model. Therefore, the proposed approach is essentially a deterministic approach as compared to traditional reliability-based simulation models for structures. In order to demonstrate the deterministic approach, the fatigue damage assessment will be conducted for a typical year. A full estimation of the fatigue performance through the service life of a long-span bridge will rely on the rational consideration of uncertainties of major variables over years, which will be discussed in the reliability-based work in the next chapter.

5.2.3.1 Time-progressive prediction of cumulative dynamic stress cycles in a typical year

As discussed earlier, the possible variations of traffic volume within an hour, a day, a week, and a month can be obtained either from the local traffic statistical data or the generic data in the specification. Vehicle classification for a particular bridge may actually vary slightly over time. In lieu of the data, constant vehicle classification data can be assumed for all weekdays and all weekends, respectively. Wind rose map can give the probability of each wind velocity (speed/direction) in a month. By considering the actual site-specific wind and traffic data in weekdays, the combination of different values of the vehicle density and wind-speed/direction is conducted randomly in any day based on the reasonable assumption that wind and traffic conditions are usually independent from one to the other.

It is assumed that the traffic or wind condition does not change within any single hour, and therefore each hour has its unique combination of wind and traffic conditions. So based on the hourly distributions of traffic volume in one weekday or weekend as well as the wind velocity data, people can assign each hour in a weekday or weekend with a representative scenario, respectively. By continuing progressively over five weekdays and two weekend days following the weekly distributions of traffic volume and wind velocity, the corresponding representative scenario can be assigned to each day in a week. Similarly, the corresponding representative scenarios of one month and finally one year can be identified based on the monthly and yearly distributions of traffic and wind data, respectively. The total hours being assigned to each representative scenario in a year will be calculated. For each representative scenario, semi-deterministic analysis will be conducted to find out the dynamic stress results. Based on the respective total hours assigned to each representative scenario throughout a typical year, the cumulative stress cycles in one typical year will be finally obtained.

5.2.3.2 Fatigue damage assessment

There have been many different fatigue theories that can be applied to bridges (e.g. Schilling et al. 1978; Fisher et al. 1980, 1983; Moses et al. 1986). Among all the fatigue theories, the traditional Miner's law (Miner 1945) is still the most popular one, which has been widely used in large-scale engineering structures (Laman 1995). In the Miner's law, the S-N curve (S: stress range, N: number of cycles to failure) is applied to form a linear damage rule which simplifies the prediction of fatigue life by the assumption of linear accumulation of fatigue damage over time (Miner 1945). In order to consider the dynamic stress amplitudes, the Rainflow Counting Method is applied to get the number of cycles for each stress-amplitude (Laman 1995).

The quantification of fatigue damage here is referred as "damage index" (DI), defined as the fraction of the total fatigue life. With the adoption of the linear fatigue theory, the "damage index" (DI) is also the ratio of accumulated cycles out of the total allowable cycles that will cause fatigue damage, which is defined as follows:

$$DI = \sum_{i=1}^{n_t} D_i = \sum_{i=1}^{n_t} \frac{1}{N_i} \tag{5.1}$$

where n_t is the number of all stress cycles in a particular period of time (e.g. one day). D_i denotes the incremental damage due to the i^{th} stress cycle and n is the total number of stress cycles in the stress history; N_i is the total number of cycles to failure for constant amplitude stress level, S_i (Miner 1945).

5.3 Demonstrative Example

The scenario-based fatigue analysis framework proposed above will be illustrated with a hypothetical cable-stayed bridge with steel girders in the New Orleans area of Louisiana. The hypothetical cable-stayed bridge shares the same structural parameters with the prototype bridge which has been studied in the previous chapters (Chapter 3 and 4). The traffic and wind data used

for this hypothetical bridge was obtained from public resources, such as wind data in the nearby areas or from generic traffic records given in the specification. Therefore, the simulation results or findings of the hypothetical bridge do not necessarily reflect the actual fatigue performance of any existing bridge.

5.3.1 Site-specific load conditions

5.3.1.1 Wind data

In the dynamic interaction model (Eq. (3.4)), wind is assumed to be perpendicular to the bridge all the time. Natural wind can come at any direction. Therefore, the natural wind speed, along with specific wind direction, will need to be converted to the "representative wind speed" which is always perpendicular to the bridge in order to be used in the simulation models. According to the Beaufort wind scale and the findings from the existing studies on Bridge/Traffic/Wind interaction analysis, totally eight "representative wind speeds" (2, 5, 8, 10, 15, 20, 25 and 32.8 m/s) are selected in Table 5.1 to represent eight segments of wind speeds (W1-W8). In Table 5.1, each of the "representative wind speed" was selected around the mean value of each wind speed range. Therefore, eight "representative wind speed" (W1-W8) in Table 5.1 represent the whole range of typical wind conditions, which span from "breeze" (W1) to "hurricane" (W8).

Table 5.1 Definition of "representative wind cases"

Representative wind cases	Representative wind speed (m/s)	Corresponding wind speed range (m/s)	Description
W1	2	≤3.5	calm to light breeze
W2	5	[3.5, 6.5]	gentle breeze to moderate breeze
W3	8	[6.5, 9]	moderate breeze to fresh breeze
W4	10	[9, 12.5]	fresh breeze to strong breeze
W5	15	[12.5, 17.5]	strong breeze to gale
W6	20	[17.5, 22.5]	gale to strong gale
W7	25	[22.5, 28.5]	strong gale to whole gale
W8	32.8	>28.5	storm to hurricane

The natural wind speed data, including both wind speed and direction, can be obtained through the local monthly wind rose maps in Year 2008 for the area of New Orleans (http://mesonet.agron.iastate.edu/sites/locate.php?network=LA_ASOS). Considering the angle (θ) between the transverse direction of the bridge and the direction of natural wind on the wind rose map, the corresponding "representative wind speed" for each natural wind velocity (both speed and direction) shown on the rose map will be obtained. Therefore, one "representative wind speed" (W1-W8) will be assigned to each combination of natural wind speed and direction (Table 5.2). By adopting the wind rose map for each month of 2008, the cumulative hours of each "representative wind speed" (W1-W8) in Year 2008 can be found out. Fig. 5.2 shows the percentage of occurrence of the eight "representative wind speeds" in Year 2008 for the prototype bridge.

Table 5.2 Representative wind cases based on natural wind data

Natural wind Speed (knot) (m/s)		2-5 1-3	5-10 3-5	10-15 5-8	15-20 8-10	20-100 10-51
Natural wind Direction	Angle θ (degree)	Corresponding "representative wind cases"				
N	-60	W1	W1	W2	W2	W7
NNE	-37.5	W1	W2	W2	W3	W8
NE	-15	W1	W2	W3	W4	W8
ENE	7.5	W1	W2	W3	W4	W8
E	30	W1	W2	W3	W3	W8
ESE	52.5	W1	W1	W2	W2	W8
SE	75	W1	W1	W1	W1	W5
SSE	97.5	W1	W1	W1	W1	W3
S	120	W1	W1	W2	W2	W7
SSW	142.5	W1	W2	W2	W3	W8
SW	165	W1	W2	W3	W4	W8
WSW	187.5	W1	W2	W3	W4	W8
W	210	W1	W2	W3	W3	W8
WNW	232.5	W1	W1	W2	W2	W8
NW	255	W1	W1	W1	W1	W5
NNW	277.5	W1	W1	W1	W1	W3

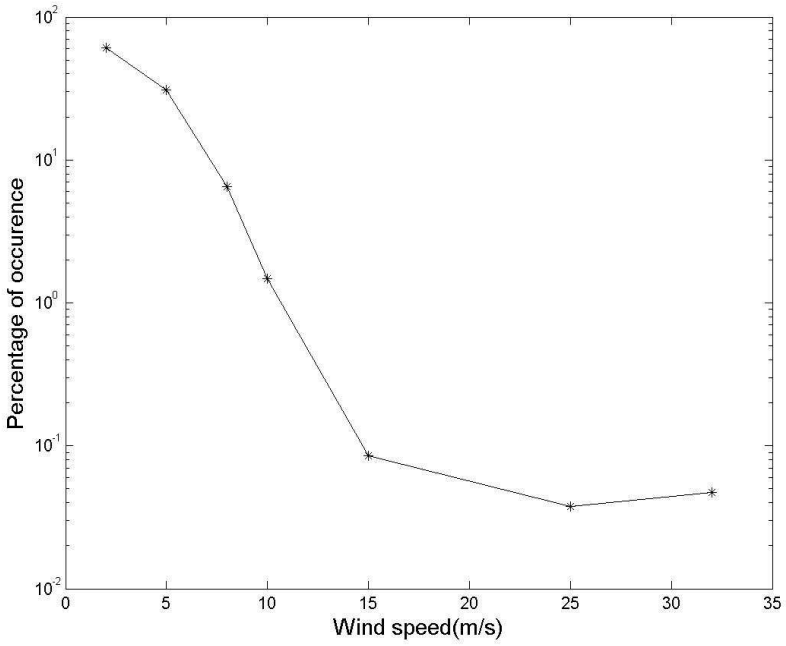

Fig. 5.2 The percentage of occurrence for different wind speeds in 2008

5.3.1.2 Traffic data

The semi-deterministic interaction analysis model of Bridge/Traffic/Wind (Chen and Wu 2010) requires two inputs for basic traffic conditions: one is vehicle density and the other is vehicle classification (i.e. ratios of different types of vehicles in the traffic flow). Based on the existing studies (Chen and Wu 2010), it has been found that to choose three typical traffic volume conditions can give reasonable representations of normal traffic conditions. Therefore, in the present study, the six levels of service (LOS) as defined in the Highway Capacity Manual (National Research Council 2000) are classified as three representative traffic conditions each of which covers two LOS:

"Free flow": LOS A ~B, $N < 1120 \ veh/hr/\ln$

"Moderate flow": LOS C~D, $1120 \ veh/hr/\ln \le N < 2015 \ veh/hr/\ln$

"Busy flow": LOS E~F, $N \ge 2015 \ veh/hr/\ln$.

The AADT of the bridge is assumed to be 40,000 vehicles for Year 2008 based on the data of the nearby highways. The traffic volume is assumed to be the same for any single hour. The generic data of variations of traffic volume over time provided by the Highway Capacity Manual (National Research Council 2000) will be used in the present study. Fig. 5.3 gives the hourly, weekly and monthly variations of the traffic volume provided by the Highway Capacity Manual (National Research Council 2000). By using the generic variation data, the traffic volume at different hours, days and months can be obtained. From the perspective of bridge dynamic analysis, various vehicle types are classified into three categories: sedan car, light truck and heavy truck (Chen and Wu 2010).

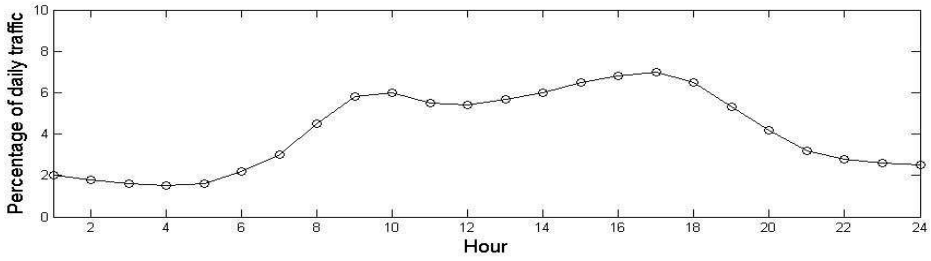

a. Hourly traffic volume distribution

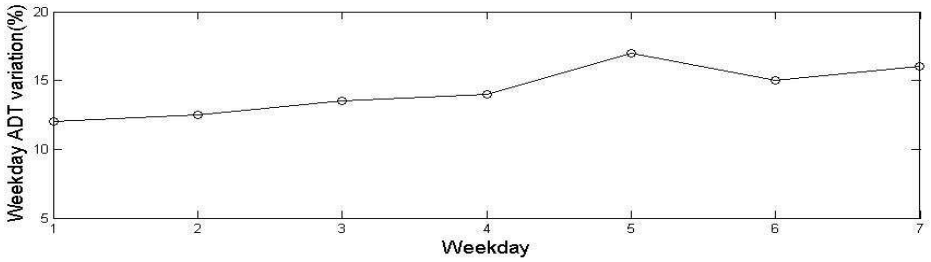

b. Weekly average daily traffic (ADT) variation

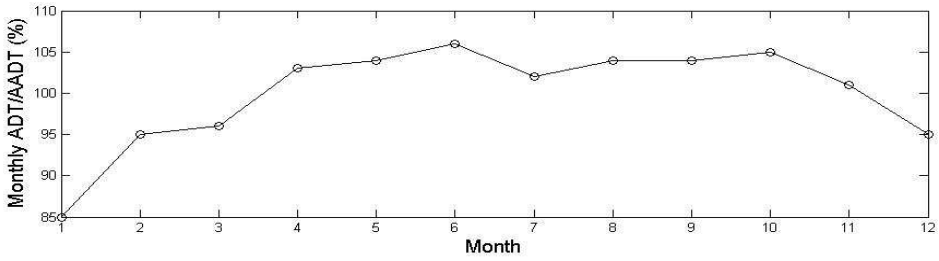

c. Monthly average daily traffic (ADT) variation

Fig. 5.3 Basic traffic data over time (National Research Council 2000)

Without the site-specific vehicle classification data, the percentages of sedan car, light truck and heavy truck are assumed to be 0.5, 0.3 and 0.2, respectively for the weekdays. While for weekends, the percentages are assumed to be 0.6, 0.2 and 0.2, respectively.

Based on the traffic-volume variation as shown in Fig. 5.3, the total vehicle number (N) through the bridge in any single hour of the simulation can be calculated with the following formula:

$$N = AADT \times K_m \times K_w \times K_h \tag{5.2}$$

where N is the flow rate in one hour (No. of vehicles/hour). AADT is the annual average daily traffic. K_m, K_w and K_h are the parameters to convert the AADT of a month, week and hour to the flow rate of a particular hour, respectively. These parameters can be obtained from simple data analysis of Fig. 5.3.

Depending on the value of N at any given hour, the traffic volume of a typical year for the prototype bridge has been categorized into one of the three representative traffic conditions (i.e. “free flow”, “moderate flow” and “busy flow”) according to the criteria of LOS introduced above. Fig. 5.4 gives the values of the percentages of the total hours for each “representative traffic condition” in each month. As expected, it can be found that the “busy flow” occurs very rare as compared to the other two categories.

5.3.2 Numerical study of fatigue damage index for representative scenarios

As discussed earlier, vehicle classifications are different on weekdays and weekends. Therefore, the normal traffic conditions include three representative traffic conditions on weekdays and weekends, respectively. In addition to normal traffic conditions, some extreme events, such as bridge-block and road-block conditions, will also be considered. For wind conditions, eight representative wind speeds will be considered. By combining different representative wind and

traffic conditions, the representative scenarios can be developed. Some numerical analysis results of several representative scenarios are given in the following.

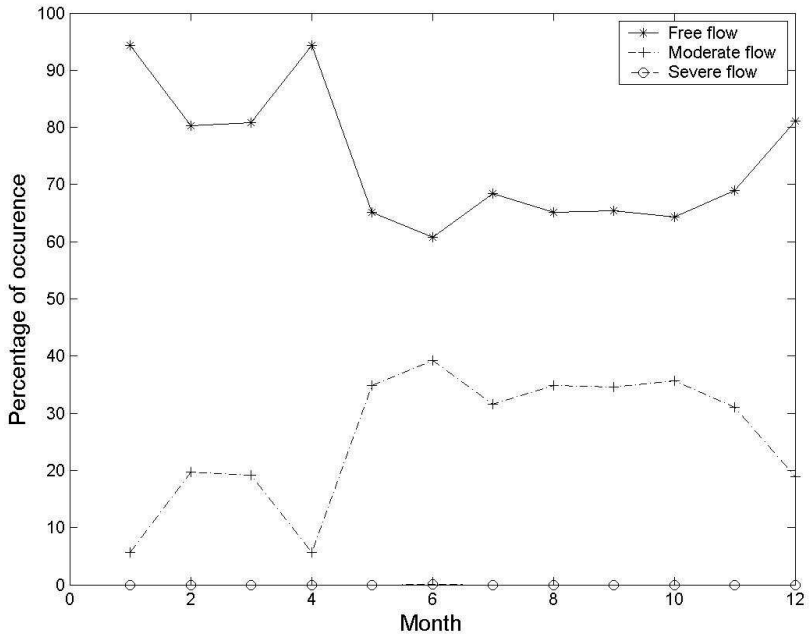

Fig. 5.4 The percentage of occurrence for different traffic conditions in 2008

Fig. 5.5 (a-b) shows the time-history response of the dynamic stress at the bottom of the girder at the middle point of the bridge in weekdays when the representative wind speed U_w=10 m/s and 25 m/s, respectively. For each wind speed, the time-history results of the "free flow" and "busy flow" are shown in the figure. As found in the previous study (Chen and Wu 2010), the dynamic stress levels are stochastic in nature subjected to the joint excitations from wind and traffic. With the increase of the wind speed, the dynamic stress amplitude increases significantly. When the wind speed gets higher (25 m/s), It is found that the difference between the results of "free flow" and "busy flow" becomes less significant as compared to that when the wind speed is low. The dynamic stress level has significant increase when the wind speed increases. When the wind speed equals to 25 m/s and the traffic flow is "busy", the dynamic stress level is around 180-200 MPa. Similar observations can be made from those results on weekends as well (Fig. 5.6).

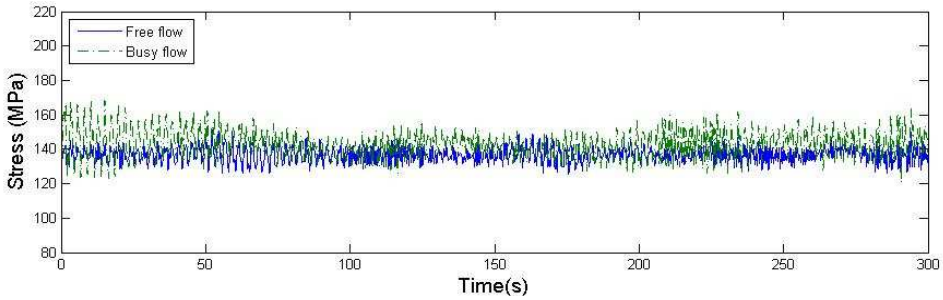

a. U_w=10 m/s

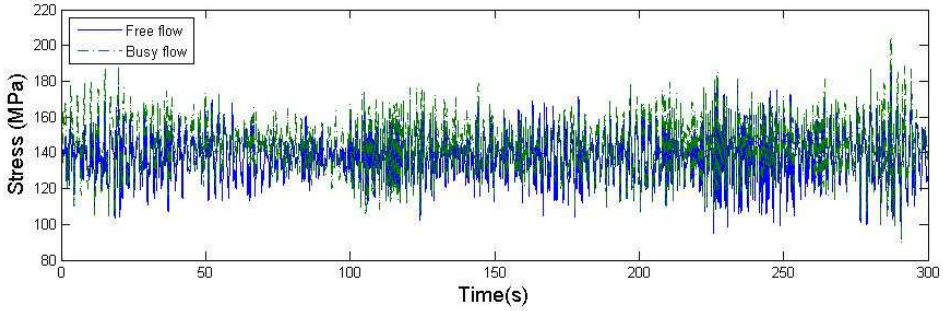

b. U_w=25 m/s

Fig. 5.5 Stress at the bottom of the girder at the midpoint of the prototype bridge (normal traffic condition, weekday)

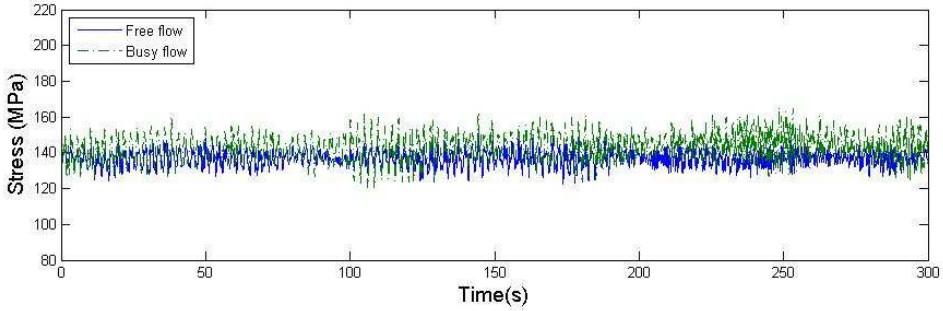

a. U_w=10 m/s

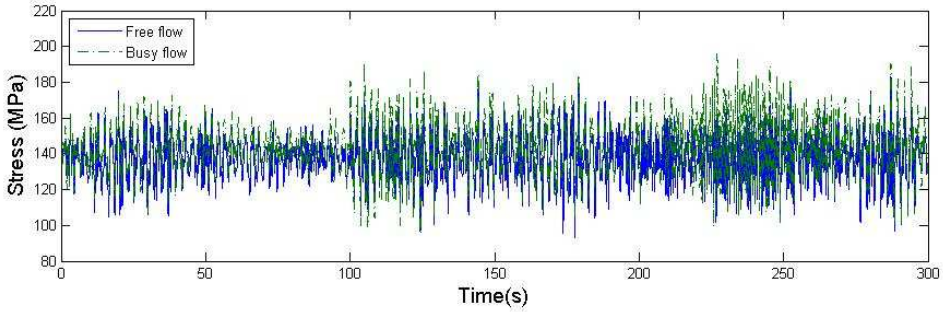

b. U_w=25 m/s

Fig. 5.6 Stress at the bottom of the girder at the midpoint of the prototype bridge (normal traffic condition, weekend)

In order to assess the possible contribution to potential fatigue damage, the damage index (DI) for each scenario is studied. By considering normal traffic conditions, the cumulative damage index in one hour for various scenarios (with different traffic and wind conditions) is shown in Fig. 5.7. Fig. 5.7(a-b) shows the results of the accumulated damage indices (per hour) under different combinations of representative wind and traffic conditions in weekdays and weekends, respectively. When wind is mild (wind speed lower than 15 m/s), it is found that the fatigue damage index is very small for all the different traffic conditions. With the increase of the wind speed, the damage index gradually increases. When the wind speed increases from 25 m/s to 32.8 m/s, the damage index dramatically increases by 4-6 times for all different traffic conditions. Since U=32.8 m/s is the starting wind speed for hurricane, the results suggest that strong wind may cause significant fatigue damage accumulation although the duration may be short. When the wind speed is higher than 15m/s, different traffic conditions may contribute to the damage indices in a complicated manner. For example, when the wind speed is at 20 m/s or 25 m/s on weekdays (Fig. 5.7(a)), busy traffic flow will cause the largest damage index while the moderate traffic flow will cause the largest damage index when the wind speed reaches 32.8 m/s. In weekends, however, busy traffic flow always causes the largest damage index when the wind speed is 25m/s or 32.8 m/s (Fig. 5.7(b)).

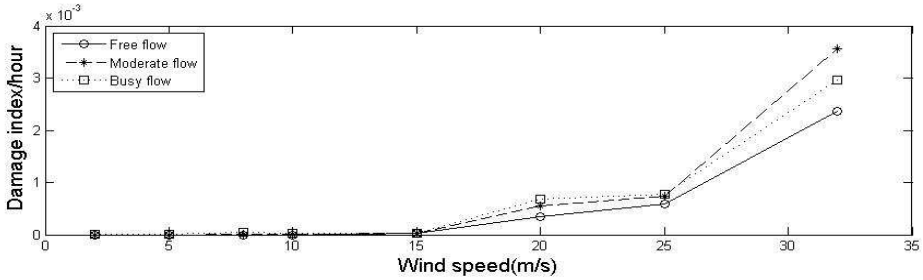

a. Weekday

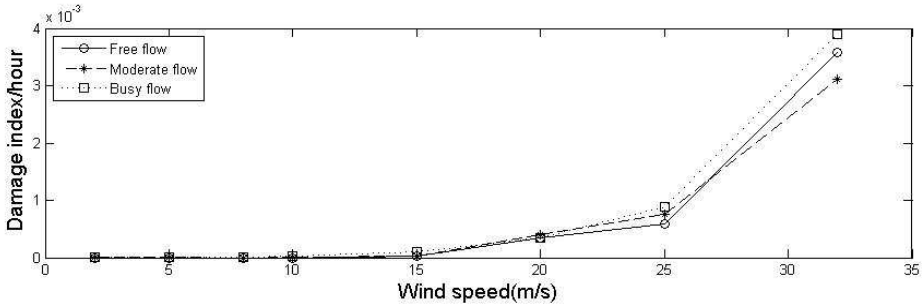

b. Weekend

Fig. 5.7 Damage index under different vehicle densities (normal traffic condition)

In addition to normal traffic conditions, extreme events may also cause fatigue damage accumulation. The comparison between normal, bridge-block and road-block conditions in weekdays is made and the results are shown in Fig. 5.8 (a-c), respectively. In order to better demonstrate the results, only the wind speeds from 15m/s to 25 m/s are shown. The *x*-axis in Fig. 5.8 shows the traffic densities corresponding to the representative traffic conditions. When the wind speed is moderate (15m/s), it is found that the accumulated damage index gradually increases in a positive way with the vehicle density (Fig. 5.8(a)). Compared to the normal service condition, the road-block condition causes higher damage accumulation while the bridge-block condition usually causes less. When the wind speed gets higher (20m/s), the accumulated damage index value in one hour significantly increases as compared to that when the wind speed is 15 m/s (Fig. 5.8(b)). When the wind speed further increases to 25 m/s (Fig. 5.8(c)), the damage index values only have limited increase with the vehicle density as compared to those when the wind speed is 20 m/s. All these observations confirm that the fatigue accumulation is not linear to the external load. Once the level of stochastic dynamic stress reaches some threshold, fatigue accumulation will start. When the number of cycles of dynamic stress that contributes to such accumulation becomes relatively stable, the fatigue damage accumulation becomes relatively constant despite the changes of the service loads. It is also found that extreme conditions exhibit complicated patterns in terms of fatigue damage accumulation as compared to normal condition. For example, bridge-block condition has the least fatigue damage accumulation among the three

traffic conditions. The road-block condition will cause more fatigue accumulation than that by normal traffic condition when the wind speed is moderate and high, especially when the vehicle density is relatively high (Fig. 5.8).

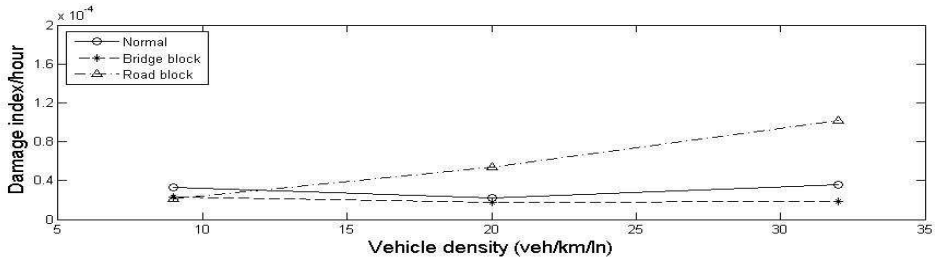

a. U_w=15m/s

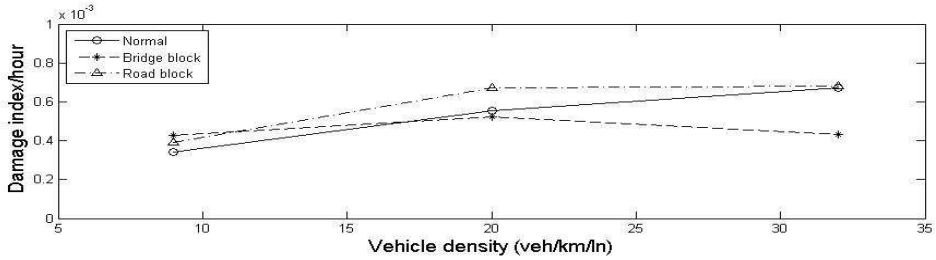

b. U_w=20m/s

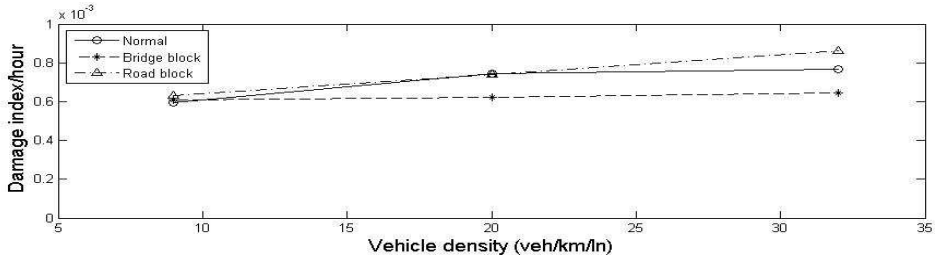

c. U_w=25m/s

Fig. 5.8 Damage index comparison between normal and incidental traffic conditions (weekday)

Fig. 5.9 (a-c) shows the fatigue damage index results for weekends. Similar to Fig. 5.8, bridge-block condition gives the lowest accumulation of fatigue damage index. The road-block condition causes more fatigue damage index accumulation than the normal condition when the vehicle density is high and the wind speed is 20 m/s. Although extreme events have been found to cause

considerably larger dynamic response than the normal conditions in many situations (Wu and Chen 2010), the results show that they are not very critical to the fatigue damage accumulation.

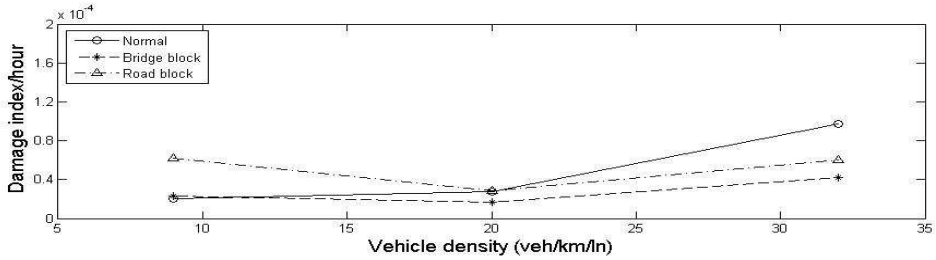

a. U_w=15m/s

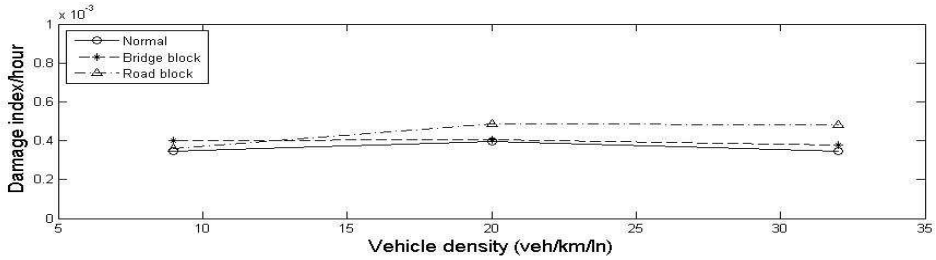

b. U_w=20m/s

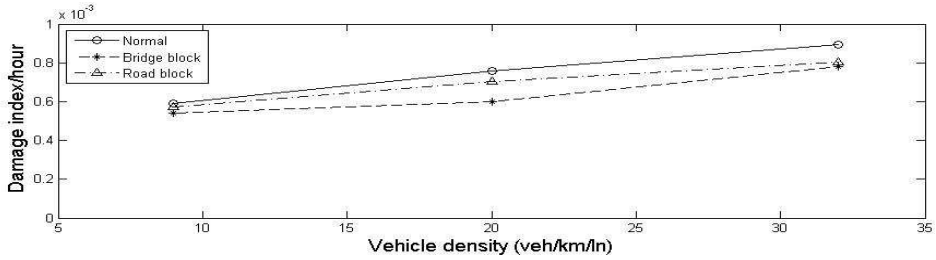

c. U_w=25m/s

Fig. 5.9 Damage index comparison between normal and incidental traffic conditions (weekend)

5.3.3 Fatigue damage assessment of a typical year

Based on the site-specific wind and traffic data specified in 5.3.1, the total hours for each representative scenario can be obtained for Year 2008. Table 5.3 and 5.4 list the detailed results of the damage index per hour, and total hours for each representative scenario in weekdays and weekends, respectively. Because of the lack of the data about possible extreme events, only normal traffic conditions were considered for the results shown in Table 5.3 and 5.4. It is easy to find that most accumulated hours in a year belong to the scenarios when the wind speed is low (breeze) and the traffic condition is “free” or “moderate”. But for these scenarios, the fatigue

damage accumulation is very small and can be ignored. The scenario, which causes the largest damage accumulation in an hour, is when the wind speed is the highest (32 m/s) and the "moderate traffic flow" (3.56E-03 in Table 5.3) for weekdays. Based on the site-specific traffic and wind data used in the present study, such a scenario actually did not happen in 2008 (i.e. 0 hour). The largest cumulative damage contribution (9.46E-03) actually happened in 2008 is made by the scenario (U=32 m/s and free traffic flow) and the second largest (5.31E-03) comes from the scenario (U=2 m/s and busy traffic flow). As shown in Table 5.3-5.4, the total cumulative damage index in weekdays and weekends in Year 2008 are 1.82E-02 and 3.40E-03, respectively.

Table 5.3 Cumulative damage index for Year 2008 (weekday)

Case No.	Representative wind speed U_w (m/s)	Representative traffic condition	Damage index/ hour	Accumulated hours	∑D
1		Free	0.00E+00	1876	0.00E+00
2	2	Moderate	0.00E+00	1806	0.00E+00
3		Busy	1.82E-05	291	**5.31E-03**
4		Free	0.00E+00	950	0.00E+00
5	5	Moderate	0.00E+00	824	0.00E+00
6		Busy	1.49E-05	36	5.36E-04
7		Free	0.00E+00	214	0.00E+00
8	8	Moderate	5.99E-07	189	1.13E-04
9		Busy	3.80E-05	5	1.90E-04
10		Free	0.00E+00	43	0.00E+00
11	10	Moderate	3.47E-06	43	1.49E-04
12		Busy	3.26E-05	0	0.00E+00
13		Free	3.35E-05	1	3.35E-05
14	15	Moderate	2.26E-05	2	4.51E-05
15		Busy	3.61E-05	0	0.00E+00
16		Free	3.41E-04	0	0.00E+00
17	20	Moderate	5.53E-04	0	0.00E+00
18		Busy	6.73E-04	0	0.00E+00
19		Free	5.93E-04	4	2.37E-03
20	25	Moderate	7.46E-04	0	0.00E+00
21		Busy	7.68E-04	0	0.00E+00
22		Free	2.36E-03	4	**9.46E-03**
23	32	Moderate	**3.56E-03**	0	0.00E+00
24		Busy	2.96E-03	0	0.00E+00
∑					**1.82E-02**

Table 5.4 Cumulative damage index for Year 2008 (weekend)

Case No.	Representative wind speed U_w (m/s)	Representative traffic condition	Damage index/ hour	Accumulated hours	∑D
1		Free	0.00E+00	706	0.00E+00
2	2	Moderate	5.03E-07	785	3.95E-04
3		Busy	8.75E-06	295	**2.58E-03**
4		Free	0.00E+00	357	0.00E+00
5	5	Moderate	1.15E-06	219	2.51E-04
6		Busy	1.18E-05	0	0.00E+00
7		Free	0.00E+00	68	0.00E+00
8	8	Moderate	0.00E+00	33	0.00E+00
9		Busy	1.58E-05	0	0.00E+00
10		Free	0.00E+00	20	0.00E+00
11	10	Moderate	9.30E-06	10	9.30E-05
12		Busy	2.96E-05	0	0.00E+00
13		Free	2.02E-05	1	2.02E-05
14	15	Moderate	2.78E-05	2	5.57E-05
15		Busy	9.77E-05	0	0.00E+00
16		Free	3.48E-04	0	0.00E+00
17	20	Moderate	3.96E-04	0	0.00E+00
18		Busy	3.46E-04	0	0.00E+00
19		Free	5.90E-04	0	0.00E+00
20	25	Moderate	7.56E-04	0	0.00E+00
21		Busy	8.93E-04	0	0.00E+00
22		Free	3.59E-03	0	0.00E+00
23	32	Moderate	3.11E-03	0	0.00E+00
24		Busy	**3.90E-03**	0	0.00E+00
∑					**3.40E-03**

Although the data about the time percentage of possible incidental conditions is not available, several assumed situations are studied in order to give some insights. Fig. 5.10 shows the cumulative damage indices in 2008 with different percentages of the time associated with incidental conditions out of the total time. With the increase of the time percentage of incidental conditions, the bridge-block condition causes decreasing damage index accumulation while the road-block condition causes increasing damage index accumulation. The results of Fig. 5.10 show that the incidental conditions only make considerable impacts on the fatigue damage when the time durations of the road-block conditions are pretty significant.

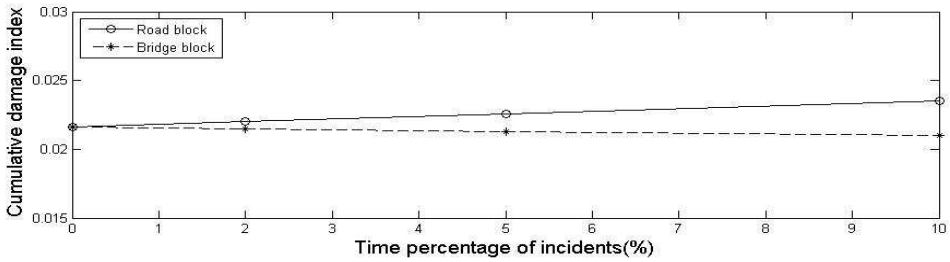

Fig. 5.10 Damage index comparison with different time percentage of incidents

5.4 Conclusions

In this chapter, a scenario-based deterministic fatigue analysis model for long-span bridges was proposed. In order to capture the unique dynamic interactions critical for long-span bridges, site-specific traffic and wind conditions were characterized. In addition to normal traffic condition, some incidental conditions were also considered.

Representative scenarios with different combinations of traffic and wind conditions were then categorized from a typical hour, day, week, month and year progressively. In order to reach a balance point among the sufficient coverage of representative scenarios, reasonable simulation efforts and limited data, some necessary assumptions and approximations were made in order to be able to develop the approach. These assumptions and approximations include:

(1) The wind and traffic conditions within an hour are assumed to be constant. This assumption is primarily due to the limited details available for typical data. More refined data can be applied once it becomes available in the future;

(2) In normal conditions, wind and traffic are deemed as mutually independent. So the combination of different wind and traffic conditions to form each representative scenario was made randomly herein. This can be improved if the detailed record is available or substituted by other reasonable combination rule.

(3) The continuous range of wind speeds is approximated into eight representative wind speeds and different traffic densities are represented by three representative traffic conditions.

By using the advanced Bridge/Traffic/Wind interaction analysis model, the dynamic response for each representative scenario was calculated. In this chapter, a linear fatigue theory was applied to assess fatigue damage. It is advisable that more advanced fatigue theory can be easily applied to the proposed framework. The fatigue damage index for each representative scenario was calculated and the cumulative damage index for a typical year was also assessed. A prototype bridge was used only for demonstration purposes of the proposed methodology. The deterministic model introduced in the present study will become the important basis for the reliability-based fatigue analysis methodology, which will be introduced in the next chapter.

5.5 References

AASHTO. (2007). LRFD bridge design spécifications, Washington, D.C.

Barker, R.M. and Puckett, J.A. (1997). Design of highway bridges, John Wiley & Sons, Inc.

Broquet, C., Bailey, S. F., Fafard, M. and Brühwiler, E. (2004). "Dynamic behavior of deck slabs of concrete road bridges." Journal of Bridge Engineering, 9(2), 137–146.

Chen, S. R. and Cai, C. S. (2007). "Equivalent wheel load approach for slender cable-stayed bridge fatigue assessment under traffic and wind: feasibility study." Journal of Bridge Engineering, 12(6), 755-764.

Chen, S. R. and Wu, J. (2008). "Performance enhancement of bridge infrastructure systems: long-span bridge, moving trucks and wind with Tuned Mass Dampers." Engineering Structures, 30, 3316-3324.

Chen, S. R. and Wu, J. (2010). "Dynamic performance simulation of long-span bridge under combined loads of stochastic traffic and wind." Journal of Bridge Engineering, 15(3), 219-230.

Chen, S. R., Cai, C. S. and Wolshon, B. (2009). "From normal operation to evacuation: single-vehicle safety under adverse weather, topographic and operational conditions." Natural Hazards Review, ASCE, 10(2), 68-76.

Chen, Y. B. and Feng, M. Q. (2006). "Modeling of traffic excitation for system identification of bridge structures." Computer-Aided Civil and Infrastructure Engineering, 21, 57-66.

Ditlevsen, O. (1994). “Traffic loads on large bridges modeled as white-noise fields.” Journal of Engineering Mechanics, 120(4), 681-694.

Ditlevsen, O. and Madsen, H. O. (1995). “Stochastic vehicle-queue-load model for large bridges.” Journal of Engineering Mechanics, 120 (9), 1829-1874.

Fisher, J. W., et al. (1980). “Fatigue behavior of full-scale welded bridge attachments.” NCHRP Report 227, National Academy Press, Washington D.C.

Gu, M., Xu, Y. L., Chen, L. Z., Xiang, H. F. (1999). “Fatigue life estimation of steel girder of Yangpu cable-stayed Bridge due to buffeting.” Journal of Wind Engineering and Industrial Aerodynamics, 80(3), 383-400.

Guo W. H., Xu Y. L. (2001). “Fully computerized approach to study cable stayed bridge-vehicle interaction.” Journal of Sound and Vibration, 248(4), 745–61.

Hallenbeck, M., Rice, M., Smith, B., Cornell-Martinez, C., Wilkinson, J., (1997). “Vehicle volume distribution by classification.” Washington State Transportation Center (http://depts.washington.edu/trac), University of Washington, 1107 NE 45th St. Suite 535, Seattle WA 98105, 54 pp.

Laman, J. A. (1995). “Fatigue load models for girder bridges.” Dissertation, University of Michigan, Ann Arbor (MI).

Miner, M. A. (1945), “Cumulative damage in fatigue.” J. Appl. Mech. 12, 1945, A159–A164.

Moses, F., Schilling, C. G., et al. (1986). Fatigue evaluation procedures for steel bridges, NCHRP Report 299, National Academy Press, Washington D.C.

Moses, F. (2001). Calibration of load factors for LRFR bridge, Transportation Research Board NCHRP Report, No. 454.

Mullard, J. A. and Stewart, M. G. (2009). “Stochastic Assessment of Timing and Efficiency of Maintenance for Corroding RC Structures.” Journal of Structural Engineering, 135(8), 887-895.

Nagel, K., Schreckenberg, M. (1992). “A cellular automaton model for freeway traffic.” Journal de Physique I France, 2(12), 2221-2229.

National Research Council (2000). Highway Capacity Manual, Washington, DC.

Nowak, A. S. (1993). “Live load models for highway bridges.” Structural Safety, 13, 53-66.

O’Connor, A. and O’Brien, E. (2005). “Mathematical traffic load modeling and factors influencing the accuracy of predicted extremes.” Canadian Journal of Civil Engineering, 32(1), 270–278.

Oh, B. H., Lew, Y. and Choil, Y. C. (2007). “Realistic assessment for safety and service life of reinforced concrete decks in girder bridges.” Journal of Bridge Engineering, 12(4), 410-418.

Pourzeynali, S and Datta, T. K. (2005). “Reliability analysis of suspension bridges against fatigue failure from the gusting of wind.” Journal of Bridge Engineering, 10(3), 262-271.

Schadschneider, A. (2006). “Cellular automata models of highway traffic.” Physica A, 372, 142–150.

Schilling, C. G., Yao, W. X. (1999). “A nonlinear damage cumulative model for uniaxial fatigue.” International Journal of Materials, ASTM 5(4), 767-778.

Simiu, E. and Scanlan, R. H. (1996). Wind Effects on Structures - Fundamentals and Applications to Design, 3rd Edition, Wiley, New York.

Stephens, R. I., Fatemi, A., Stephens, R. R., Fuchs, H. O. (2001). Metal fatigue in engineering, 2nd edition, John Wiley & Sons, Inc.

TRANSIMS Travelogues, Transportation analysis and simulation system, Los Alamos National Laboratory, Los Alamos, <http://www-transims.tsasa.lanl.gov/travel.shtml>, lastly accessed on April 30th 2008.

Wu, J. and Chen, S. R. (2008). “Traffic flow simulation based on cellular automaton model for interaction analysis between long-span bridge and traffic.” Inaugural International Conference of the Engineering Mechanics Institute (EM08), May 18-21, 2008.

Wu, J. and Chen, S. R. (2010). “Probabilistic dynamic behavior of long-span bridge under extreme events.” Engineering Structures (under re-review with minor change).

Xu, Y. L. and Guo, W. H. (2003). “Dynamic analysis of coupled road vehicle and cable-stayed bridge system under turbulent wind.” Engineering Structures, 25, 473-486.

CHAPTER 6: FATIGUE ASSESSMENT OF SLENDER LONG-SPAN BRIDGES: A RELIABILITY APPROACH

6.1 Introduction

A bridge starts the deterioration process from the first day it goes into service. Rational evaluation of the fatigue performance of a bridge is a key to assessing its lifetime performance including general planning such as maintenance and associated costs. A fatigue analysis is different from a strength or aerodynamic stability problem (e.g. flutter) which focuses on the worst-case scenario, in that it is examined over an extended time period, which can be as long as the design lifetime of the bridge. As a result, realistically simulating time-variant service loads and the response of a slender long-span bridge throughout its lifetime becomes essential for an accurate prediction of the fatigue performance.

It is known that stochastic wind and traffic loads, dynamic interaction and fatigue accumulation for a slender long-span bridge vary over time and are inherently uncertain. In the several decades, reliability theory has been applied in the field of structural engineering to consider the uncertainties associated with structures, the environment and resulting loads (Ellingwood et al. 1980; Nowak 1999). Most existing reliability-based research on bridges focused on short and medium span bridges (Caprani and O'Brien 2006; Akgul and Frangopol 2004; Akgul and Frangopol 2005a; Akgul and Frangopol 2005b; Czarnecki and Nowak 2008). For slender long-span bridges, only a few studies have been completed on aerodynamic performance such as flutter or buffeting (Cheng et al. 2005; Pourzeynali and Datta 2002; Ge et al. 2000; Jakobsen and Tanaka 2003). In addition, several researchers have studied the reliability of long-span bridges

through the analysis of field monitoring data (Frangopol and Imai 2004; Frangopol et al. 2008; Catbas et al. 2008; Imai and Frangopol 2002). To date, no study has focused on reliability-based fatigue analysis, considering traffic and wind loads as well as their dynamic interactions, for slender long-span bridges.

In this chapter, a framework for the reliability-based fatigue assessment of a slender long-span bridge is presented. Initially, a scenario-based deterministic fatigue damage analytical model is introduced. Then, the reliability-based fatigue life prediction is conducted. Finally, using the proposed model, the reliability index for fatigue damage of the main component of a typical slender long-span bridge is assessed for demonstrative purposes.

6.2 Scenario-Based Fatigue Damage Model for a Typical Year -Deterministic Basis

The basic deterministic scenario-based fatigue damage model for a long-span bridge has already been described in Chapter 5. For the sake of completeness and some different points with Chapter 5, the deterministic fatigue analysis model will be presented briefly. As shown in Fig. 6.1, the fatigue model consists of two major parts: (1) categorization of representative scenarios; and (2) deterministic fatigue damage assessment for a typical year. More details of each part will be introduced in the following sections.

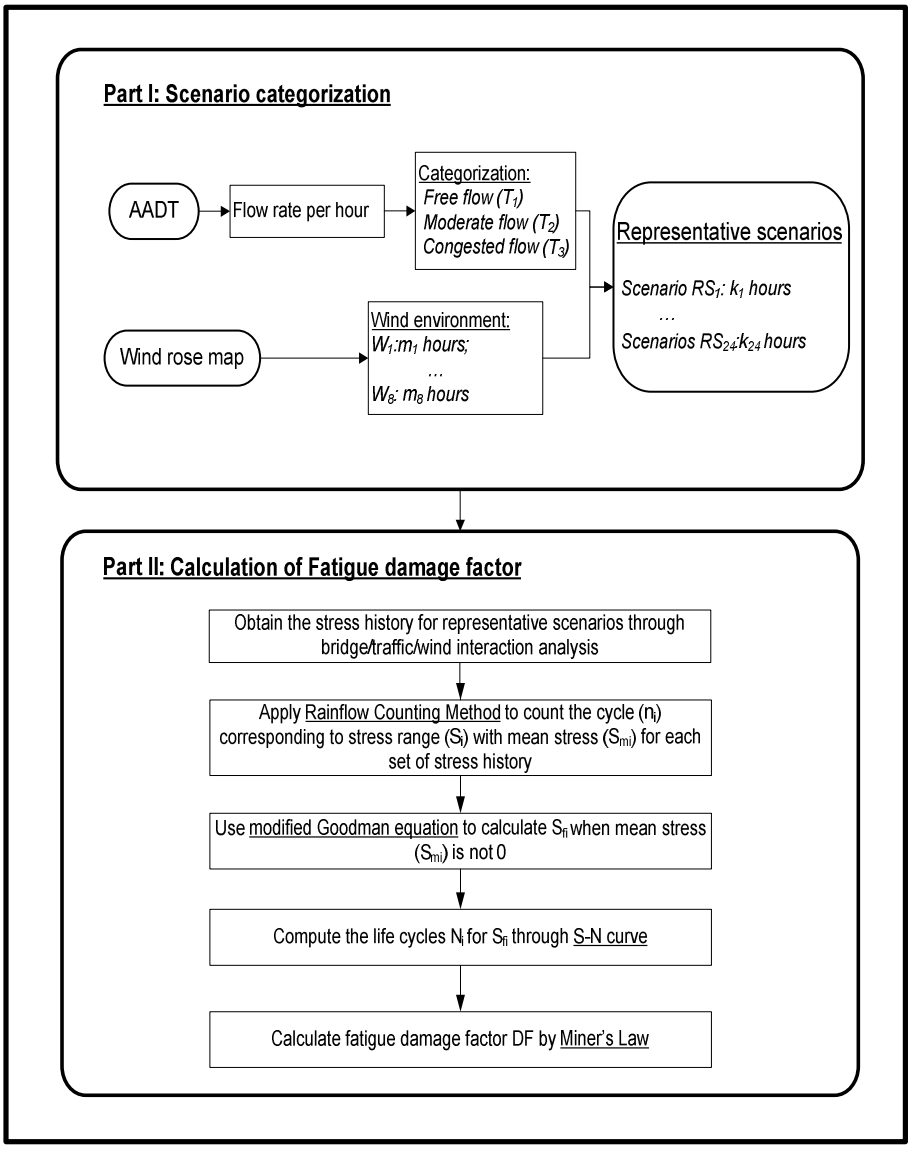

Fig. 6.1 Flowchart of scenario-based deterministic fatigue analysis

6.2.1 Part I- Categorization of representative scenarios

6.2.1.1 Representative scenarios

Representative scenarios are defined to cover the typical load combinations of the stochastic traffic and wind acting on a slender long-span bridge. According to the Highway Capacity Manual (HCM) (National Research Council 2000), the traffic flow on a freeway is typically

classified into six levels of service (LOS) from A to F, ranging from free flow to severe congestion. To maintain acceptable numerical simulation effort in the following analysis, some reasonable simplifications are needed. In the present study, six LOS will be reduced to three representative traffic conditions (T_i, i=1-3) by combining similar LOS: (a) Free (T_1): A~B LOS; (b) Moderate (T_2): C~D LOS; (c) Busy (T_3): E~F LOS. The Beaufort wind scale is often used to define the severity of wind effects with respect to wind speed from Scale 1 to Scale 12. Similar to LOS, "representative wind speeds" are defined by combining similar categories of wind conditions. In this study, eight representative wind speeds (W_j, j=1-8) are defined as 2m/s (W_1), 5m/s (W_2), 8m/s (W_3), 10m/s (W_4), 15m/s (W_5), 20m/s (W_6), 25m/s (W_7) and 32m/s (W_8) which correspond to the ranges of wind speeds between [0 - 3.5], (3.5 - 6.5], (6.5 - 9], (9 - 12.5], (12.5-17.5], (17.5-22.5], (22.5-28.5] and (28.5-32] (m/s), respectively. As a result, the combination of one representative traffic condition and one representative wind speed will eventually generate twenty-four possible representative scenarios (RS) of wind/traffic conditions as shown in Table 6.1.

Table 6.1 Representative scenario

Wind condition (W_i)	Wind speed (m/s)	Traffic flow condition (T_i)		
		Free (T_1)	Moderate (T_2)	Congested (T_3)
W_1	2	RS_1	RS_2	RS_3
W_2	5	RS_4	RS_5	RS_6
W_3	8	RS_7	RS_8	RS_9
W_4	10	RS_{10}	RS_{11}	RS_{12}
W_5	15	RS_{13}	RS_{14}	RS_{15}
W_6	20	RS_{16}	RS_{17}	RS_{18}
W_7	25	RS_{19}	RS_{20}	RS_{21}
W_8	32	RS_{22}	RS_{23}	RS_{24}

6.2.1.2 Categorization process from local traffic and wind record to representative scenario

Traffic flow

The traffic flow varying over hours, weeks, and months will generally follow similar trends among different highways (National Research Council 2000). For example, the daily traffic flow

may reach two peaks in the morning and evening, respectively, when most people commute between home and work or school. In this study, an hour is taken as the basic time period during which the traffic flow rate and wind velocity are both assumed to be constant. When the continuous long-term traffic monitoring data for a particular bridge is available, theoretically the flow rate for each hour can be statistically obtained, as long as the records are sufficiently long. In reality, long-term and continuous traffic monitoring data specific to the bridge may not always be available, and the data from nearby highways as well as generic data are then considered as an acceptable alternative. In this case, the flow rate (N) for a certain hour can be calculated through the transformation from the AADT to the monthly, weekly and hourly variation of the flow rate by applying Eq. (5.2). Once the flow rate (N) for any hour is obtained, one of the representative traffic conditions (T_i) will be assigned based on the definitions of LOS. Cumulatively, the occurrence probability of any representative traffic condition T_i during the study period (e.g. one year) can be identified.

Wind environment

The representative wind speeds (W_j, j=1-8) are classified based on the equivalent wind velocity (U_{eq}) perpendicular to the longitudinal direction of the bridge. The natural wind velocity, including both wind speed and direction, can be linked with the corresponding U_{eq} by considering the angle between the direction of natural wind and the transverse direction of the bridge as:

$$U_{eq} = U_n \cos\theta \tag{6.1}$$

where θ is the angle between the bridge's transverse direction and the direction shown on the wind rose map. U_n and U_{eq} are the natural and equivalent wind velocities, respectively.

For some critical long-span bridges, long-term wind velocity monitoring data may be available. In this case, the actual historical wind data can be adopted to define the natural wind velocities

over time. If the long-term monitoring data is not available, the local wind rose maps close to the site of the bridge can provide the probability of occurrence for each natural wind velocity (including wind speed and direction) in a certain period of time (e.g. a month or a year). Accordingly, the equivalent wind speed U_{eq} can be obtained using Eq. (6.1), which will be checked against the classification criteria of representative wind speeds as introduced earlier to finish the categorization. As a result, the probability of each representative wind speed W_j (j=1-8) for each month is obtained. By repeating the process for the wind rose maps for each month within a year, the cumulative probability of occurrence for each representative wind speed in a year can be obtained.

Combination of traffic flow and wind

Traffic and wind can be typically regarded as two mutually independent random processes most of the time, except some rare cases such as when extremely strong wind events (e.g. hurricane) exists and the bridge may be closed to traffic for very short periods of time. Due to the negligible time periods of these extreme events as compared to normal situations, wind and traffic load modeling are treated as independent from one another in the present study.

Therefore the probability of the k^{th} "representative scenario (RS_k)" can be easily computed through the following equation.

$$P\left(RS_k\right) = P\left(T_i\right) P\left(W_j\right) \tag{6.2}$$

where $P(RS_k)$ is the occurrence probability of the k^{th} representative scenario, $P(T_i)$ and $P(W_j)$ are the occurrence probability of the representative traffic condition i and the wind condition j, respectively. In the present study, i=1-3, j=1-8 and k=1-24(=3×8).

So the total hours of the k^{th} representative scenario $H(RS_k)$ that occurred in the duration period (e.g. one year) can be easily calculated by using the following equation:

$$H\left(RS_k\right) = T_{study} \cdot P\left(RS_k\right) \tag{6.3}$$

where T_{study} is the time length (in hours) of the study period (e.g. one year).

6.2.2 Part II- Fatigue damage assessment in a typical year

For each representative scenario (RS_k), the time-variant stress levels at a particular location of the bridge member in an hour will be calculated through the bridge/traffic/wind interaction analysis (Chen and Wu 2010). The stress history in a typical year can be computed by linearly superimposing the hourly stress results.

In the present study, Miner's rule (Miner 1945) is used to evaluate the fatigue performance based on the results of the stress calculations and the S-N curve (S: stress range, N: number of cycles to failure). It is known that S-N curve is based on the assumption that the loading is constant. The realistic load is random in nature and the equivalent stress range and cycles will be derived from the Rainflow Counting Method (Matsuishi and Endo 1968). The Rainflow Counting Method, which has been widely used in fatigue damage assessment, is based on the stress cycle identification to consider the segment of a stress-time history between any two subsequent local extremes (from peak to a valley or from valley to a peak) (Matsuishi and Endo 1968). Modified Goodman Equation (Eq. (6.4)) is used to transfer the stress range unless the cycle is fully reversed, i.e., the mean stress is non-zero since the S-N (stress-life) curve corresponds to the fully-reversed cycle (Smith 1942; Stephens et al. 2001):

$$\frac{S_a}{S_f} + \frac{S_m}{S_u} = 1 \tag{6.4}$$

where S_a is the alternating stress. S_m is the mean stress. S_f is the corresponding stress amplitude for the fully reversed ($S_m = 0$) fatigue limit of smooth specimens and S_u is the ultimate tensile strength.

The hourly fatigue damage factor (DF) for the k^{th} representative scenario (DF_k) caused by the combined loads is computed through Eq. (6.5) following Miner's Law (Miner 1945):

$$DF_k = \sum \frac{n_j}{N_j} \tag{6.5}$$

where DF_k is the damage factor per hour caused by the stress cycles of the representative scenario *k*. N_j is the fatigue life corresponding to stress amplitude S_j. n_j is the number of the cycles at the stress amplitude S_j.

The yearly cumulative fatigue damage factor (DF_y) can be calculated as

$$DF_y = \sum_{k=1}^{n_k} DF_k \cdot H\left(RS_k\right) \tag{6.6}$$

where n_k is the total number of representative scenarios (k=24 in this study).

6.3 Reliability Model for Fatigue Life Assessment

6.3.1 Uncertainties of major parameters used in fatigue life prediction

There are uncertainties related to the structural modeling, wind environment and traffic loads for slender long-span bridges. For example, climate change has resulted in variations in wind environment over time (Sterr et al. 2003). The expansion of the population in coastal areas has also led to an increase in traffic volume on major highways (Farahmand 1997). As discussed earlier, the fatigue performance of a long-span bridge is actually a lifetime serviceability issue

which may range from 50 to 100 years, depending on the design life of the bridge. Therefore, the traffic growth during the lifespan of a long-span bridge should be considered. Wind flutter derivatives have been considered as random variables in past studies related to flutter analysis (Cheng et al. 2005). A buffeting analysis encompasses a collection of different values of flutter derivatives corresponding to a wide range of different wind speeds. As a result, to consider flutter derivatives as random variables in buffeting analysis may require prohibitively high computational effort. Since the present study focuses on developing a framework of fatigue analysis subjected to the combined loads of wind and traffic, the flutter derivatives will be treated as deterministic variables to avoid excessive computational costs in the present study. As a result, the uncertainties related to the growth factor of AADT, wind velocity and mechanical properties of a long-span bridge are those considered in this study.

6.3.1.1. Growth factor of AADT

To evaluate the fatigue life, AADT is an important variable which directly affects the specific traffic loads on the bridge. AADT varies over years and is influenced by numerous factors like local birth rate and local gross domestic product (GDP) (National Research Council 2000). Local traffic departments often adopt a growth factor (*gf*) to predict future traffic flow, which is typically calculated using Eq. (6.7) (Sliupas 2006):

$$gf = \sqrt[k]{\frac{E_t}{E_{t-k}}} - 1 \tag{6.7}$$

where k is the number of the total years in which AADT data is available, t is the most recent year with the available AADT data, E_t denotes the AADT of the t^{th} year, and E_{t-k} denotes the AADT of the $(t\text{-}k)^{th}$ year.

In the present study, the Cellular Automaton (CA) traffic flow model (Nagel and Schreckenberg 1992) is used to simulate each representative traffic condition (T_i), in order to determine the

instantaneous information of each vehicle for the stochastically modeled traffic, such as its speed and location.

6.3.1.2 Wind velocity data

As discussed earlier, the actual wind speeds on a long-span bridge are random in nature and may vary over years. In situations when long-term wind velocity monitoring data on a long-span bridge is available, the actual wind velocity data for all the service years can be adopted directly. If the actual wind monitoring data is not available, it will be also straightforward to repeat the characterization process of wind velocity for each year if the wind rose maps of all the service years are available. However, if wind rose maps of only a few years are available, some reasonable assumptions on the typical statistical distributions will be needed in order to rationally extrapolate to the whole service time period of the bridge. This is especially critical for coastal long-span bridges which may experience a few extreme wind events (e.g. hurricanes) each year, while the trend of hurricanes each year is hard to be modeled with a standard distribution. Given the substantial difference and the complex nature of wind environments on different long-span bridges in different regions (e.g. coastal, inland), a bridge-specific characterization process, rather than a generic assumption, is necessary to accurately consider the yearly difference of wind velocities on a slender long-span bridge.

In addition to yearly difference, the wind velocities also bear inherent uncertainties due to the random nature and possible errors from data measurements and processing. Rather than taking the wind velocity as a random variable directly, the present study considers the uncertainties associated with wind speeds through a derived variable - "the occurrence probability of each representative wind speed ($P(W_j)$)" as the random variable.

As discussed above, please be noted that various refined characterizations of wind velocity data can be made within the proposed framework for any particular long-span bridge, depending on the availability of the bridge-specific data and the location of the bridge. Since the present study focuses on developing a general methodological framework, the characterization of the wind velocity for a specific long-span bridge deserves a separate case study.

6.3.1.3. Mechanical properties of bridge

A long-span bridge is a complex three-dimensional structure which consists of a number of components with different mechanical properties. From the perspective of dynamic response and fatigue analysis, the elastic modulus, the moment of inertia of the girder and the damping ratio are especially important according to the observations from previous studies (Cheng et al 2005, Pourzeynali and Datta 2002). Therefore, in the present study, these variables will be treated as random variables.

6.3.2 Reliability method

Recall the scenario-based fatigue damage model introduced earlier. This fatigue model formulation results in an implicit limit state function which can be expressed as:

$$g = \sum_{y=1}^{n_y} DF_y - 1 \tag{6.8}$$

where $\sum_{y=1}^{n_y} DF_y$ is the cumulative damage factor during the total n_y years of the service for the concerned component. When the cumulative damage factor reaches one, the member is regarded as failure due to fatigue damage (Stephens, et al. 2001).

The flowchart depicting the proposed reliability analysis framework is shown in Fig. 6.2. Because the limit state function defined in Eq. (6.8) is an implicit function, the response surface method

(RSM) (Bucher and Bourgund 1990) is applied as it can approximate an implicit function with a polynomial explicit function expressed as Eq. (6.9) through regression analysis.

$$\hat{g}(x) = a_0 + \sum_{i=1}^{n} b_i x_i + \sum_{i=1}^{n} c_i x_i^2 \tag{6.9}$$

where $\hat{g}(x)$ is the approximated limit state function. a_o, b_i, c_i are the coefficients to be calculated. x_i is the i^{th} basic random variable and n is the total number of random variables.

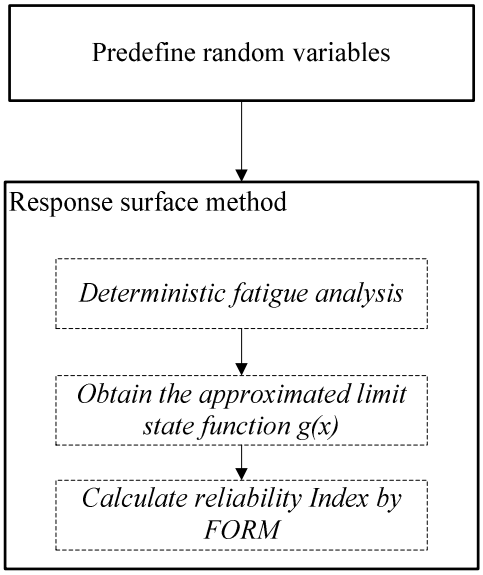

Fig. 6.2 Reliability analysis framework

To form the approximated limit state function $\hat{g}(x)$, the mean value (μ), low value (μ-$l\sigma$) and high value (μ+$l\sigma$) (σ is the standard deviation) for each random variable as defined in Table 6.2 will be used, where l is set as 3.0 for the first iteration and 0.99 for the second (also final) iteration (Bucher and Bourgund 1990). The combination of the mean, low and high values for each variable will form $2n$+1 initial sets of input parameters. The coupled bridge/traffic/wind analysis (Chen and Wu 2010) and the scenario-based fatigue analysis will be conducted for each set of the random variables. After obtaining the approximate limit state function $\hat{g}(x)$, the first-order reliability method (FORM) is applied to estimate the reliability index β.

Table 6.2 Statistical properties of random variables

Random variables		Unit	Mean	Std	Distribution type	Description	Source
Mechanical properties	ξ	/	0.005	0.001	Normal	Damping ratio	Assumed
	E	GPa	200	20	Normal	Elastic modulus of girder	Cheng et al. (2005)
	I	m^4	3.0856	0.30856	Normal	Moment of inertia of girder	Cheng et al. (2005)
Traffic volume	gf	/	0.05	0.015	Normal	AADT growth factor	Assumed
Occurrence probability of representative wind speeds $P(W_i)$*	$P(W_1)$	%	53.6 (195.64 days)	5.36	Normal	$P(U_{eq}=2m/s)$	Assumed
	$P(W_2)$	%	27.2 (99.28days)	2.72	Normal	$P(U_{eq}=5m/s)$	Assumed
	$P(W_3)$	%	5.80 (21.17days)	0.58	Normal	$P(U_{eq}=8m/s)$	Assumed
	$P(W_4)$	%	1.31 (4.78days)	0.131	Normal	$P(U_{eq}=10m/s)$	Assumed
	$P(W_5)$	%	0.07 (0.26days)	0.007	Normal	$P(U_{eq}=15m/s)$	Assumed
	$P(W_6)$	%	0	0	N/A	$P(U_{eq}=20m/s)$	Assumed
	$P(W_7)$	%	0.23 (0.84days)	0.023	Normal	$P(U_{eq}=25m/s)$	Assumed
	$P(W_8)$	%	0.81 (2.967days)	0.081	Normal	$P(U_{eq}=32m/s)$	Assumed

* The mean value of P(Wi) is derived from local wind rose map. The std value and distribution type are assumed.

6.4 Illustrative Example

6.4.1 Prototype long-span bridge and service loads

A typical long-span cable-stayed bridge in costal Louisiana with steel girders shares the same structural parameters which has been studied in the previous chapters is used to illustrate the proposed model. The random variables, such as the mechanical variables, growth factor (*gf*) of AADT and the occurrence probability of each representative wind speed for this illustrative example are shown in Table 6.2. All the variables are assumed to follow the normal distribution. Regarding mechanical properties, the mean values of random variables as listed in Table 6.2 were determined based on the prototype bridge data and the standard deviation is assumed to be 10% (E, I) or 20% (ξ) of the respective mean values. The mean value of the probability of any representative wind speed *j* $P(W_i)$ is derived from local wind rose maps and the stand deviation value is assumed to be 10%.

The prototype bridge was opened to traffic in 1983 with a design life of 75 years and the AADT of this bridge in 2008 was 40,000. Since the AADT for other years are not available for the prototype bridge, the AADT for other years is calculated based on Eq. (6.7). The mean (μ) and the standard deviation (σ) for the growth factor (*gf*) are assumed to be 0.05 and 0.015, respectively (Table 6.2). The variation of AADT caused by different values of the growth factor used in the reliability model during the service life (75 years) was plotted in Fig. 6.3. As discussed earlier, due to the lack of site-specific traffic monitoring data, the variations of the traffic flow rate with respect to AADT will be derived from the generic data of ADT provided in the Highway Capacity Manual (National Research Council 2000) (Fig. 5.3). The vehicle flow rate *N* (veh/hr) is then categorized into one of the predefined three representative traffic conditions (T_i) "Free", "Moderate" or "Busy" as introduced earlier. In the CA traffic model, the representative

traffic density of 9veh/km/ln, 20veh/km/ln and 32veh/km/ln are chosen respectively to compute for the three traffic conditions. The combination of vehicle types is set as 50%, 30% and 20% for cars, light trucks and heavy trucks (Chen and Wu 2010), respectively. Due to the lack of the relevant data, no maintenance or repair is assumed during the 75 years of service. In reality, any maintenance or repair can be considered later by adjusting the fatigue damage factors and associated reliability index accordingly.

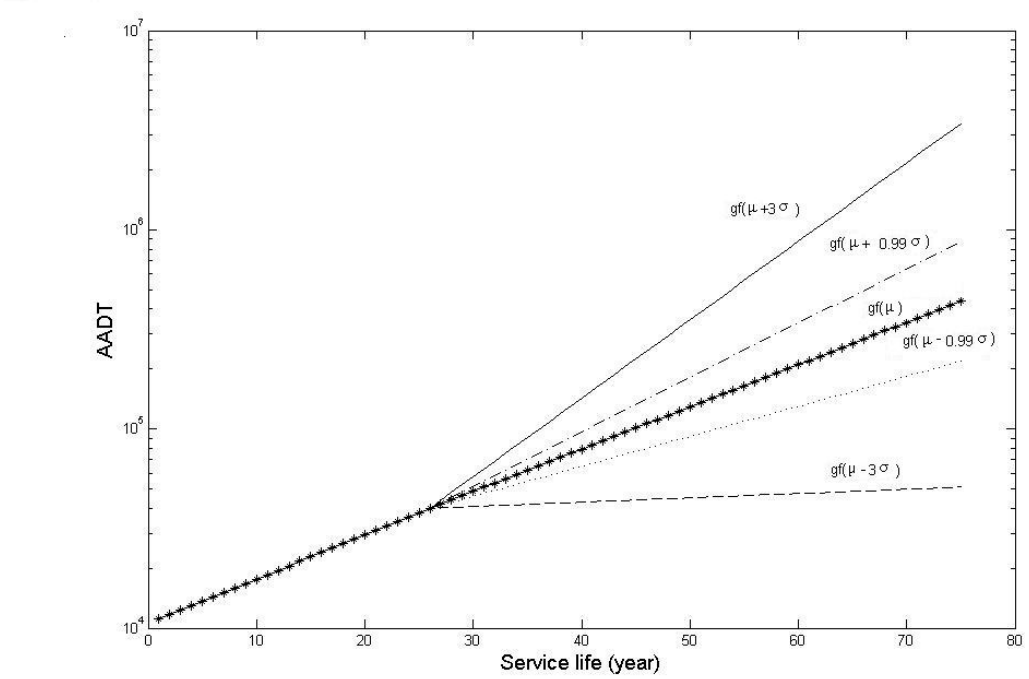

Fig. 6.3 The variation of AADT

As discussed earlier, typically the multi-year wind velocity data can be either characterized by long-term actual wind monitoring on a bridge or wind rose maps during the period of the service time. Obviously, when the full records of wind velocity data over years are available, regardless from actual monitoring data or the whole sets of wind rose maps, it is pretty straightforward to characterize the cumulative probability of occurrence for each representative wind speed simply by repeating the process for each year. In order not to lose generality of the proposed framework, the limited number years of wind rose maps which are available in the public domain, will be

used for the demonstrative purpose. Specifically, the wind rose maps in the New Orleans area close to the location of the bridge (IEM 2010) will be used to characterize the wind data for the prototype bridge. Only three years of wind rose maps (Year 2007-2009) were found to be available in the public domain (IEM 2010). As discussed earlier, for a coastal slender long-span bridge which experiences frequent hurricanes, bridge-specific wind velocity data, either from long-term monitoring or the comprehensive wind rose maps covering all the service years, is critical to any rational prediction of fatigue performance. Therefore, the fatigue assessment of this prototype slender long-span bridge based on wind rose maps in only three years is merely for demonstrative purpose, rather than a realistic case study.

By repeating the characterization process of representative wind velocities for all the three years (Year 2007-2009), the probability of each representative wind speed (W_j) can be derived. The probability values of different representative wind speeds are shown in Fig. 6.4. These probability values will be adopted as the mean values which are assumed to be the same for all the service years of the prototype bridge because of the lack of the actual wind velocity data of each year. Such an approximation is probably the most reasonable way given the limited available wind data. However, the hurricane records in Louisiana showed that there were four noteworthy hurricanes (i.e. Humberto (2007), Gustav (2008), Ike (2008) and Ida (2009)) happening between Year 2007-2009. While within seven years (Year 2000-2007), there were only three noteworthy hurricanes (i.e. Lili (2002), Katrina and Rita (2005)). Therefore although this is just a demonstrative example, it should also be noted that such an approximation for this particular bridge in Louisiana may cause overestimated wind velocities over the service lifespan due to considerably more frequent occurrence of hurricanes between Year 2007-2009.

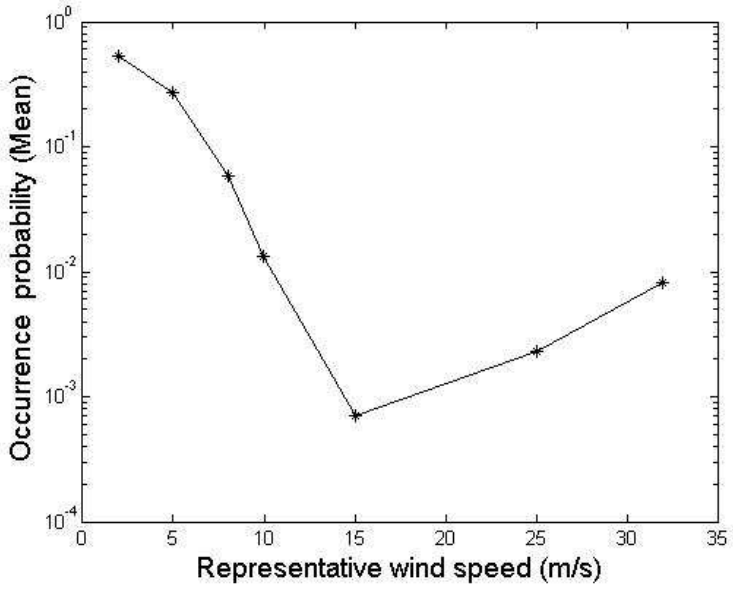

Fig. 6.4 The occurrence percentage of representative wind speeds (W_j)

According to the AASHTO LRFD specification (AASHTO 2007), the members of a bridge are categorized into different types with respective S-N curves and threshold values. In this study, the main member of Type B (an unpainted weathering plain member or the well-prepared welded connections in a built-up member without attachments) is selected to study the fatigue performance. Its stress-life relationship can be expressed as (AASHTO 2007):

$$N(S) = 39.3\times10^{11} / S^3 \tag{6.10}$$

where S is the stress cycle range (MPa), N is the total number of cycles for working stress. The fatigue threshold of a type B member is 110MPa (AASHTO 2007).

Based on the deterministic scenario-based fatigue damage analysis, it was found that the representative wind speeds of W_1~W_6 do not cause any fatigue damage for the main bridge member examined herein regardless of the traffic condition. Thus, only the probabilities of the representative wind speeds W_7 and W_8 are eventually taken as random variables in the reliability study.

6.4.2 Fatigue analysis result- deterministic-based

Fig. 6.5 (a-c) shows the extreme stress comparison of the bottom fiber at the midspan of the bridge (the critical location) under the minimum (μ-3σ), mean (μ) and maximum (μ+3σ) values of the damping ratio, elastic modulus and moment of inertia of the girder, respectively. Two wind speeds, W_7 (25m/s) and W_8 (32 m/s), are studied. The complex coupling effect of traffic density and wind can be observed from Fig. 6.5. For example, it is found that strong wind can cause larger extreme stress. However, the extreme stress does not always increase with traffic density such as the case with heavy traffic, U_{eq}=32m/s and the mean value of moment of inertia (right window in Fig. 6.5(c)). As shown in Fig. 6.75, lower damping ratios, higher elastic modulus and lower moment of inertia of the main girder generally result in higher dynamic stress.

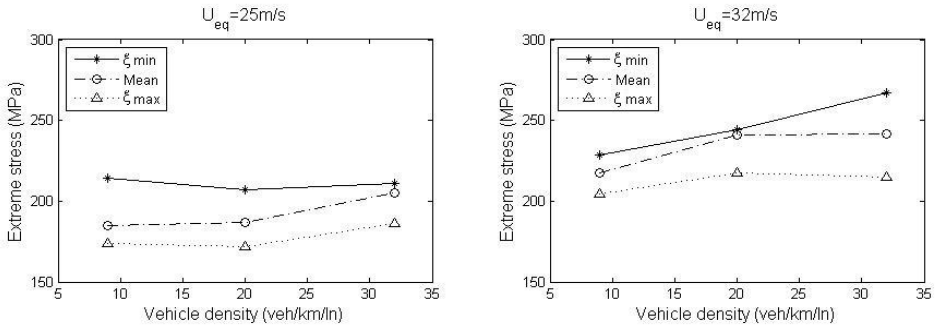

a. ξ_{min} vs ξ_{max}

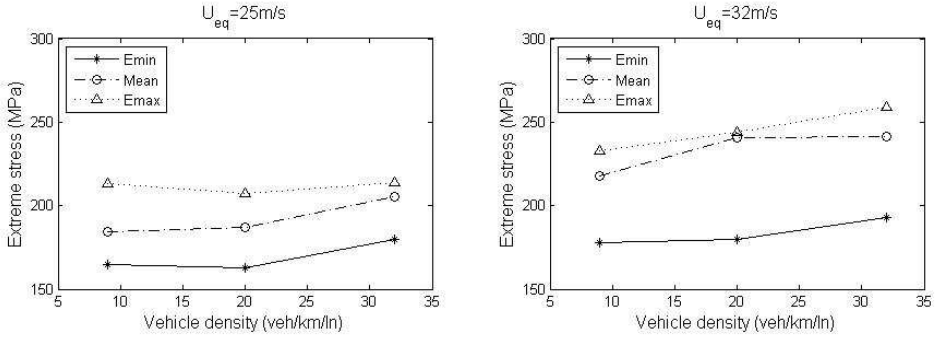

b. E_{min} vs E_{max}

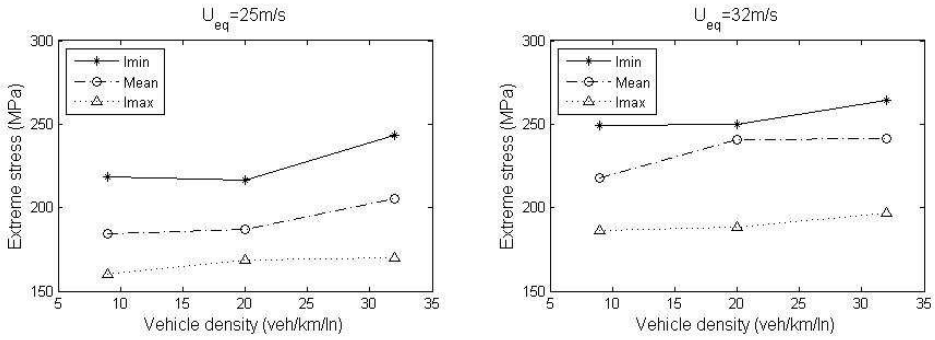

c. I_{min} vs I_{max}

Fig. 6.5 Extreme stress comparison

As introduced in Section 6.2.1, the Rainflow Method is employed to count cycles for each stress range from the stress history. The cycle-counting results for the variables being set as the respective mean values are shown in Fig. 6.6(a-c) for different traffic conditions when the wind speeds are 25m/s (W_7) and 32m/s (W_8), respectively. As shown in Fig. 6.6, the amplitude of the stress generally increases with wind speeds. However, the counts for different stress ranges vary in a complicated manner with different traffic conditions (densities). Based on the rainflow matrix and Miner's law, the fatigue damage factors for the member type B are derived for different wind and traffic conditions and the results are shown in Table 6.3. When the wind speed is 25m/s, the damage factor per hour does not always increase with the density of traffic flow, similar to the stress results. It was found that the damage factor is more sensitive to the change in wind speeds than the change in traffic conditions.

Table 6.3 Damage factor per hour for critical cases

Variable	U_{eq}=25m/s (W_7)			U_{eq}=32m/s (W_8)		
	Free flow (T_1)	Moderate flow (T_2)	Congested flow (T_3)	Free flow (T_1)	Moderate flow (T_2)	Congested flow (T_3)
Mean	0.00E+00	0.00E+00	2.36E-06	5.94E-05	1.57E-04	1.17E-04
ξ_{max}	0.00E+00	0.00E+00	0.00E+00	4.81E-05	7.31E-05	3.78E-05
ξ_{min}	6.95E-05	7.79E-05	7.99E-05	1.04E-04	2.11E-04	4.93E-04
E_{max}	6.54E-06	0.00E+00	2.15E-06	1.69E-04	3.02E-04	2.31E-04
E_{min}	5.51E-06	2.08E-06	1.12E-05	6.39E-05	7.18E-05	1.21E-04
I_{max}	0.00E+00	0.00E+00	0.00E+00	2.55E-06	8.55E-05	6.74E-05
I_{min}	1.80E-05	1.01E-05	5.11E-05	4.59E-04	4.78E-04	6.60E-04

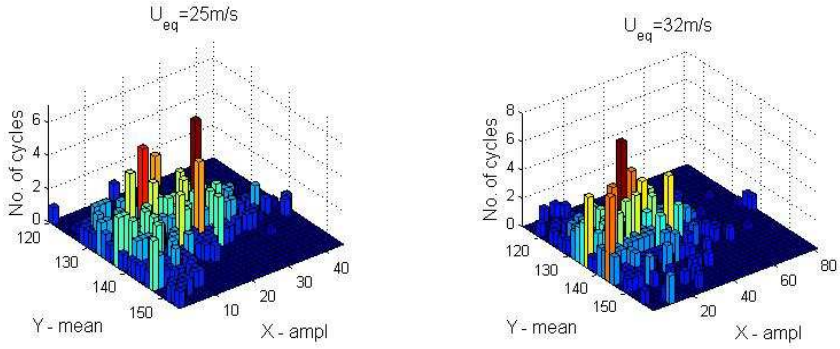

a. Free traffic flow

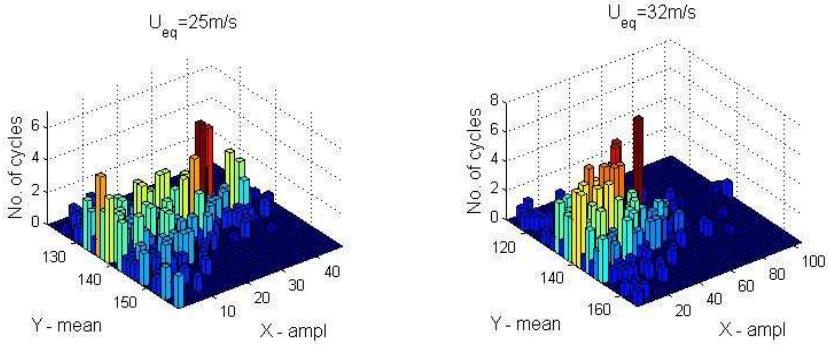

b. Moderate traffic flow

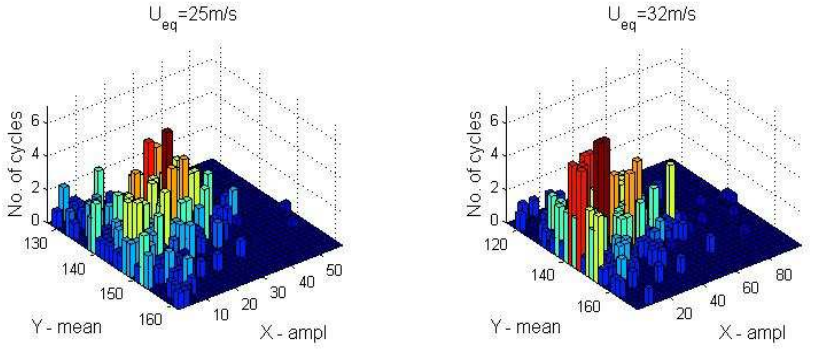

c. Congested traffic flow

Fig. 6.6 Rainflow matrix for critical cases

The results of the cumulative hours for each representative scenario with the minimum, mean and maximum values of the growth factor of AADT are all similar. The cumulative hours of the critical scenarios (RS19~RS24 as defined in Table 6.1) are shown in Table 6.4. From Table 6.4, it can be seen that the case of heavy traffic (T_3) becomes more dominant with the increase of the

service life. As shown in Fig. 6.7, the cumulative yearly damage factor (DF_y) gradually increases throughout the lifespan of the bridge and can reach 0.5452 at the 75th year of the service when all the variables remain as their respective mean values.

Table 6.4 Accumulated hours for critical cases

Case	Service life (year)				
	15	30	45	60	75
$RS_{19}(T_1+W_7)$	298	480	552	555	554
$RS_{20}(T_2+W_7)$	4	109	187	232	232
$RS_{21}(T_3+W_7)$	0	16	168	421	722
$RS_{22}(T_1+W_8)$	1052	1684	1940	1951	1950
$RS_{23}(T_2+W_8)$	13	382	653	819	820
$RS_{24}(T_3+W_8)$	0	64	601	1489	2553

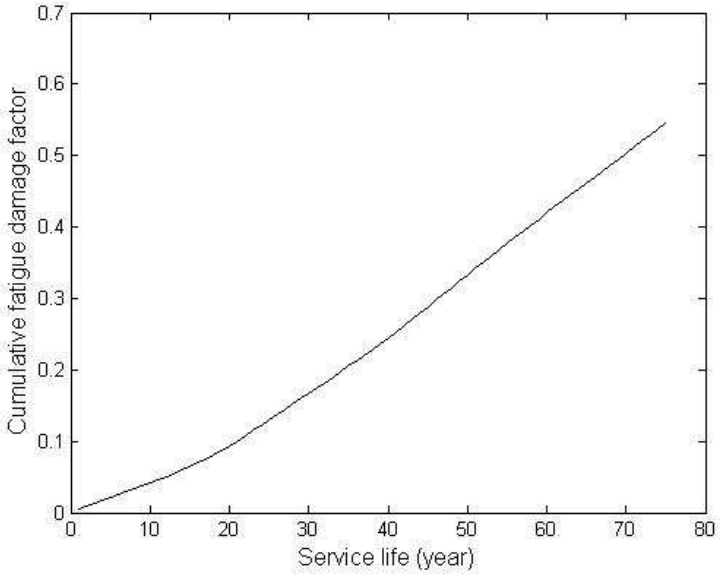

Fig. 6.7 Cumulative damage factor vs. service life

6.4.3 Reliability index

In order to study the fatigue performance at different stages in the lifespan of the prototype bridge, the reliability indices β are calculated for different service lives of the type B member located at the bottom of the midspan of the bridge. As seen in Fig. 6.8, the reliability index β for fatigue damage decreases dramatically with the increase of the service life. β for the service life of 75 years reduced about 65% from that for the service life of 45 year. It can clearly be seen that the

reliability index for a design life of 75 years of the prototype bridge is quite low. As discussed earlier, because the bridge-specific records of wind velocities are not available, the results are more for illustrative purposes, rather than actual assessment results. In fact, there are two approximations which may contribute to the relatively low reliability index: (1) no maintenance or repair was assumed during the design life; and (2) the wind speed conditions were extrapolated with the wind data from the wind rose maps in New Orleans only between Year 2007-2009, when more frequent hurricanes occurred. In order to demonstrate the impact of high wind speeds on the fatigue reliability index, a simple trial analysis is conducted. By simply reducing the current cumulative time period for W8 (2.967 days) to around 1.5 days, the reliability index for the service life of 75 years will increase by 3.4 times of the current value. It is obvious the reliability index is very sensitive to the cumulative time duration of high wind speeds. It has also confirmed that the accuracy of the bridge-specific wind velocity data, especially high wind speed data, is very critical to the fatigue life prediction of a slender long-span bridge, especially in hurricane-prone areas. Long-term wind monitoring data on slender long-span bridges, especially coastal bridges, is desired in order to rationally characterize the lifetime wind conditions.

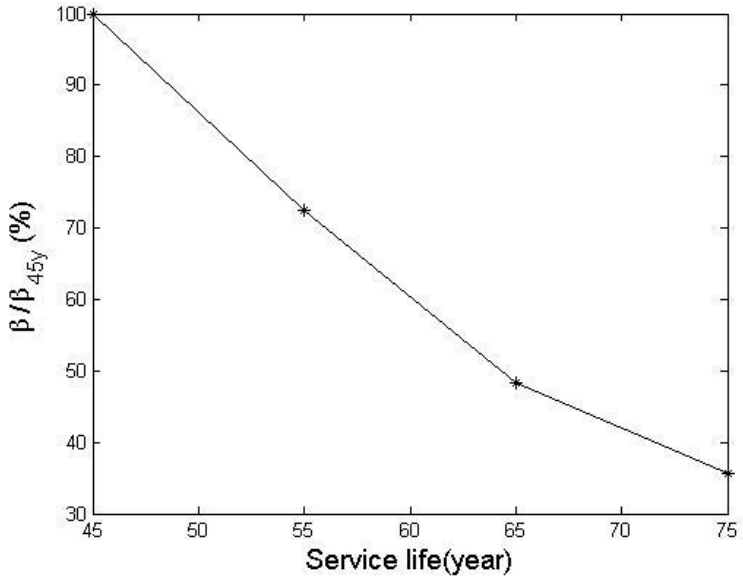

Fig. 6.8 Reliability index ratio vs. service life

6.5 Conclusions

The goal of the study presented in this chapter was to develop and propose a reliability-based framework to account for the main impacts on the fatigue damage of slender long-span bridges that are susceptible to cumulative damage from wind and traffic loads. By adopting the proposed framework, the reliability index for fatigue performance of any member of a long-span bridge can be obtained. The following conclusions can be reached as a result of this work:

(1) The fatigue assessment for the critical scenarios discloses that the hourly fatigue damage factor (DF) is more sensitive to changes in the wind condition than changes in the traffic conditions.

(2) The dynamic analysis of bridge/traffic/wind interaction for each scenario requires substantial computational time. In order to make the fatigue analysis practically possible for various combinations of traffic and wind conditions, limited representative scenarios must be selected for a particular bridge. Such a simplification is necessary to enable the assessment of the lifetime fatigue performance of a major bridge both rationally and efficiently. The accuracy can be further improved by selecting more refined representative scenarios, if necessary.

(3) Although Miner's Rule is the most common model applied in fatigue analysis of large structures, the proposed framework is flexible enough to accommodate other nonlinear fatigue models, if needed.

(4) The study also suggests that the fatigue reliability index is quite sensitive to the high wind velocity data. For coastal bridges which frequently experience hurricanes, long-term wind monitoring data on the bridge of interest would be ideal for this type of analysis.

6.6 References

AASHTO. (2007). LRFD bridge design specifications, Washington, D.C.

Akgul, F., Frangopol, D. M. (2004). “Lifetime performance analysis of existing steel girder bridge superstructures.” Journal of Structural Engineering 12, 1875-1888.

Akgul, F., Frangopol, D. M. (2005a). “Lifetime performance analysis of existing reinforced concrete bridges. I: theory.” Journal of Infrastructure Systems, 6, 122-128.

Akgul, F., Frangopol, D. M. (2005b). “Lifetime performance analysis of existing reinforced concrete bridges. II: Application.” Journal of Infrastructure Systems, 6, 129-141.

Bucher, C. G., Bourgund, U. (1990). “A fast and efficient response surface approach for reliability analysis.” Structural Safety 7(1), 57-66.

Cai, C. S. and Chen, S. R. (2004). “Framework of vehicle-bridge-wind dynamic analysis.” Journal of Wind Engineering & Industrial Aerodynamics, 92 (7-8), 579-607.

Caprani, C. C., O’Brien, E. J. (2006). “Statistical computation for extreme bridge traffic load effects.” Civil-Comp Press, Proceedings of the Eighth International Conference on Computational Structures Technology, Paper 139.

Catbas, F. N., Susoy, M., Frangopol, D. M. (2008). “Structural health monitoring and reliability estimation: Long span truss bridge application with environmental monitoring data.” Engineering Structures, 30, 2347-2359.

Chen, S. R. and Cai, C. S. (2007). “Equivalent wheel load approach for slender cable-stayed bridge fatigue assessment under traffic and wind: feasibility study.” Journal of Bridge Engineering, 12(6), 755-764.

Chen, S. R. and Wu, J. (2010). “Dynamic performance simulation of long-span bridge under combined loads of stochastic traffic and wind.” Journal of Bridge Engineering ASCE, 15(3), 219-230.

Chen, X. and Lind, N. C. (1983). “Fast probability integration by three-parameter normal tail approximation.” Structural Safety, 1, 269-276.

Cheng, J., Cai, C. S., Xiao, R. C., Chen, S. R. (2005). “Flutter reliability analysis of suspension bridges.” Journal of Wind Engineering and Industrial Aerodynamics, 93, 757-775.

Czarnecki, A. A., Nowak, A. S. (2008). “Time-variant reliability profiles for steel girder bridges.” Structural Safety, 30, 49-64.

Ellingwood, B., Galambos, T. V., MacGregor, J. C. and Cornell, C. A. (1980). “Development of a probability-based load criterion for American standard A58.” National Bureau of Standards Special Publication No. SP 577, Nat. Bureau of Standards, Washington, D.C.

Farahmand, K. (1997). “Application of simulation modeling to emergency population evacuation.” Proceedings of the 1997 Winter Simulation Conference, 1181–1188, Atlanta, Georgia.

Frangopol, D. M., Imai, K. (2004). “Reliability of long span bridges based on design experience with the Honshu-Shikoku bridges.” Journal of Constructional Steel Research, 60, 373-392.

Frangopol, D., Strauss, M. A., Kim, S. Y. (2008). “Use of monitoring extreme data for the performance prediction of structures: general approach.” Engineering Structures, 30, 3644-3653.

Ge, Y. J., Xiang, H. F., Tanaka, H. (2000). “Application of a reliability analysis model to bridge flutter under extreme winds.” Journal of Wind Engineering and Industrial Aerodynamics, 86, 155-167.

Gu, M., Xu, Y. L., Chen, L. Z. and Xiang, H. F. (1999). “Fatigue life estimation of steel girder of Yangpu cable-stayed Bridge due to buffeting.” Journal of Wind Engineering and Industrial Aerodynamics, 80(3), 383-400.

Guo, W. H., Xu, Y. L. (2001). “Fully computerized approach to study cable-stayed bridge-vehicle interaction.” Journal of Sound and Vibration, 248(4), 745-761.

Iowa Environmental Mesonet (IEM) (2010). <http://mesonet.agron.iastate.edu/sites/locate.php>, Iowa State University of Agronomy, lastly accessed on Oct 5th 2010.

Imai, K., Frangopol, D. M. (2002). “System reliability of suspension bridges.” Structural Safety, 24, 219-259.

Jakobsen, J. B., Tanaka, H. (2003). “Modeling uncertainties in prediction of aeroelastic bridge behavior.” Journal of Wind Engineering and Industrial Aerodynamics, 91, 1485-1498.

Matsuichi, M. and Endo, T. (1968). “Fatigue of metals subjected to varying stress”, Presented in Proceedings of Japan Society of Mechanical Engineering, Fukuoka, Japan.

Miner, M. A. (1945). “Cumulative damage in fatigue.” Trans. ASME. Journal of Applied Mechanics, 67, A159-A164.

Nagel, K. and Schreckenberg, M. (1992). “A cellular automaton model for freeway traffic.” Journal de Physique I France, 2(12), 2221-2229.

National Research Council (2000), Highway Capacity Manual, Washington, D. C.

Nowak, A. S. (1999), “Calibration of LRFD Bridge Design Code.” National Cooperative Highway Research Program Report 368, Washington D.C., USA, NCHRP.

Pourzeynali, S., Datta, T. K. (2002). “Reliability analysis of suspension bridges against flutter.” Journal of Sound and Vibration, 254(1), 143-162.

Pourzeynali, S., Datta, T. K. (2005). “Reliability Analysis of Suspension Bridges against Fatigue Failure from the Gusting of Wind.” Journal of Bridge Engineering, 10(3), 262-271.

Simiu, E. and Scanlan, R. H. (1996). Wind Effects on Structures-Fundamentals and Applications to Design, 3rd Edition, Wiley, New York.

Sliupas, T. (2006). “Annual average daily traffic forecasting using different techniques.” Transport XXI (1), 38–43.

Smith, J. O. (1942). “The effect of range of stress on the fatigue strength of metals”, Bulletin No. 334, University of Illinois, Engineering Experiment Station, Urbana, IL.

Stephens, R. I., Fatemi, A., Stephens, R. R., Fuchs, H. O. (2001). Metal fatigue in engineering, 2nd edition, John Wiley & Sons, Inc.

Sterr, H., Klein, R. J. T. and Reese, S. (2003). “Climate Change and Coastal Zones: An Overview of the State-of-the-Art on Regional and Local Vulnerability Assessments.” In: Giupponi, C. and Shechter, M. (eds.), Climate Changes in the Mediterranean. Cheltenham, UK: Edward Elgar Publishing, 245–278.

Wu, J. and Chen, S. R. (2008). “Traffic flow simulation based on cellular automaton model for interaction analysis between long-span bridge and traffic.” Inaugural International Conference of the Engineering Mechanics Institute (EM08), May 18-21, 2008

CHAPTER 7: CONCLUSIONS AND RECOMMENDATION FOR FUTURE STUDY

7.1 Summary and Conclusions

The dissertation aims to propose a general framework to quantify the performance of long-span bridges through the rationalized dynamic model of Bridge/Traffic/Wind interaction. To achieve this goal, the cellular automaton (CA) traffic flow model was introduced. The CA traffic flow model was integrated with the equivalent dynamic wheel loading approach to study the bridge dynamic response under normal and incidental traffic condition and different wind environment. The serviceability of the long-span bridge under both normal and extreme load conditions was studied. The scenario-based fatigue model was further developed based on the developed Bridge/Traffic/Wind dynamic framework. The reliability-based analysis was finally applied to assess the fatigue damage caused by the coupling effects among bridge, traffic flow and wind throughout the bridge's service life. The main conclusions of this dissertation research are summarized in the following.

(1) A framework of microscopic probabilistic traffic flow simulations for bridge infrastructure system (BIS) using the Cellular Automaton (CA) simulation technique was developed. The framework can adapt to different local conditions such as the traffic densities, speed limits, bridge spans and the length of approaching way as well as some special events such as the partial blockage of lanes due to construction, maintenance or accident. The results of the BIS calculation can offer detailed traffic flow information for various bridge-related studies, such as the time-dependent position, velocity and vehicle type of each individual vehicle through replicating the

main traffic rules. The parametric study on the BIS framework was also conducted and some guidelines on carrying out appropriate CA traffic simulation for different bridges were also given.

(2) Through integrating the CA traffic flow model and EDWL approach, a novel and efficient "semi-deterministic" Bridge/Traffic/Wind interaction analysis model considering stochastic traffic flow and wind was developed to predict the performance of long-span bridges in a more realistic way. The proposed approach was demonstrated through a long-span cable-stayed bridge and can be expanded to other types of long-span bridges without problems. In the case study, the statistical dynamic responses such as displacement and stress of the bridge under normal condition (wind speed is not high and all the lanes are open) and extreme conditions were studied.

(3) The scenario-based deterministic fatigue analysis model was proposed by taking account of the Bridge/Traffic/Wind framework developed for long-span bridges. This was the first simulation model so far that considers the contributions from both traffic and wind loads in bridge fatigue performance. Representative scenarios were defined with different combinations of traffic and wind conditions. Each hour in a typical day, week, months and a year can be categorized with the appropriate representative scenario progressively. The fatigue damage index of the concerned member of a prototype bridge for each representative scenario was calculated and the cumulative damage index for a typical year was assessed. Such a scenario-based fatigue model can served as the basis for the reliability-based model introduced later.

(4) The reliability approach for the fatigue assessment of the long-span bridge was finally proposed based on the above scenario-based fatigue analysis model. Firstly, the representative scenarios of traffic flow and wind loads on bridge during its service life were identified through incorporating the local information of AADT and the wind rose map. Secondly, the fatigue assessment of the concerned member of the bridge subjected to the bridge/traffic/flow interaction

was conducted over years. Finally, the reliability indices of fatigue damage were obtained based on rational considerations of uncertainties. The reliability index results can help prioritize the inspection and renovation of critical members for all the bridges. Through providing more rational predictions of possible damage, the study will also help the transportation authorities to improve the new bridge design and implement effective prevention strategies to avoid any severe fatigue damage on the main components.

7.2 Future Work

Based on the research experience from this study, the writer believes that the following issues can be addressed in the future work to improve the design and reliability analysis of long-span bridges.

(1) The quantification of live load and its dynamic impacts are critical to the serviceability of long-span bridges. However, the current LRFD specification does not cover long-span bridges and very little research has been conducted for long-span bridges by considering rational load scenarios, such as the combination of wind and traffic loads. Based on the general framework of Bridge/Traffic/Wind dynamic interaction analysis developed in this dissertation, more comprehensive studies on the design loads can be carried out in the future, which may contribute to future addition to the specification.

(2) In the dynamic analysis of bridges under normal and extreme situations, few cases were studied in the dissertation because of the limit of the time and scope of the study. More inclusive studies on various extreme events, including some events with other natural or man-made hazards, can be conducted. Moreover, the related studies on effective warning and prevention system for bridge management may also be conducted in the future.

(3) In the present study on fatigue damage assessment, the simple fatigue model, i.e. Miner' law, was applied. The accuracy of the damage prediction can be further improved through adopting some advanced nonlinear fatigue models.

BIBLIOGRAPHY

Ms. Jun Wu was born in 1982 in Xi'an, Shaanxi Province, China. She has pursued the doctoral degree in structural engineering at Colorado State University since 2007. She got her Master of Science and Bachelor of Science degrees from Department of Bridge Engineering, School of Highway Engineering, Chang'an University, China, in 2007 and 2004, respectively.

Dr. Wu has worked as a Graduate Research Assistant at Colorado State University since Jan 2007. From 2004 to 2006, Ms. Wu worked as a Graduate Research Assistant at Chang'an University, China.

Dr. Wu has been involved in research in several areas, such as structural dynamics, construction control, structural damage detection, wind engineering and transportation engineering. She has nearly 15 publications which are listed below:

1. **Wu, J.** and Chen, S. R. (2010). "Probabilistic dynamic behavior of long-span bridge under extreme events", Engineering Structures (under re-review with minor change).

2. Chen, S. R. and **Wu, J.** (2010). "Dynamic performance simulation of long-span bridge under combined loads of stochastic traffic and wind", Journal of Bridge Engineering ASCE, 15(3), 219-230.

3. Chen, S. R., Chen, F., Liu, J. H., **Wu, J.** and Bienkiewicz, B. (2010). "Mobile mapping technology of wind velocity data along highway for traffic safety evaluation", Transportation Research Part C: Emerging Technology, 18, 507-518.

4. Chen, F., Chen, S. R., Liu, J. H. and **Wu, J.** (2009). "Site-specific wind data acquisition and analysis with geospatial mobile testing technology", 11th American Conference on Wind Engineering, Puerto Rico, June 22-26 2009.

5. **Wu, J.** and Chen, S. R. (2009). "An innovative approach to estimate long-span bridge's safety under extreme events", NSF CMMI Research and Innovation Conference, June 22-25 2009, Hawaii (poster presented by J. Wu).

6. **Wu, J.** and Chen, S. R. (2009). "Traffic flow simulation on bridge with cellular automaton technique", 88th Transportation Research Board Annual Meeting, Jan 13-17, 2009.

7. Chen, S. R., Liu, J. H., Chen, F. and **Wu, J.** (2008). "Mobile testing scheme about wind measurement, vehicle dynamic monitoring and geospatial multimedia technology", 1st American Association of Wind Engineers Workshop, Vail, Colorado, August 21-22, 2008 (presented).

8. Chen, S. R. and **Wu, J.** (2008). "Long-span bridge dynamic analysis based on equivalent wheel loading and traffic flow simulation", First American Academy of Mechanics Conference, New Orleans, June 17-20, 2008 (presented).

9. Chen, S. R. and **Wu, J.** (2008). "Performance enhancement of long-span bridge and moving trucks under wind using Tuned Mass Dampers", Inaugural International Conference of the Engineering Mechanics Institute (EM08), ASCE, May 18-21, 2008 (presented).

10. **Wu, J.** and Chen, S. R. (2008). "Traffic flow simulation based on cellular automaton model for interaction analysis between long-span bridge and traffic", Inaugural International Conference of the Engineering Mechanics Institute (EM08), ASCE, May 18-21, 2008 (presented).

11. Chen, S. R. and **Wu, J.** (2008). "Control of long-span bridge and moving trucks under wind using tuned mass dampers (08-2900)", 87th Transportation Research Board Annual Meeting, Jan 13-17, 2008.

12. Chen, S. R. and **Wu, J.** (2008). "Performance enhancement of bridge infrastructure systems: Long-span bridge, moving trucks and wind with tuned mass dampers", Engineering Structures, 30, 3316-3324.

13. Di, J., Zhou, X. H. and **Wu, J.** (2006), Time-domain buffeting analysis and safety assessment on main pylon construction of cable-stayed bridge for north navigational channel of Hangzhou Bay Sea-Crossing Bridge. Highway, 9, 150-154 (in Chinese).

14. Zhou, X. H., **Wu, J.** and Di, J. (2006), Mechanical analysis of long-span self-anchored suspension bridge. China Civil Engineering Journal, 2(2), 42-45. (in Chinese).

15. Di, J. and **Wu, J.** (2005), Calculation methods for cable curve of self-anchored suspension bridge. Journal of Traffic and Transportation Engineering, 4(3), 38-43. (in Chinese).